12-2020

MICRORNAs ASSOCIATED WITH MELANOMA INFLAMMATION AND RESPONSE TO PD-1 INHIBITION

Robert Szczepaniak Sloane

MICRORNAs ASSOCIATED WITH MELANOMA INFLAMMATION AND RESPONSE TO PD-1 INHIBITION

by

Robert Szczepaniak Sloane, BSc

APPROVED:

_____

Jennifer A. Wargo, M.D., M.M.Sc.

_____

Michael A. Davies, M.D., Ph.D.

_____

Richard E. Davis, M.D.

_____

Giulio F. Draetta, M.D., Ph.D.

_____

Padmanee Sharma, M.D., Ph.D.

APPROVED:

_____

Dean, The University of Texas

MD Anderson Cancer Center UTHealth Graduate School of Biomedical Sciences

MICRORNAs ASSOCIATED WITH MELANOMA INFLAMMATION

AND RESPONSE TO PD-1 INHIBITION

A

DISSERTATION

Presented to the Faculty of

The University of Texas

MD Anderson Cancer Center

University of Texas Health Science Center at Houston

Graduate School of Biomedical Sciences

in Partial Fulfilment

of the Requirements

for the Degree of

DOCTOR OF PHILOSOPHY

By

Robert Szczepaniak Sloane, BSc.

Houston, Texas

December 2020

MICRORNAS ASSOCIATED WITH MELANOMA INFLAMMATION AND RESPONSE TO PD-1 INHIBITION

Robert Szczepaniak Sloane, BSc

Advisory Professor: Jennifer Wargo, M.D., M.M.Sc.

Melanoma is an aggressive malignancy of melanocytes with historically poor outcomes. Melanoma therapy has improved markedly over the past decade with advances in molecularly targeted agents and immunotherapies. Immune checkpoint inhibitors achieve T-cell mediated anti-tumor efficacy by blocking engagement of inhibitory checkpoints on T-cells to overcome immunosuppressive signals from tumor cells and the broader microenvironment. Despite these advances, there are a significant proportion of patients who do not benefit from existing immunotherapy strategies making it a priority to identify and target the mechanisms that confer resistance to therapy. We demonstrate that microRNAs are accurate markers of microenvironment composition with prognostic value for overall survival in melanoma. We also identified networks of microRNA and mRNA expression in melanoma tissue and melanoma cell lines that are associated with previously identified melanoma transcriptomic subsets. These microRNA networks encompass several key oncogenic processes including epithelial to mesenchymal transition and expression of melanoma specific transcription factors including MITF. Furthermore, investigation of these microRNAs in a cohort of PD-1 inhibitor treated melanoma patients identified a survival benefit in patients whose melanomas had high expression of miR-100-5p and miR-125b-5p. These findings indicate that microRNA regulation of gene expression in melanoma is relevant to melanoma biology, composition of the immune microenvironment and outcomes to PD-1 checkpoint blockade.

TABLE OF CONTENTS

CHAPTER SIX

LIST OF ILLUSTRATIONS

LIST OF TABLES

CHAPTER ONE

INTRODUCTION

This chapter is based upon the following work:

- Szczepaniak Sloane RA, Gopalakrishnan V, Reddy SM, Zhang X, Reuben A, Wargo JA. Interaction of molecular alterations with immune response in melanoma. Cancer. 2017 Jun 1;123(S11):2130-2142. doi: 10.1002/cncr.30681. PMID: 28543700; PMCID: PMC6105277.

TARGETED AND IMMUNE THERAPY FOR MELANOMA

Recent Advances in Clinical Care

Significant advances in the treatment of metastatic melanoma have been made over the last decade, translating into meaningful survival benefit for patients. Therapeutic strategies may be broadly characterized into targeted therapy versus immunotherapy approaches—with several agents now approved by the US Food and Drug Administration (FDA) in each category. These agents are also being used to treat patients with earlier stage disease; however, resistance to therapy remains an issue across treatment types.

One of the most frequent mutations in melanoma involves the B-Raf proto-oncogene serine/threonine kinase (BRAF) gene, with BRAF mutations present in approximately 50% of melanomas, leading to constitutive signaling of the mitogen-activated protein kinase (MAPK) pathway in affected cells [1, 2]. Pharmacologic targeting of this oncogenic mutation has been a qualified success, leading to the approval of several different BRAF inhibitors (vemurafenib in 2011, dabrafenib in 2013)[3, 4]. However, despite a high

response rate, the durability of responses has been limited (<6 months), and a deep query into resistance has ensued, uncovering numerous mechanisms of therapeutic resistance to BRAF-inhibitor monotherapy, many of which contribute to MAPK reactivation [5-14]. On the basis of these findings, investigators developed combinatorial strategies incorporating mitogen-activated protein kinase kinase (MEK) inhibition and BRAF-inhibitor monotherapy with some success and a near doubling of progression-free survival [15, 16]. Therapeutic resistance remains an issue even with combined BRAF and MEK inhibition, and the majority of patients experience relapse of disease within 1 year of initiating therapy [17-19]. Nonetheless, durable responses may be observed in a subset of patients, and from 20% to 30% of patients remain progression free 4 years into therapy [17].

Concurrent with the clinical development of BRAF-targeted therapy was the clinical development of immune-checkpoint inhibitors. This class of agents blocks immunomodulatory molecules on the surface of T cells (or their ligands), resulting in reactivation of potentially anergic T cells [20, 21]. Ipilimumab and tremelimumab are monoclonal antibodies that block the cytotoxic T-lymphocyte antigen 4 (CTLA-4) receptor on the surface of T lymphocytes. CTLA-4 functions to down-regulate the priming phase of an immune response, and blocking this interaction results in T-cell activation through the engagement of antigen-presenting cells. CTLA-4 blockade may also function through depletion of immune-suppressive regulatory T cells by antibody-dependent cellular cytotoxicity, increased mobilization of CD8 T cells to the tumor, and prevention of trans-endocytosis of costimulatory molecules on antigen-presenting cells, thereby enhancing their capacity to prime T-cell responses [22-24]. Two large phase 3 clinical trials investigating treatment with ipilimumab in patients with metastatic melanoma

demonstrated a survival benefit over then standard-of-care chemotherapy, substantiating its FDA approval in 2011 [25, 26]. Although overall objective response rates are modest (range, 10%-15%), treatment with CTLA-4 blockade is associated with long-term disease control in a subset of patients, with approximately 20% of treated patients achieving durable disease control (>10 years after initiating therapy) [25, 27].

Other immune-checkpoint inhibitors were also developed during this time, including those targeting the programmed death-1 (PD-1) pathway and its ligands (PD-L1, PD-L2). PD-1 ligation leads to inactivation of T cells, although this mainly affects the effector phase of a T-cell response in peripheral tissues (such as in the tumor microenvironment) [28, 29]. Treatment with monoclonal antibodies that block PD-1 is associated with response rates of approximately 40% in patients with metastatic melanoma, and 2 such agents were approved by the FDA in 2014 (pembrolizumab and nivolumab) [30, 31]. It is noteworthy that treatment with these agents is associated with a lower incidence of toxicity compared with CTLA-4 blockade [30, 32-35]. More recently, combination regimens with CTLA-4 and PD-1 blockade were tested in clinical trials and demonstrated a high response rate (>60%) and improvement in overall survival, although treatment with this regimen is also associated with a very high rate of toxicity [36, 37].

Additional forms of immunotherapy have been investigated and have demonstrated efficacy with the FDA approval of talimogene laherparepvec (TVEC) in 2015. TVEC is an oncolytic herpesvirus that was engineered to express human granulocyte-monocyte colony–stimulating factor and is used as an intratumoral injection [38]. TVEC selectively replicates within tumor cells, causing tumor lysis and is also believed to elicit antitumor immune responses through enhanced antigen presentation by dendritic cells (DCs) [39-41].

This agent was FDA approved for the treatment of unresectable stage IIIB, IIIC, and IV melanoma based on an improved durable response rate compared with granulocyte-monocyte colony–stimulating factor alone [42]. More recently, TVEC was tested in combination with immune-checkpoint inhibitors (ipilimumab and pembrolizumab) and demonstrated greater efficacy than expected with either drug alone; however, these agents were not compared in a randomized prospective design [43, 44].

Despite these advances, there are still significant proportions of patients who do not respond to therapy, and therapeutic decision making remains difficult based on different treatment choices and a paucity of reliable biomarkers for response. However, tremendous insights into molecular and immune mechanisms of response and resistance to these therapies have been gained and ultimately may help guide rational approaches to optimizing treatment.

Insights into the Effects of Mutations on Antitumor Immunity

Over the past decade, we have made significant progress in understanding the effects of mutations on antitumor immunity. With the advent of next-generation sequencing and the use of targeted sequencing panels at the time of melanoma diagnosis, we now have more information on which to base therapeutic decisions, although the approach to date has been somewhat rudimentary.

Detailed genomic analyses of large melanoma cohorts have provided understanding of the key molecular features that contribute to the development of melanoma, including widespread dysregulation of the MAPK signaling pathway driven predominantly by BRAF and RAS (neuroblastoma rat sarcoma viral oncogene homolog [NRAS], Harvey rat

sarcoma viral oncogene homolog [HRAS], Kirsten rat sarcoma viral oncogene homolog [KRAS]) mutations. Additional significant alterations include phosphatase and tensin homolog (PTEN) inactivation either by mutation or deletion, and neurofibromatosis type 1 (NF-1) mutations [45, 46]. It is also known that cutaneous melanoma has the highest mutational burden among all cancers, likely related to damage by ultraviolet (UV) radiation [47]. Over the last decade, it has become apparent that the different molecular alterations can have distinct effects on the tumor microenvironment, which, in turn, influence the response to targeted therapies and immunotherapies [48, 49]. Thus, a deeper understanding of the immune effects of genomic mutations (and consequences of targeting these mutations) may facilitate the design of effective treatment strategies. Specific aspects of selected mutations and/or genomic alterations are discussed below. It is worth noting that several additional mutations may influence immune responses, but here we are highlighting the high-frequency mutations with strong evidence for an impact on antitumor immunity.

BRAF Valine-to-Glutamic Acid Mutations at Codon 600

Activating mutations in the BRAF gene (most commonly the valine-to-glutamic acid mutation at codon 600 [V600E]), lead to 10-fold greater kinase activity than that observed in normal cells, resulting in aberrant MAPK pathway activation, which protects melanocytes from apoptosis while driving tumorigenesis, invasiveness, and metastatic behavior [50]. It is noteworthy that this mutation also reportedly plays a role in immune evasion [51-53]. The first mechanistic report of the immunosuppressive effects of BRAF in melanoma came from Sumimoto et al in 2006 [51]. In their study, interleukin 6 (IL-6), IL-10, and vascular endothelial growth factor (VEGF) were identified and validated as immunosuppressive factors from the supernatant of cultured BRAFV600E melanoma cells,

and these factors and their immunosuppressive function were reduced with pharmacologic MEK inhibition or BRAFV600E RNA interference treatment [48, 51]. At the same time, Kono et al demonstrated that BRAFV600E can suppress the expression of the melanoma antigens melanoma antigen recognized by T cells 1 (MART-1) and glycoprotein 100 (gp100), whereas MEK inhibition reverses this effect, also leading to increased recognition and killing by MART-1–specific cytotoxic T cells [52]. Khalili and colleagues also observed that BRAFV600E mutations caused immunosuppression by inducing IL-1 transcription in both melanocytes and melanoma cell lines, resulting in enhanced ability of melanoma tumor-associated fibroblasts to suppress cytotoxic T-cell activity [54].

These in vitro findings are supported by preclinical models and translational work in human melanomas by several groups [48, 49, 53-58]. Notably, longitudinal tissue immune profiling of patients undergoing selective BRAF inhibition with or without MEK inhibition demonstrated an increase in CD8-positive T-cell infiltrate within 2 weeks of initiation of treatment, an increase in the expression of melanoma antigens on tumor cells, an increase in markers of T-cell cytotoxicity, and a decrease in levels of immunosuppressive cytokines IL-6 and IL-8 (Figure 1.1) [49, 59]. It is noteworthy that immunomodulatory molecules PD-1 and PD-L1 were also increased with treatment. This is likely a mechanism of adaptive immune resistance, induced by tumor-infiltrating lymphocyte (TIL)-derived interferon gamma (IFN-γ). However, it is important to note that, although PD-1/PD-L1 interaction is inhibitory, induction of these molecules as a result of BRAF therapy provides additional therapeutic targets in light of FDA approval of anti-PD-1 and anti-PD-L1 therapies, strengthening the rationale for combining targeted therapies with immune-checkpoint blockade.

Figure 1.1 Immune Effects of Molecular Alterations in Melanoma

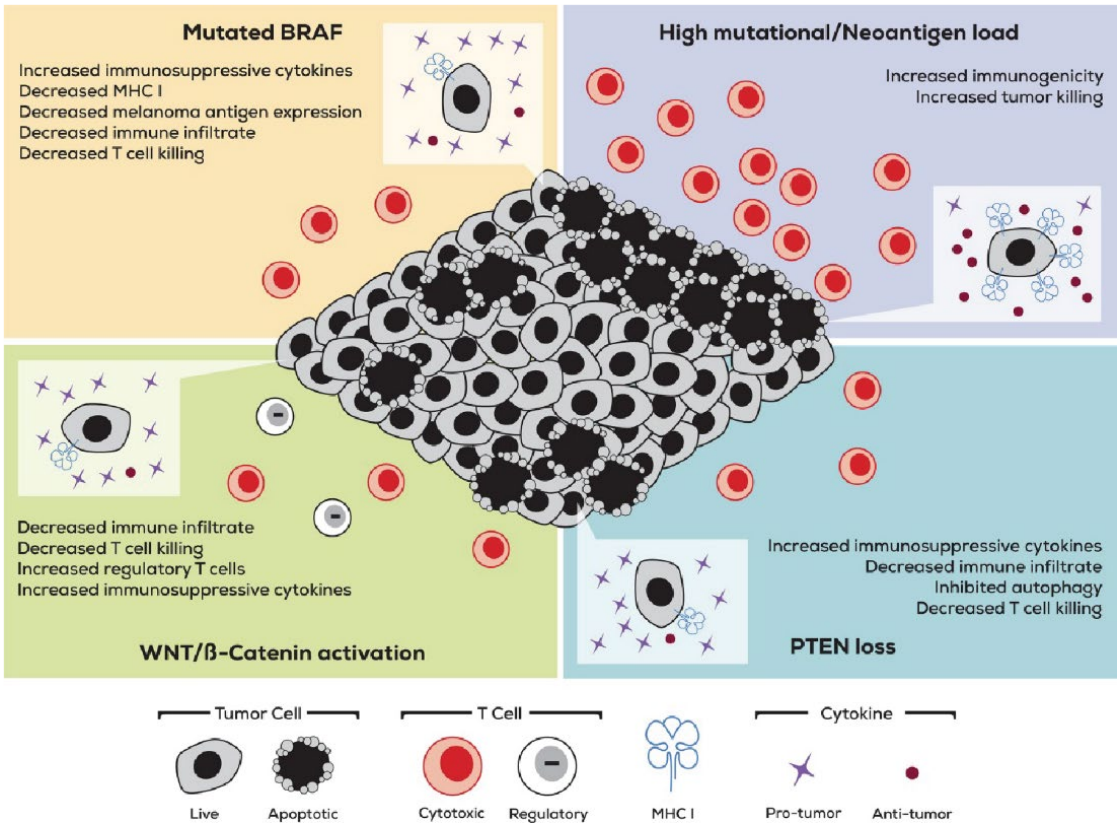

Figure 1.1 Immune Effects of Molecular Alterations in Melanoma

Immune effects of molecular alterations within the tumor microenvironment are illustrated. Immune effects of the B-Raf proto-oncogene serine/threonine kinase (BRAF) valine-to-glutamic acid mutation at codon (BRAFV600E) and phosphatase and tensin homolog (PTEN), β-catenin, and passenger mutations resulting in neoantigens on the immune tumor microenvironment are described. It has been established that the BRAFV600E mutation up-regulates the immunosuppressive cytokines vascular endothelial growth factor (VEGF), interleukin 1 (IL-1), IL-6, and IL-10 and down-regulates immunogenic melanoma antigens. It also has been demonstrated that PTEN loss increases the expression of VEGF, IL-6, IL-10, and C-C motif chemokine ligand 2 (CCL2), leading to reduced T-cell infiltration and poor response to checkpoint blockade. Aberrant β-catenin activity leads to increased expression of IL-10, reducing the ability of dendritic cells to mediate an antitumor T-cell response. Increases in mutational load and neoantigens result in a potential increase in the antigenicity of the tumor. MHC I indicates major histocompatibility complex class 1.

Despite evidence for the immunosuppressive role of BRAF in vitro and in translational studies, meta-analyses of immunotherapy trials have not demonstrated a significant difference in response rates for patients with versus without a BRAF mutation [60]. This could have been because of insufficient power to detect a difference, or it may be related to the presence of other molecular and microenvironment factors affecting antitumor immunity. Nonetheless, it suggests that BRAF mutation status as a single variable is not sufficient to predict response to immunotherapy.

PTEN

Expression of the tumor suppressor PTEN is lost in up to 30% of melanomas, and loss of PTEN function is associated with aberrant activation of the phosphoinositide 3-kinase (PI3K) pathway, which can cooperate with mutant BRAF during tumorigenesis [61, 62]. In melanoma, PTEN loss is associated with both reduced T-cell infiltration and reduced T-cell function in vitro and in vivo, and 2 separate studies have outlined the mechanisms of immune suppression that occur with PTEN loss [45, 63]. Like in BRAF-mutant melanoma, IL-6, IL-10, and VEGF expression levels are key immunosuppressive features of PTEN inactivation, with PI3K signaling through signal transducer and activator of transcription 3 (STAT3) mediating the expression of these cytokines [63]. Furthermore, the immunosuppressant C-C motif chemokine ligand 2 (CCL2) is also overexpressed in PTEN-inactivated tumors [45]. It is encouraging to know that the effects of PTEN loss on both cytokine expression and T-cell infiltration and function are reversible with PI3K inhibitors, which increased the efficacy of anti–PD-1 therapy when administered in combination in a murine model [45]. These studies also demonstrated that PTEN loss is associated with reduced T-cell infiltration, reduced efficacy of ex vivo expansion of TILs,

and poor response to anti-PD-1 checkpoint blockade in human studies (Figure 1.1)[63]. This concept is now being translated to the clinic, and a trial is underway to test the safety and efficacy of combining a PI3K inhibitor with pembrolizumab in melanoma and other tumor types (clinicaltrials.gov identifier NCT02646748). One of the stated aims of this study is to investigate effects on the tumor microenvironment, which may help clarify the immune-related role of PI3K and the clinical feasibility of this combination. Notably, potential nuances exist with this type of approach, because studies have indicated that different isoforms of PI3K inhibitors have differential effects on T lymphocytes [64].

NRAS

NRAS mutations are present in approximately 20% of melanomas, representing the second largest molecular subtype after BRAF-mutant melanoma [65, 66]. Activating mutations in NRAS, like BRAF, result in constitutive over-activation of the MAPK pathway [67, 68]. However, NRAS-mutant melanomas are also clinically distinct from BRAF-mutant melanomas, with a higher incidence in chronically sun-damaged skin, thicker lesions at presentation, and poorer prognosis [69].

The clinical response to immunotherapy is also different in the presence or absence of an NRAS mutation. Two independent studies have now observed a higher response rate to immunotherapy in NRAS-mutated melanomas. In an analysis of 208 patients with stage III/IV melanomas who received treatment with high-dose IL-2 (HD-IL-2), those who had NRAS mutations achieved significantly higher response rates compared with those who had BRAF-mutant or wild-type (WT) melanomas [70]. These findings were recently corroborated in a study that included HD-IL-2, ipilimumab, and anti–PD-L1/PD-1

therapies. Although increased response rates were observed in all immunotherapies, the benefits were most pronounced with the anti–PD-L1/PD-1 treatments [71].

The mechanism of these improved responses has not yet been fully elucidated. Joseph et al reported a correlation between serum lactate dehydrogenase (LDH) levels and response to HD-IL-2, although LDH is a surrogate of disease burden and a prognostic biomarker in melanoma and this may be the basis of the association, rather than a specific association with an immune phenotype [70, 72]. Elevated expression of PD-L1 in the NRAS cohort described by Johnson et al could explain these clinical differences, although their observations were in a small cohort and were not statistically significant [71]. The differential response to immunotherapies may also be explained in part by the specific immunosuppressive effects of BRAF mutation and PTEN loss in the other cohorts, especially because NRAS mutations are generally exclusive of both BRAF mutation and PTEN loss, which would clearly delineate these cohorts [69].

Wnt/β-Catenin Signaling Pathway

Although mutations in the Wnt/β-catenin pathway occur at a relatively low rate in melanoma, it has been reported that dysregulation of this pathway is common, with 1 report of abnormal cytoplasmic/nuclear accumulation in one-third of melanomas [73, 74]. It is noteworthy that defects in the Wnt/β-catenin signaling pathway have been implicated in immunosuppression as an intrinsic mechanism within melanomas and also within local DCs [75-77]. Activation of β-catenin signaling directly increases expression of the immunosuppressive cytokine IL-10 in human melanoma, and this is linked to a reduced ability of DCs to stimulate a melanoma-specific, CD8-positive T-cell response [78]. Two studies have demonstrated that DC-mediated inhibition of CD8-positive T-cell cross-

priming itself is a process regulated by the Wnt/β-catenin pathway within the DCs [76, 79]. In addition, tumor-induced β-catenin activity in DCs can also induce regulatory T-cell differentiation [77]. Recent evidence also suggests that Wnt/β-catenin signaling in melanoma cells is linked to T-cell exclusion from the tumor microenvironment and that this is mediated by CCL4 transcription and a reduction in the recruitment of CD103-positive DCs [75].

When considering the potential clinical relevance of these findings, it is interesting to note that Wnt/β-catenin signaling-linked immunosuppressive effects can be reversed by pharmacologic targeting of the pathway [77, 79]. It may also be of therapeutic benefit that Wnt/β-catenin signaling can regulate immunosuppressive processes in different cell types through various mechanisms. Therefore, any targeting of this pathway may be broadly immunosensitizing, and this may improve efficacy and limit potential mechanisms of resistance (Figure 1.1).

Mutational Load/Neoantigens

Cutaneous melanoma is the most heavily mutated of all cancers because of induction of C-T transitions at dipyrimidine sites through exposure to UV irradiation [47, 65, 80]. Accumulation of these mutations often leads to alterations in the MAPK pathway in melanoma and in other melanoma driver genes, although UV exposure also leads to the generation of large numbers of other mutations that affect genes unrelated to proliferation or apoptosis and thus are unlikely to directly contribute to cancer progression [65]. However, recent work has brought to light the role that these “passenger mutations” may play in altering tumor immunogenicity [80].

Although high mutational load was once considered to be deleterious in cancer, it is now thought to have potentially beneficial immunogenic properties [80, 81]. The reasoning behind this is that a higher mutational load is generally associated with a higher level of neoantigens, which are defined as tumor-restricted antigens derived from mutations within transformed cells [82]. Considering the origin and randomness of their generation, neoantigens may be associated with increased tumor immunogenicity, because they are excluded from self-tolerance and deletion mechanisms at play during T-cell development. Increased mutational load and neoantigen burden therefore potentially allow for increased tumor immunogenicity through presentation of unique peptides more likely to be recognized by T cells (Figure 1.1).

Accordingly, neoantigen burden has been studied in the context of treatment with immune-checkpoint blockade as well as other forms of immunotherapy, such as adoptive T-cell therapy [80, 81, 83]. In the setting of treatment with CTLA-4 and PD-1 blockade, a higher mutational burden is correlated with favorable responses [80, 81, 84]. However, this is not specific to melanomas and has been observed in other cancer types, including non-small cell lung cancer as well as colorectal cancer, with high mismatch-repair mutations [85]. Although original reports relied on whole-exome sequencing to derive mutational load, algorithms have now been developed to calculate the "predicted total mutational load" from targeted sequencing panels of 200 genes [86]. In addition to these quantitative assessments, qualitative assessments of neoantigens have been used to develop personalized cancer therapies through the identification of neoantigens in tumors and validation of expression and reactivity against these antigens by autologous T cells [83]. Targeting of patient-restricted neoantigens has proven successful in this context, as

demonstrated in a study by Tran and colleagues in which exome sequencing was performed, neoantigens were predicted based on patient human leukocyte antigen alleles, and infusion of mutated Erbb2 interacting protein (ERBB2IP)-specific T cells mediated the response of multiple metastases in a patient with epithelial cancer [80, 83].

Molecular Alterations with Response/Resistance to Immunotherapy

In addition to interrogating known melanoma mutations for their influence on antitumor immunity, tremendous progress has been made in identifying resistance-conferring molecular alterations through the analysis of patient cohorts that received immunotherapy. Several high-impact studies have been done over the last several years, and the insights gained are informing strategies to overcome therapeutic resistance.

In addition to the influence of mutational load, as described above, several other factors have been associated with response or resistance to immune-checkpoint blockade [80]. Genomic and transcriptomic characterization of a cohort treated with CTLA-4 blockade revealed that neoantigen burden and the expression of cytolytic markers also are associated with long-term clinical benefit [84]. Additional studies in the setting of CTLA-4 blockade have identified other mutations associated with improved survival, such as serpin peptidase inhibitor, clade B, member 3 (SERPINB3) and SERPINB4 mutations, which are hypothesized to enhance tumor immunogenicity [87]. Defects in IFN signaling may also serve as a mechanism of resistance to therapy, and studies have demonstrated that functional IFN-γ is necessary for a successful immune response to CTLA-4 therapy [88, 89].

Several recent reports have also described molecular alterations associated with response and resistance to PD-1 blockade. Like CTLA-4 blockade, high mutational load is also associated with long-term clinical benefit [90, 91]. In addition, it has been demonstrated that responding tumors have a higher burden of mutations in breast cancer 2 (BRCA2), a DNA repair gene [90]. Therapeutic resistance is associated with defects in the antigen processing and presentation machinery (such as β2-microglobulin) and IFN-γ signaling as well as up-regulation of genes involved in angiogenesis, extracellular matrix remodeling, cell adhesion, and mesenchymal transition [89, 90]. In addition, a recent study incorporating targeted sequencing revealed that patients with NF-1 mutations had high mutational load and high response rates to anti-PD-1, whereas patients who lacked BRAF/NRAS/NF-1 mutations had low mutational load [91]. One study to date has been published analyzing sequential treatment with CTLA-4 and PD-1 blockade that performed immune and gene-expression profiling in longitudinal tumor samples in the context of therapy [92]. In those studies, immune signatures in pretreatment samples were only modestly predictive of response to both CTLA-4 blockade as well as PD-1 blockade; however, the presence of a favorable immune signature in on-treatment tumor biopsies was highly predictive of response, particularly to anti–PD-1 therapy. More recently, genomic characterization of tumor samples has been performed in the same cohort, demonstrating copy number alterations as drivers of resistance to both forms of immune-checkpoint blockade [93].

Combining Targeted Therapy and Immunotherapy

With an understanding of the immune effects of oncogenic mutations and consequences of their therapeutic targeting, coupled with a growing appreciation of molecular resistance

mechanisms to immunotherapy—one may question if synergy will be seen when these agents are combined. Indeed this hypothesis has been posed, though early interest in combining targeted therapy and immunotherapy was largely clinically based—hoping to achieve high response rates (characterized by targeted therapy) and durable responses (characterized by immunotherapy). Since these trials were initiated, there is now also growing scientific rationale for combining these 2 treatment modalities, and a large number of trials exploring this strategy are currently underway [94-97].

One of the first phase 1 clinical trials testing a BRAF inhibitor with immunotherapy involved the combination of BRAF inhibitor monotherapy (with vemurafenib) and a checkpoint inhibitor (targeting CTLA-4, ipilimumab). Although responses were observed and there was evidence of synergy based on assessment of T-cell infiltrates within tumors from these patients, accrual to the trial was halted early, because grade 3 hepatotoxicity was observed in a significant proportion of these patients (6 of 12), highlighting the potential toxicity of these combinations [94, 98].

Another trial focused on the combination of BRAF and MEK inhibitors (dabrafenib and trametinib) with immune-checkpoint blockade targeting CTLA-4 (ipilimumab; clinicaltrials.gov identifier NCT107767454) in patients with stage IV, BRAF-mutant melanoma. In that trial, hepatotoxicity was still observed, although the magnitude was far less, suggesting that this may be drug specific rather than target specific [96]. Notably, the arm of the trial that incorporated treatment with the triplet combination was closed after several patients (2 of 7) developed colitis, with 1 patient requiring surgery [99]. This again highlights the unpredictability of toxicity profiles and the need for carefully designed and monitored, early phase clinical trials.

Compared with concurrent therapy, a phase 2 trial of sequential vemurafenib and ipilimumab demonstrated a more tolerable and manageable toxicity profile—65% of patients had grade ≥3 toxicities, the majority of which were skin toxicities—suggesting that combining these drugs in this manner may prove more beneficial [97]. Finally, given the improved tolerability of anti–PD-1/PD-L1 axis-targeting therapies compared with ipilimumab, trials are investigating combinations of these agents with targeted therapies. A recent report on a phase 1 trial of durvalumab/dabrafenib/trametinib for BRAF-mutant melanoma, durvalumab/trametinib for BRAF-WT melanoma, and sequential trametinib/durvalumab in BRAF-WT melanoma has also demonstrated a relatively more manageable toxicity profile, suggesting that combination with anti–PD-1/PDL-1 agents may be preferable [100].

In recent years the combination of a BRAF and MEK inhibitor (Vemurafenib and Cobimetinib) with an anti-PDL-1 agent (Atezolizumab) has been investigated in a multi-center, randomized, double blind, placebo-controlled phase III trial (NCT02908672). This trial reported increased progression free survival of melanoma patients treated with the triple combination compared to those treated with Vemurafenib and Cobimetinib and a placebo (15.1 months vs 10.6 months) [101]. There was no significant difference in objective response rates between the different arms of this trial and the largest differences in PFS were observed after 6 months. The results of this trial lead to the FDA approval of this combination in July 2020 for melanoma patients with BRAFV600E mutated, unresectable or metastatic melanoma.

Additional trials are underway exploring combinations of immunotherapy and targeted therapy. However, as results emerge, it is becoming increasingly clear that complexities

exist with this approach; therefore, efforts must be made to use scientific evidence and iterative input from ongoing and completed trials to guide next-generation combination studies.

Refining Combination Strategies through Biomarker-Driven Clinical Trials

Insights from preclinical models and translational research are paramount as we charter a path forward with rational combination strategies. This is important, because the numbers of patients required to test all possible combinations of molecular-targeted and immune-targeted therapies using conventional clinical trial designs far exceed the numbers of available patients for such studies. Thus it may be necessary to move to more novel, biomarker-heavy clinical trial designs in an effort to incorporate insights gained from genomic and immune analyses (Figure 1.2).

Figure 1.2 Adaptive Trial Design to Utilize Personalized Medicine

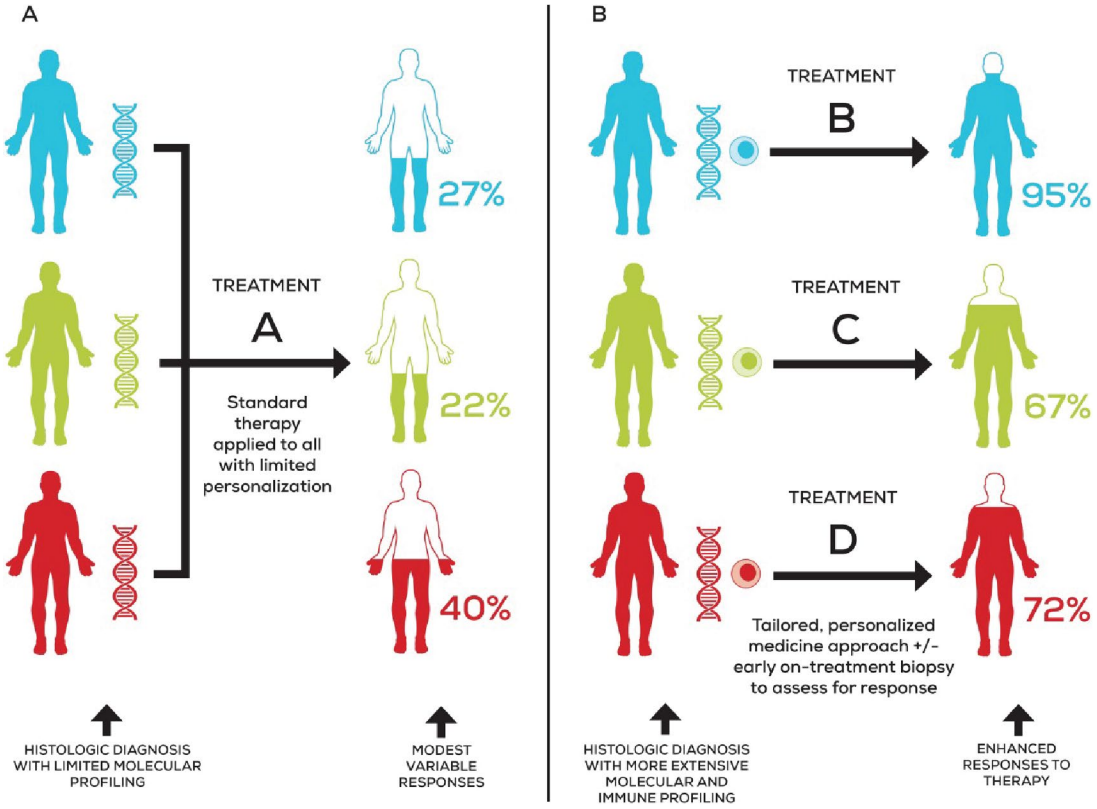

Figure 1.2. Adaptive clinical trial design allows improved therapeutic decisions. (A) Current approaches investigate limited molecular biomarkers before initiation of a standard therapy in a heterogeneous patient population with little personalization. This results in modest and variable responses. (B) Increasing numbers of trials now allow for adaptive decision making. These trials include more extensive molecular and immune profiling before a personalized medicine approach. Then, after treatment initiation, an early on-treatment biopsy is obtained for molecular and immune profiling to evaluate the success of the current therapy. Because of this profiling, patients are either continued on this therapy or switched to an alternate treatment regimen, enhancing responses to therapy.

From a trial standpoint, adaptive trial design provides 1 possible means of more efficiently assessing combination therapies [102]. In this design, Bayesian modeling may be used to combine a priori hypotheses and estimation of variables along with data collected from the ongoing trial regarding efficacy and toxicity. On the basis of an adjusted set of parameters at prespecified interim analyses, the trial design can be modified regarding dose escalation, sample size, population or subpopulations studied, treatment allocation, randomization probabilities, and study endpoint (for example, changing from superiority to noninferiority endpoint), among other variables [102]. An example in melanoma in which an adaptive trial design was used is the LOGIC 2 trial, which was designed to combine initial treatment with BRAF and MEK inhibitors, binimetinib and encorafenib, until the time of progression, at which point patients received 1 of several different treatments based on the molecular profile of their biopsy at the time of progression. The trial also incorporated Bayesian modeling based on accumulating toxicity data to minimize the number of patients on doses with excessive toxicity and maximized exposure to doses that were both tolerable and efficacious. Such a flexible design approach allows for more efficient testing of combinations that can ascertain efficacy, minimize toxicity, and use data from biomarker analysis.

Furthermore, it is prudent to take findings gained from translational research studies back to appropriate preclinical models, with validation and optimization of different combination strategies, before returning these insights to patients (Figure 1.3). An example of this type of an approach was recently published, describing the immunosuppressive effects of PTEN loss and responses to immunotherapy [45]. In those studies, tumor samples from patients with melanoma were interrogated and noted to have exclusion of CD8-

Figure 1.3 Translational Research to Improve Melanoma Treatment

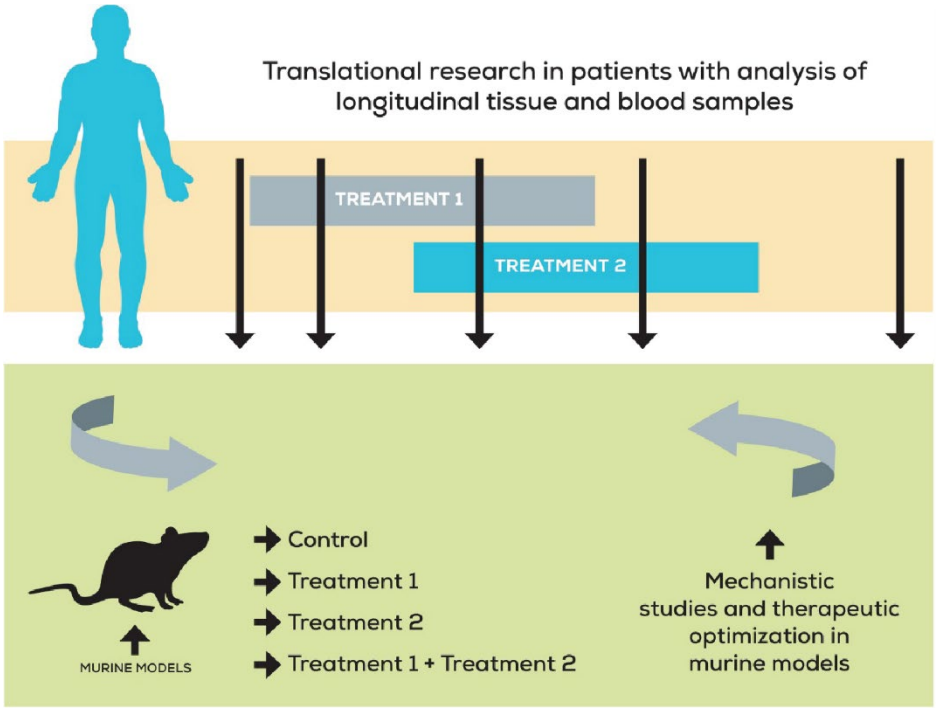

Figure 1.3. Translational studies provide an optimal approach to understanding mechanisms and accelerating patient benefit. Much success has come from approaches investigating longitudinal patient samples from clinical trials. These samples are then used to formulate hypotheses and develop appropriate animal models in which therapeutic mechanisms of response and resistance can be investigated and better understood to improve patient outcomes.

positive T cells in regions of PTEN loss within tumors. The impact of this on response to anti–PD-1 therapy was assessed, and an association was demonstrated between PTEN loss in tumors from patients with lack of response to PD-1–based therapy [45]. These findings were then translated to a murine model and indicated that treatment of mice with combined PI3K pathway inhibitors and PD-1 checkpoint blockade was associated with delayed tumor outgrowth and enhanced survival. This research is now being translated again back to patients in the form of clinical trials combining PI3K inhibitors with immune-checkpoint inhibitors (clinicaltrials.gov identifier NCT02646748).

Challenges

Despite the successes and insights gained from these studies, major obstacles inherently remain. First, although several molecular features, such as total mutational load, the burden of copy number losses, and others described in this review, are associated with responses to immunotherapy, there is significant overlap between responders and non-responders with regard to each of these variables; therefore, each on its own is not a reliable biomarker. Recent studies suggest that an integrated analysis of several of these variables may prove more useful in predicting responses, although this needs to be validated in larger cohorts and across cancer types [93].

In addition, recent studies suggest that early on-treatment biopsies may be far superior to baseline biopsies in predicting therapeutic response; however, tumors are not always readily accessible for sampling, and limitations in the amount of tissue obtained with biopsies may limit the analyses that may be performed [45, 103]. In addition, despite their better predictive ability, these on-treatment signatures require treatment of patients with 1 or 2 cycles of their therapies, which is not ideal in the long term and highlights the need to

identify pretreatment biomarkers of response to therapy. Although it is currently limited, the identification of biomarkers within liquid biopsies may hold the most promise in the least invasive manner and make on-treatment biopsies more pragmatic. “Liquid-biopsy” approaches are in development for melanoma and other cancers. Another promising approach is using a quantitative methods to analyze positron emission tomography (PET) and computerized tomography (CT) scans to identify previously unappreciated metrics from diagnostic and staging images that may have prognostic or predictive value. These techniques are non-invasive and already routinely used clinically [104]. Another related technique is using deep learning tools to assess histopathological images, again to identify previously unappreciated features within routinely used diagnostic images that may have utility as biomarkers [105]; however, large studies will be needed to validate their prognostic and predictive role [106, 107].

MicroRNAs as Potential Biomarker and Therapeutic Options in Melanoma

Targeted therapy and immunotherapy, as described above, represent major advances in the treatment of melanoma, offering a real and tangible opportunity to help achieve long-term disease control and cures. However, resistance mechanisms to these therapies, either alone or in combination, continue to emerge. A more comprehensive understanding of molecular alterations in melanoma and of the molecular mechanisms that contribute to immune evasion will allow us to design better and more effective treatment strategies in this age of personalized cancer therapy. One area of research that offers insight into molecular mechanisms of melanoma biology and immune evasion, as well as a potential source of prognostic and predictive biomarkers are the posttranscriptional regulators of gene expression, microRNAs.

Canonical MicroRNA Biogenesis in Humans

MicroRNA genes are transcribed by RNA Polymerase II, generating the primary microRNA transcript (pri-miRNA)[108]. The principal feature of the pri-miRNA is a ~80 nucleotide hairpin structure containing what will become the functional, mature microRNA [109, 110]. The pri-miRNA is processed in the nucleus by a 'microprocessor complex' comprised of the RNAIII-family nuclease Drosha and the double stranded RNA binding protein DGCR8 [111, 112]. The microprocessor complex excises the hairpin from the RNA strand to form a precursor microRNA (pre-miRNA), which is then transported to the cytoplasm by the nuclear export protein Exportin 5 [113]. Once in the cytoplasm, the pre-miRNA is further processed into a 22 nucleotide long, double stranded microRNA duplex. This is achieved by excising the loop of the pre-miRNA hairpin, a process mediated by another RNAIII-family nuclease, Dicer [114, 115]. The microRNA duplex contains two potential mature microRNAs and are named according to which end of the pre-miRNA hairpin they are from, either 3' or 5', thus each microRNA gene can potentially generate two mature microRNAs [116]. The second role of Dicer is to transfer one strand of the microRNA duplex to an Argonaute(AGO) protein to form the functional microRNA induced silencing complex (miRISC). Dicer and the microRNA duplex associate with a trans-activation-responsive-RNA-binding-protein (TRBP) and the AGO protein to form the miRISC loading complex [117]. One strand of the microRNA duplex is then preferentially loaded onto the AGO protein to create the miRISC - a functional complex capable of interacting and regulating mRNA sequences complementary to the loaded microRNA [118]. Preferential loading of the 3' or 5' microRNA is normally determined by the strength of nucleotide interactions at the 5' end of each strand in the microRNA

duplex, typically leading to one microRNA strand being overrepresented in the final miRISC [116]. However, post-transcriptional modifications of pre-miRNA can disrupt this equilibrium and skew expression of 3' or 5' microRNAs [116, 119]. The mature RISC complex resides primarily on rough endoplasmic reticulum, where mRNA:miRISC interactions can be concentrated [120].

MicroRNA Induced Silencing Complex Specificity and Function

The mature miRISC complex presents two regions of the microRNA molecule on the external surface of the miRISC complex that bind complementary sequences located on available mRNA molecules [121]. The two regions of the microRNA that are available to bind are nucleotides 2-8, known as the seed region, and nucleotides 13 to 16, known as the supplementary region; the complementary sequence in the mRNA molecule is located in the 3' UTR and is called the microRNA Response Element (MRE) [121]. The primary and highest affinity determinant of the miRISC-mRNA binding is 100% sequence complementarity between the seed sequence and the MRE as well as an Adenine in the MRE corresponding to microRNA nucleotide [122, 123]. Functional binding can still occur without the corresponding Adenine or with a mismatch between nucleotide 8 although this is of lower affinity [122, 123]. A miRISC-mRNA complex prevents translation and can lead to degradation of the bound mRNA, thus the miRISC complex can repress gene expression with high specificity and precision. Two additional features of miRISC-mRNA interactions provide layered regulation of gene expression; microRNA multiplicity and cooperation. MicroRNA multiplicity refers to the number of MREs present in the transcriptome. Each microRNA will normally have complementary MRE in dozens of genes and each mRNA allowing a single microRNA to regulate multiple genes.

MicroRNA cooperation refers to the number of MREs for more than one microRNA in a single mRNA. This allows more than one microRNA to cooperatively regulate shared mRNA targets. Together, variations in the abundance of each microRNA, abundance of MREs specific to each microRNA and competition between multiple microRNAs for MREs on the same mRNA leads to a highly complex but organised regulatory system where cell-type specific microRNA stoichiometry can lead to distinct phenotypes [124].

MicroRNAs in Melanoma

MicroRNAs have an established role as tumor suppressors and oncogenes across multiple cancer types, with extensive mechanistic evidence related to the hallmarks of cancer [124, 125]. MicroRNA expression has been extensively characterized in melanoma tissue, the most comprehensive example of this is the microRNA sequencing within the melanoma TCGA dataset [126, 127]. In this study three distinct transcriptomic subsets of melanoma were identified that were independent of their mutation status. These subsets were classified as 'Keratin', 'MITF-low' and 'Immune' based on their unique transcriptomic features. Of note, a distinct group of microRNAs were associated with each transcriptomic profile providing evidence for a unique post-transcriptional regulatory microRNA network associated with different molecular subtypes of melanoma. Clinical and preclinical studies of individual microRNAs have yielded extensive evidence for their roles in multiple oncogenic processes in melanoma including sustained proliferative signaling, resisting cell death, invasion and metastasis, tumor-promoting inflammation and avoiding immune destruction (Figure 1.4)[128].

MicroRNAs in Immuno-Oncology

In addition to their proven role as oncogenes and tumor suppressors, there is emerging evidence for the role of microRNAs in tumor immune evasion [129-134]. Several notable examples exist from different cancer types that illustrate the potential for microRNA regulation of immunological molecules and pathways that may have clinical applications in support of immune checkpoint blockade. The first of these examples is the identification of the role of miR-200 in epithelial to mesenchymal transition and metastasis in non-small lung cancer [134]. In this study, Chen et, al demonstrated that miR-200 could simultaneously suppress metastasis and PD-L1 expression and when miR-200 was itself repressed by the pro-metastatic ZEB1, there was increased metastasis, and immunosuppression through expression of PD-L1 [134]. In Glioma, miR-124, was identified as a repressor of STAT3 signaling, which normally allows glioma cells to generate an immunosuppressive microenvironment through T-cell suppression and T-regulatory cell induction [135]. By expressing miR-124 in Glioma cancer stem cells, STAT3 signaling was diminished and markers of immunosuppression in the tumor microenvironment were reversed [135]. Separately, miR-138 was identified as a regulator of both CTLA-4 and PD-1 checkpoint molecules and subsequent expression of miR-138 in murine CD4 T-cells improved the immune-clearance of glioma *in vivo* [136]. Also in T-cells, miR-155 has been shown to have an important role in cytotoxic activity and in-vivo models lacking miR-155 expression have defective T-cell activity and impaired anti-tumor efficacy [130, 131].

Figure 1.4 MicroRNAs Associated with Hallmarks of Cancer in Melanoma

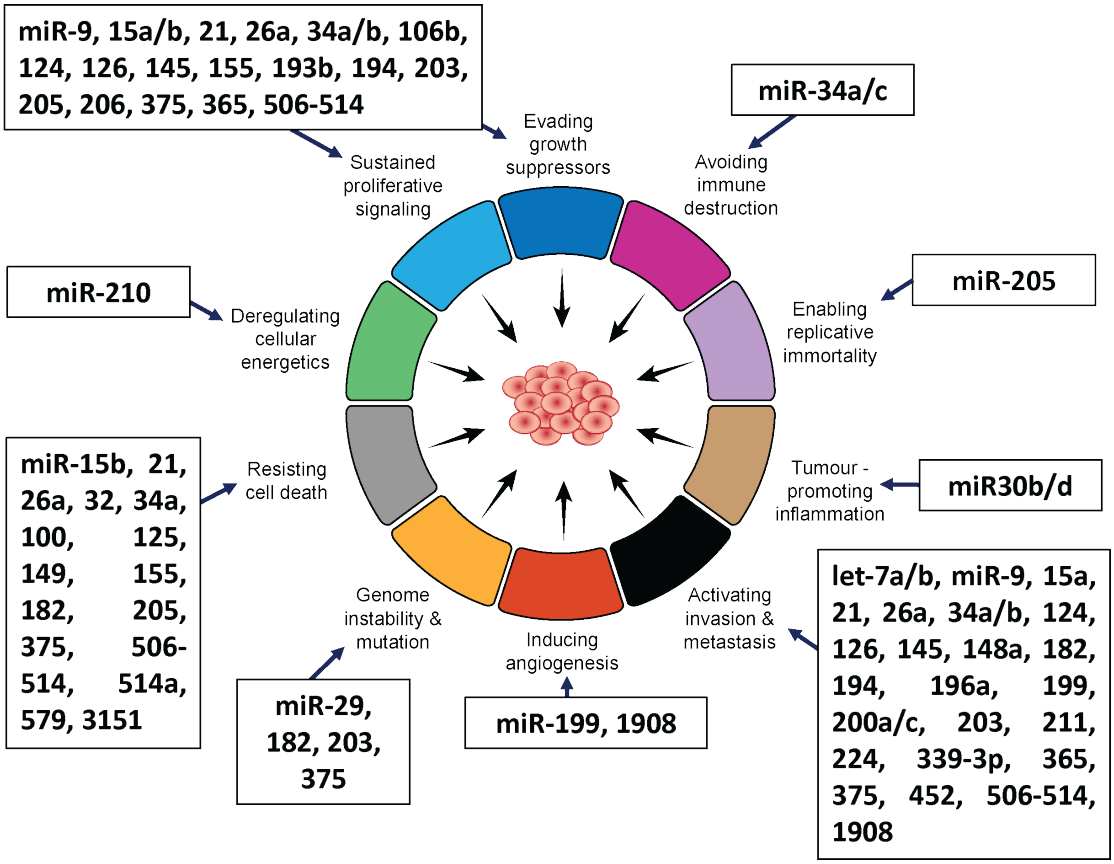

Figure 1.4 MicroRNAs in Melanoma: Extensive evidence for the role of microRNAs in melanoma biology exists. Presented is a summary of microRNAs with published evidence for regulatory roles of the hallmarks of cancer in melanoma [128].

In melanoma, there is pre-clinical evidence for the role of miR-146a in immune-evasion [137]. In this study, Mastroianni et.al identified miR-146a as overexpressed in melanoma and a subsequent miR-146a-/- knockout mouse model was shown to improve immune control of melanoma tumors, indicating that miR-146a is a negative regulator of immune activation [137].

Dissertation Overview

Immunotherapy has dramatically improved the outcome for many melanoma patients, however, approximately half of patients do not receive durable responses. The mechanisms of resistance to immunotherapy are only partly understood and effective therapies to overcome them are urgently required.

MicroRNAs are major post-transcriptional regulators of gene expression and the aberrant expression and activity of microRNAs is involved in multiple oncogenic processes. In melanoma, these processes include proliferation, resisting cell death and activation of invasion and metastasis. There is also evidence that microRNAs can also regulate the tumor microenvironment and response to immunotherapy. To date, this has not been extensively studied in humans and could reveal important mechanisms of immune evasion that could be targeted therapeutically.

The central hypothesis that we tested is: **Micro-RNAs are contributing to the differential responses of melanomas to checkpoint blockade through post-transcriptional regulation of immunomodulatory molecules and pathways.**

We tested the central hypothesis by investigating the following specific aims:

Aim 1: Identify microRNAs associated with immune infiltration and exclusion in TCGA Melanomas and elucidate mechanisms of immune regulation. RNA and microRNA sequencing data from TCGA melanoma tissue samples were used to characterize the immune landscape of melanoma and identify microRNAs that were enriched or depleted in samples with specific immune features. Using databases of known microRNA targets we were able to identify immune-associated microRNAs, miR-155-5p, miR-508-3p and miR-509-3p that had known roles in immune signaling pathway regulation, cytokine secretion and expression of other immune-regulatory molecules. Additionally, we validated these targets *in vitro*, demonstrating their role in modulating cytokine secretion, MHC expression and sensitivity to T-cell killing. The results from this aim are shown in Chapter 2.

Aim2: Characterize the mRNA and microRNA profiles associated with response to PD-1 immunotherapy in melanoma. RNA and microRNA-sequencing data from pre-treatment melanoma biopsies from PD-1 treated patients was used to identify similar groups of tumors based on their gene expression using an unsupervised clustering approach: Clusters identified by this approach largely overlapped with clinical and immune parameters, including RECIST response. Differential expression analysis and pathway analysis identified known and novel enriched genes and pathways associated with PD-1 inhibitor response. We then identified miR-31-5p, miR-200b-3p and miR-205-5p were associated with response to PD-1 therapy and validated their role in melanoma sensitivity to T-cell killing *in vitro*. The results of this aim are shown in Chapter 3.

Aim3: Construct Melanoma Tissue and Cellular MicroRNA-mRNA Networks to Identify Melanoma Intrinsic MicroRNA-mRNA Networks and Test Their

Association with PD-1 Inhibitor Outcomes. We constructed microRNA-mRNA networks using two large databases of melanoma tissue and melanoma cell lines with microRNA and mRNA sequencing data available. We identified shared as well as tissue specific networks comprising known 'Immune', 'Keratin' and 'MITF-low' transcriptomic profile associated microRNAs. We identified known and novel gene set enrichment associated with each network, indicating distinct phenotypic associations. Using Cox's proportional hazard model we were able to demonstrate that the microRNAs, miR-100-5p and miR-125b-5p, identified as central to the 'MITF-low' network, were positively associated with overall survival in PD-1 inhibitor treated melanoma patients.

CHAPTER TWO

MICRORNAs ARE ASSOCIATED WITH AND CAN REGULATE IMMUNE FEATURES IN MELANOMA

INTRODUCTION

Melanoma and Resistance to Immunotherapy

Melanoma is an aggressive malignancy of melanocytes with a 5-year survival rate of 20% for metastatic disease. Melanoma diagnoses are predicted to reach 91,270 and to cause 9,320 deaths in the US in 2018 [138]. Melanoma therapy has improved markedly over the past decade with advances in molecularly targeted agents and immunotherapies. Immune checkpoint inhibitors achieve T-cell mediated anti-tumor efficacy by blocking engagement of inhibitory checkpoints on T-cells to overcome immunosuppressive signals from tumor cells and the broader microenvironment [21, 139]. Monoclonal antibodies that target the immune checkpoint molecules cytotoxic T-lymphocyte antigen 4 (CTLA-4) and programmed death-1 (PD-1) have achieved a response rate of 61% and 3 year overall survival of 58% in combination [37, 140]. Despite these advances, there are a significant proportion of patients who do not benefit from existing immunotherapy strategies. While some melanoma intrinsic mechanisms of resistance have been identified, such as impaired antigen presentation and defects in IFN-γ signaling, our understanding is still incomplete, making it a priority to identify and target the mechanisms that confer resistance to therapy [88, 141].

MicroRNAs in Melanoma

MicroRNAs (miRs) are 17-24 nucleotide long, non-protein-coding RNAs that bind to complementary sequences on messenger RNA (mRNA) molecules, inhibiting translation and increasing degradation of the target transcripts. One miR has multiple mRNA targets, allowing a single miR to regulate the expression of many genes, often converging on a particular pathway or biological process. Through this mechanism, it is estimated that miRs can directly regulate translation of approximately 60% of human genes, making them important post-transcriptional regulators of gene expression [142]. MiRs have been demonstrated to directly influence specific cellular functions including proliferation, survival, metastasis and resistance to targeted therapy across multiple cancer types including melanoma [134, 143-151]. In glioma, miR-124 and miR-138 exert immune-mediated anti-tumor effects by inhibiting STAT3 signaling and reducing expression of immune checkpoint molecules, while miR-142 and miR-155 play important roles in macrophage and effector T cell responses against cancer [131, 135, 136, 152]. To date there has not been a comprehensive analysis of the role of miRs in melanoma immunity.

RESULTS

Characterizing the Immune Landscape of Melanoma

To identify candidate immunomodulatory microRNAs, our strategy was to compare microRNA expression in the human skin cutaneous melanoma (SKCM) dataset from The Cancer Genome Atlas (TCGA) with a selection of immune correlates: a) pathological assessment of tumor infiltrating lymphocytes (TIL), b) cytolytic score comprising Granzyme A and Perforin 1 gene expression levels and c) CIBERSORT, a bioinformatics method using transcriptomic data to infer the composition of immune cells within a tumor immune infiltrate [126, 153, 154]. We hypothesized that microRNAs with strong associations with immune exclusion or infiltration would be compelling candidates for further investigation as immunomodulatory genes. For this comparison, we first estimated the immune infiltration status of 322 melanoma samples from the TCGA dataset using the tumor microenvironment deconvolution tool CIBERSORT (LM22) (Figure 2.1 a). From this analysis we can see the immune content of this melanoma dataset mostly consists of macrophage and T-cell lineages. Specifically M0, M2 and M1 macrophage populations are three of the five most abundant immune populations while CD8, follicular helper, CD4 memory and T regulatory cells comprise four of the eight most abundant immune populations. Other less abundant components of the immune microenvironment by this methodology include naïve and memory B cells, plasma cells, NK cells, monocytes and mast cells. Other immune populations such as eosinophils, neutrophils, gamma delta T cells and dendritic cells are estimated to be mostly absent from these tumors although there are some exceptions to this. As the TCGA dataset consists of tumors from multiple disease sites, and knowing that there is potential for differential immune involvement at

Figure 2.1 Immune Profiling of TCGA Melanoma Samples

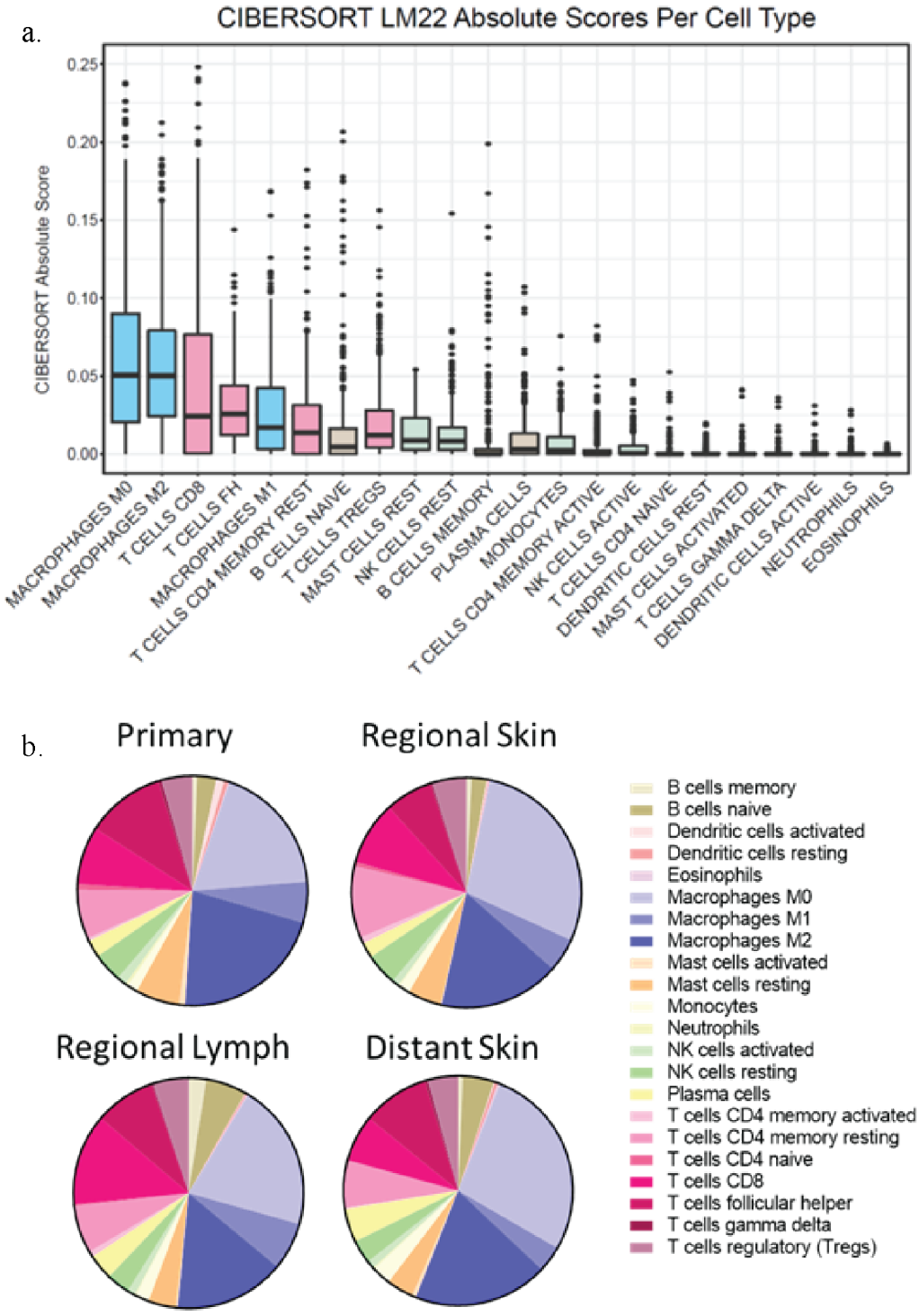

Figure 2.1 Immune Profiling Reveals Significant Immune Populations in TCGA Melanoma Tumors. CIBERSORT analysis of n TCGA melanoma samples from primary, regional skin, regional lymph and distant skin metastases quantifies the abundance of pertinent immune cell populations. Box and whisker plot (A) represent median, IQR and min/max abundance of each immune population estimated by MCP counter. Outliers are defined as ± 1.5 * the IQR beyond the upper and lower quartiles and represented by black dots. Pie charts represent the average relative abundance of each immune population in tumors from differing disease stage / sites.

different sites, notably lymph nodes, we compared the relative abundance of each immune population across each disease site (Figure 2.1 b). Although we did previously observe higher absolute immune scores in regional lymph tumors relative to other sites, the relative abundance of each immune cell type remained remarkably stable across disease sites. Some slight variation was observed, most notably when comparing the regional lymph and distant skin tumors, where there are generally higher proportions of B cells. In the regional lymph samples, this seems to be at the expense of macrophages, while in the distant skin samples it seems to be at the expense of T-cells. However, since relative measures of abundance are dependent variables and absolute abundance varies by disease site it is difficult to make robust comparisons between immune markers across disease sites.

Previous analysis of TCGA melanoma samples revealed that immune markers including LCK protein expression and histopathological assessment of immune infiltration (Lymphocyte-score) were prognostic indicators for overall survival. We investigated if any of the immune markers we had calculated had a similar prognostic value. To this end we performed a survival analysis with each of the CIBERSORT immune estimates as well as for CD8A mRNA expression and the cytolytic score which is derived from perforin and granzyme mRNA expression (Figure 2.2). We also included LCK and the Lymphocyte score from the original analysis. Our results replicated the previously published findings that LCK and Lymphocyte Score were associated with increased overall survival (Hazard ratio, log rank p; 0.28, 0.015 and 0.49, 0.057 respectively). In addition to this, four of our immune markers also demonstrated some prognostic utility. The strongest results came from the M1 macrophage gene signature (Hazard ratio = 0.35 (95%CI = 0.16-0.74) log

Figure 2.2 TCGA SKCM IMMUNE FEATURES : KAPLAN MEIER & HAZARD RATIOS

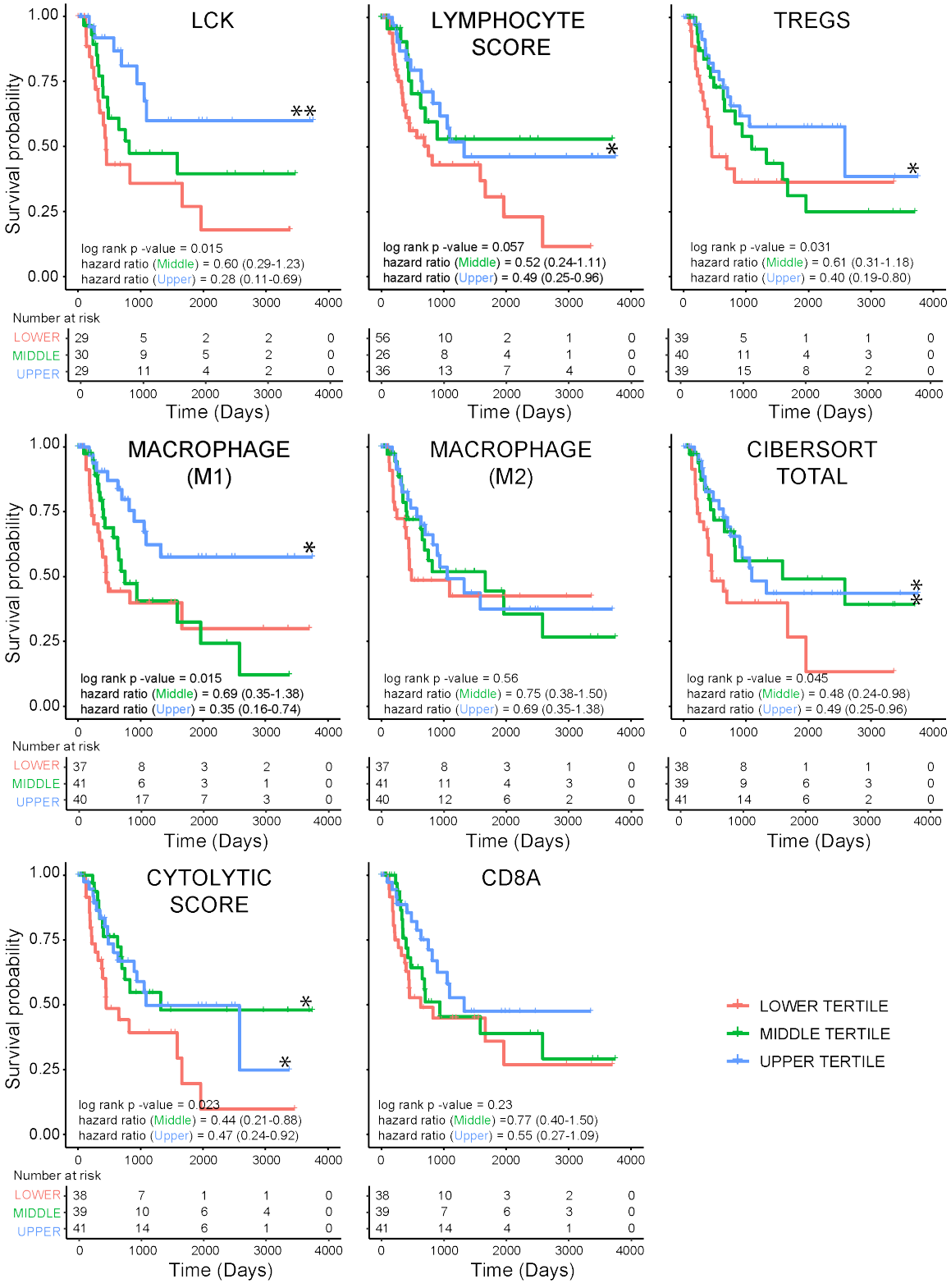

Figure 2.2 Melanoma Immune Markers Are Associated with Improved Overall Survival in TCGA Melanoma Samples. We measured survival outcomes in TCGA melanoma patients based on the abundance of different immune features in their tumors. (**a**) Kaplan Meier curves for each immune feature displaying curves for samples divided into tertiles based on expression of each immune feature, using time to death as the event value. Log rank p-value and hazard ratios ± 95% confidence intervals are shown for upper and middle tertiles compared to lower tertile in each plot. * represents P-value < 0.05 ** represents P-value < 0.01 compared to the lowest tertitle in each plot.

rank p=0.015). Interestingly, although their expression is correlated, the M2 macrophage signature did not show any significant prognostic value (Hazard ratio = 0.69 (95% CI = 0.35-1.35) log rank p=0.56), highlighting the polarized biology of these differentiated states of macrophages. Two other intuitive results were the prognostic value of the total CIBERSORT score, the sum of all estimated immune populations in the tumour microenvironment (hazard ratio = 0.49 (95% CI = 0.25-0.96) log rank p=0.045), and the cytolytic score (hazard ratio = 0.47 (95% CI = 0.24-0.92) log rank p=0.023). Both of these markers indicate a significant cytotoxic immune infiltrate. One counterintuitive result was the positive prognostic indication of regulatory T cell abundance (hazard ratio = 0.4 (95% CI = 0.19-0.8) log rank p=0.031, since we normally associate this population with negative regulation of cellular immunity. This discrepancy may be due to infidelity of the CIBERSORT algorithm, since FOXP3 is a classic marker of regulatory T cells but may also be expressed during early activation of cytotoxic T cells, making it uncertain if we are accurately counting the regulatory T cell population using this method.

Characterizing the microRNA landscape of melanoma:

The next step of this project was to identify microRNAs associated with microenvironment features of melanoma, including the immune markers described above and also transcriptomic markers of tumor purity and melanoma lineage markers. For this analysis we correlated normalized microRNA counts from TCGA melanoma samples from all disease sites with the markers described above (Figure 2.3) To visualize the pattern of microRNA associations we plotted the correlation coefficients from each microRNA with each microenvironment feature with hierarchical clustering in a heatmap (Figure 2.3 a).

Figure 2.3: Landscape of Melanoma MicroRNA Expression

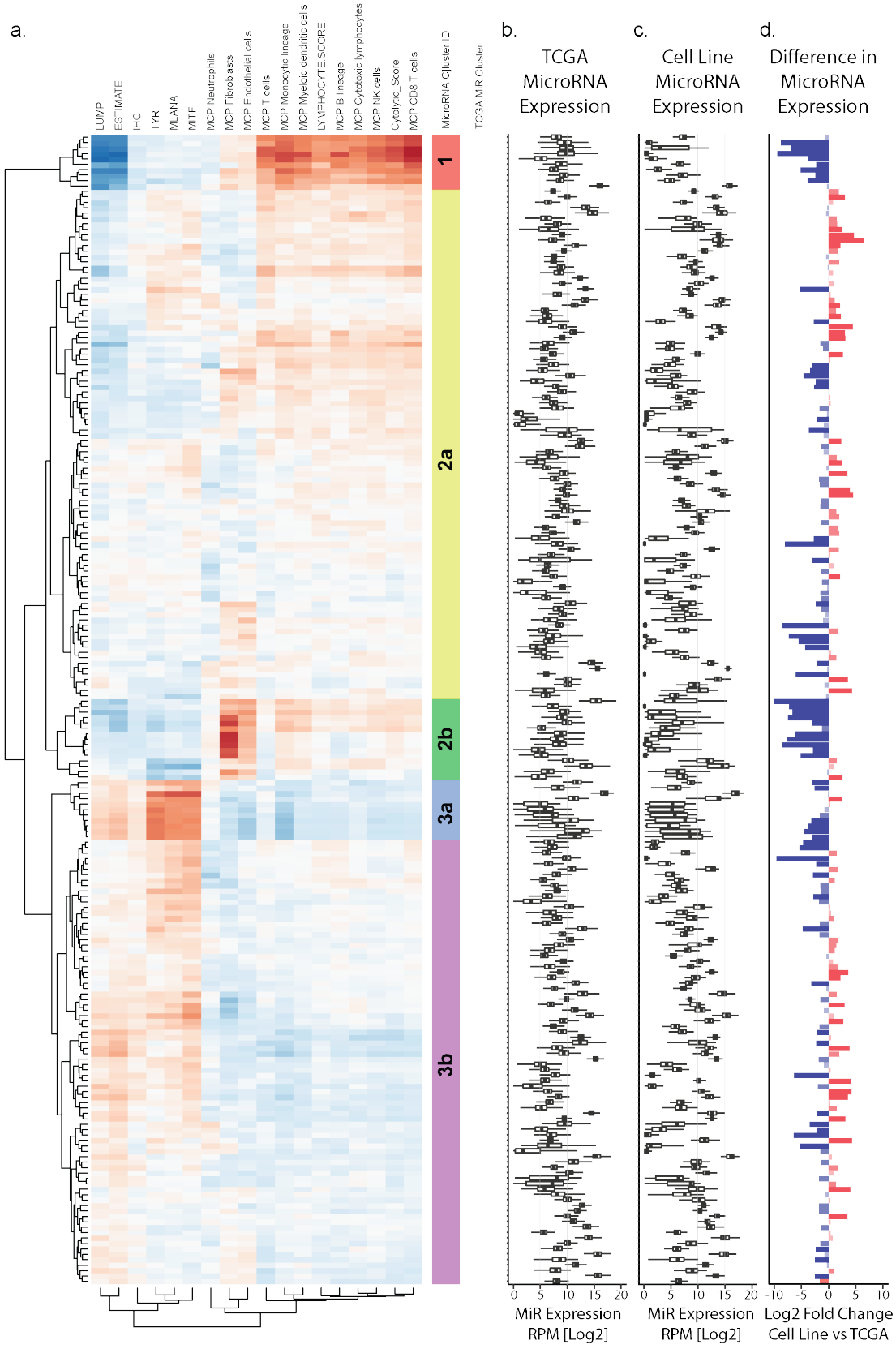

Figure 2.3 Melanoma MicroRNA Expression is Associated with Tumor Microenvironment Composition. We examined the relationship between TCGA microRNA expression and a panel of melanoma and immune markers. (**a**) A clustered heatmap representing Spearman's correlation coefficients between expression of each microRNA and each melanoma or immune marker measured from transcriptomic data. Major microRNA clusters are denoted on the track on the right of the heatmap. (**b**) Box and whisker plot showing microRNA expression in TCGA samples (log2 median ± interquartile range and IQR x1.5). (**c**) Box and whisker plot showing microRNA expression in melanoma cell lines (n=62) (log2 median ± interquartile range and IQR x1.5). (**d**) A barplot comparing microRNA expression in TCGA samples and melanoma cell lines to identify melanoma intrinsic microRNA expression. MicroRNAs that are expressed at higher levels in tumor samples are blue. MicroRNAs that are expressed at higher levels in cell lines are red.

The most striking result from this analysis was the observation of five distinct clusters of microRNA associations with broad categories of microenvironment markers. We named these clusters sequentially from the top of the heatmap to the bottom. Cluster 1 contains microRNAs predominantly correlated with expression of immune markers including T-cells, monocytes, NK cells, B cells, cytolytic score and the L-score of lymphocyte infiltration, this cluster also had strong inverse correlations with LUMP and ESTIMATE markers of tumor purity indicating that these microRNAs are expressed at higher levels in melanoma samples where the microenvironment content is inflamed and melanoma markers are diluted. We defined this cluster as the 'Immune' cluster. Cluster 2a contains a mixture of relatively weak correlations of immune markers but also some stromal and melanoma markers and is therefore classified as the 'Intermediate' cluster. Cluster 2b also contains some weak correlations with immune markers and inverse correlations with melanoma markers but is defined by the highest correlations with fibroblast and endothelial cell signatures amongst any microRNAs in this dataset. We therefore classified this group as the 'Mesenchymal' cluster. Cluster 3a appears to have the opposite associations with cluster 2b, with high correlations with melanoma lineage markers, TYR, MLANA and MITF with moderate correlations with LUMP and ESTIMATE markers of immune purity and moderate inverse correlations with immune and stromal markers. Due to the strongest associations with melanoma markers this group was classified as the 'Melanoma' microRNA cluster. The fifth and final cluster, 3b, shared similar characteristics to the 'Melanoma' cluster 3a but the strength of correlations was weaker and is therefore classified as the 'Intermediate Melanoma' cluster. Since correlative analyses are sensitive to biological variation we next repeated the analysis across sites of disease to understand

Figure S2.4: Landscape of Melanoma MicroRNA Expression - Site

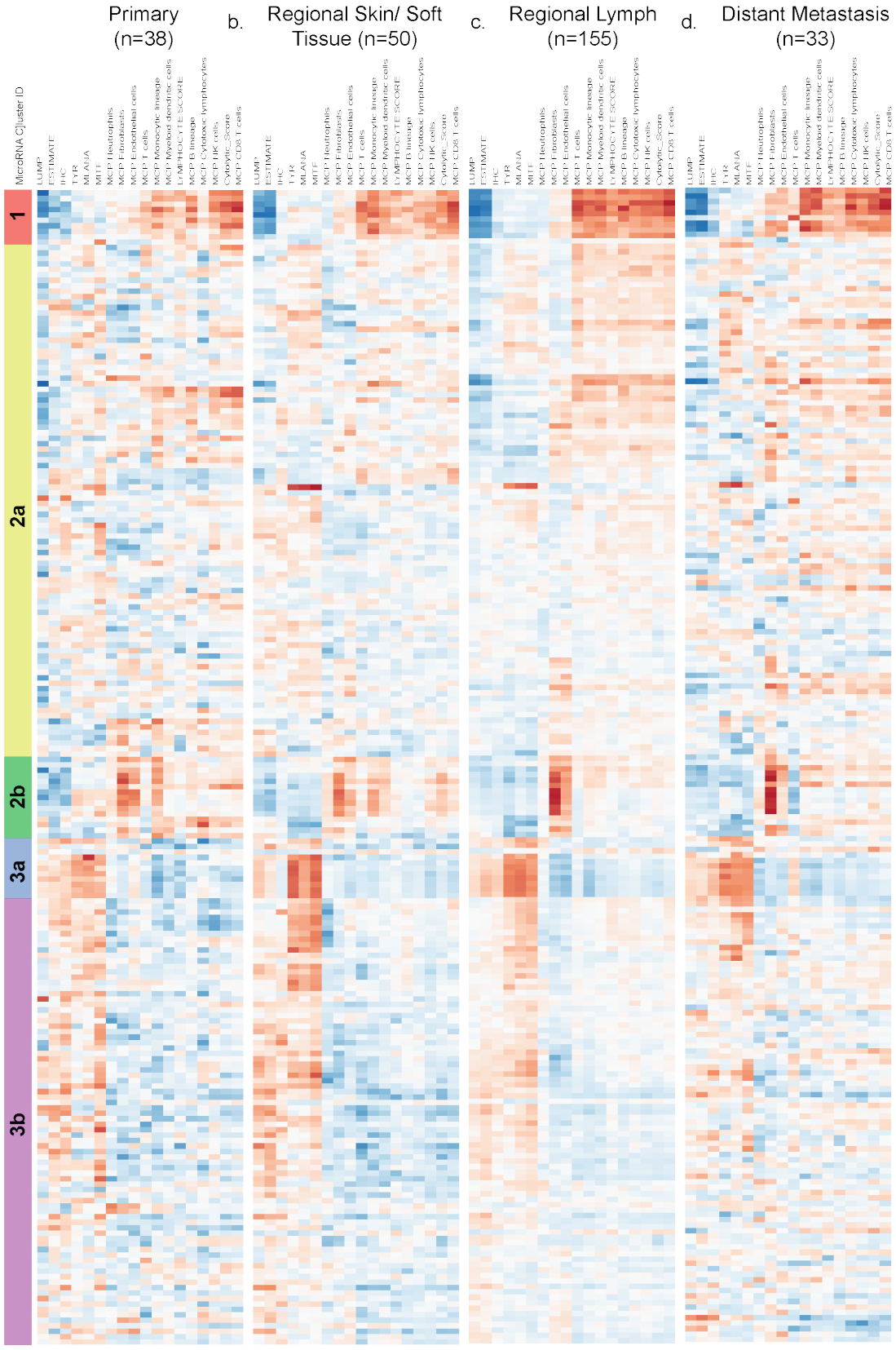

Figure 2.4 Immune:MicroRNA Relationships Maintained Across Sites of Disease We examined the relationship between TCGA microRNA expression and a panel of melanoma and immune markers across 4 different sites of disease using heatmaps with supervised clustering based on figure 2.3. (**a**) A heatmap representing Spearman's correlation coefficients between expression of each microRNA and each melanoma or immune marker measured from transcriptomic data in primary melanoma biopsies (n=38). Major microRNA clusters are denoted on the track on the left of the heatmap. (**b)** A heatmap representing Spearman's correlation coefficients between expression of each microRNA and each melanoma or immune marker measured from transcriptomic data in regional skin / soft tissue biopsies (n=50). (**c**) A heatmap representing Spearman's correlation coefficients between expression of each microRNA and each melanoma or immune marker measured from transcriptomic data in regional lymph node biopsies (n=155). (**d**) A heatmap representing Spearman's correlation coefficients between expression of each microRNA and each melanoma or immune marker measured from transcriptomic data in distant metastases (n=33).

if the variation of microenvironment compositions affected our data (Figure 2.4). In this analysis we supervised the clustering of our samples using the clusters obtained when comparing all samples (Figure 2.3). Using this approach we can compare the integrity of each microRNA cluster across disease sites. We observed that generally the clusters remained consistent despite the relatively low numbers in the primary and distant metastasis groups (n=38 and 33, respectively. We next investigated the individual microRNA membership of these clusters. In the 'Immune' cluster we noted exclusive membership of canonical immune-miRs with established roles in immune-biology such as miR-155-5p, miR-142-5p, miR-146b-5p, miR-342-3p and miR-29c-3p. Interestingly these microRNAs were also previously associated with the 'Immune' transcriptomic subset of melanoma identified in the SKCM TCGA dataset. We also identified well defined melanoma transcriptomic subset associated microRNAs in the 'Melanoma' cluster and 'Stromal' cluster. Specifically we identified miR-211-5p, miR-508, miR-509, miR-514a-3p and miR-146a-5p in the 'Melanoma' cluster which associates with the "Keratin' transcriptomic subset of melanoma and the 'MITF-low' transcriptomic subset associated microRNAs miR-100-5p and miR-125b-5p in our 'Stromal' cluster. Taken together we surmised that this methodology could effectively identify microRNAs associated with immune infiltrated melanomas, melanomas with high stromal content and high purity melanomas.

Identification of Immune-Associated MicroRNAs in Melanoma

Since immune content of melanomas has prognostic value, we hypothesized that the microRNAs with strongest associations with immune infiltration may also have prognostic values. To test this hypothesis we filtered microRNAs expressed in one hundred and

Figure 2.5 Schematic of Immuno-MicroRNA Identification in TCGA Samples. We used this work flow to define 'Immuno-MicroRNAs' as microRNAs significantly associated with at least one immune feature in TCGA melanoma samples.

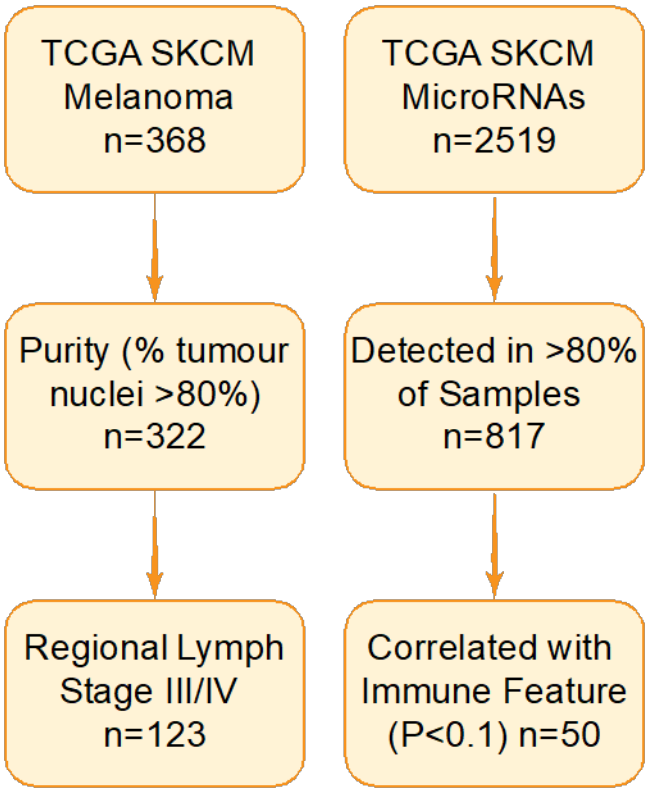

Figure 2.6 Identification of Immuno-MicroRNAs in Melanoma TCGA

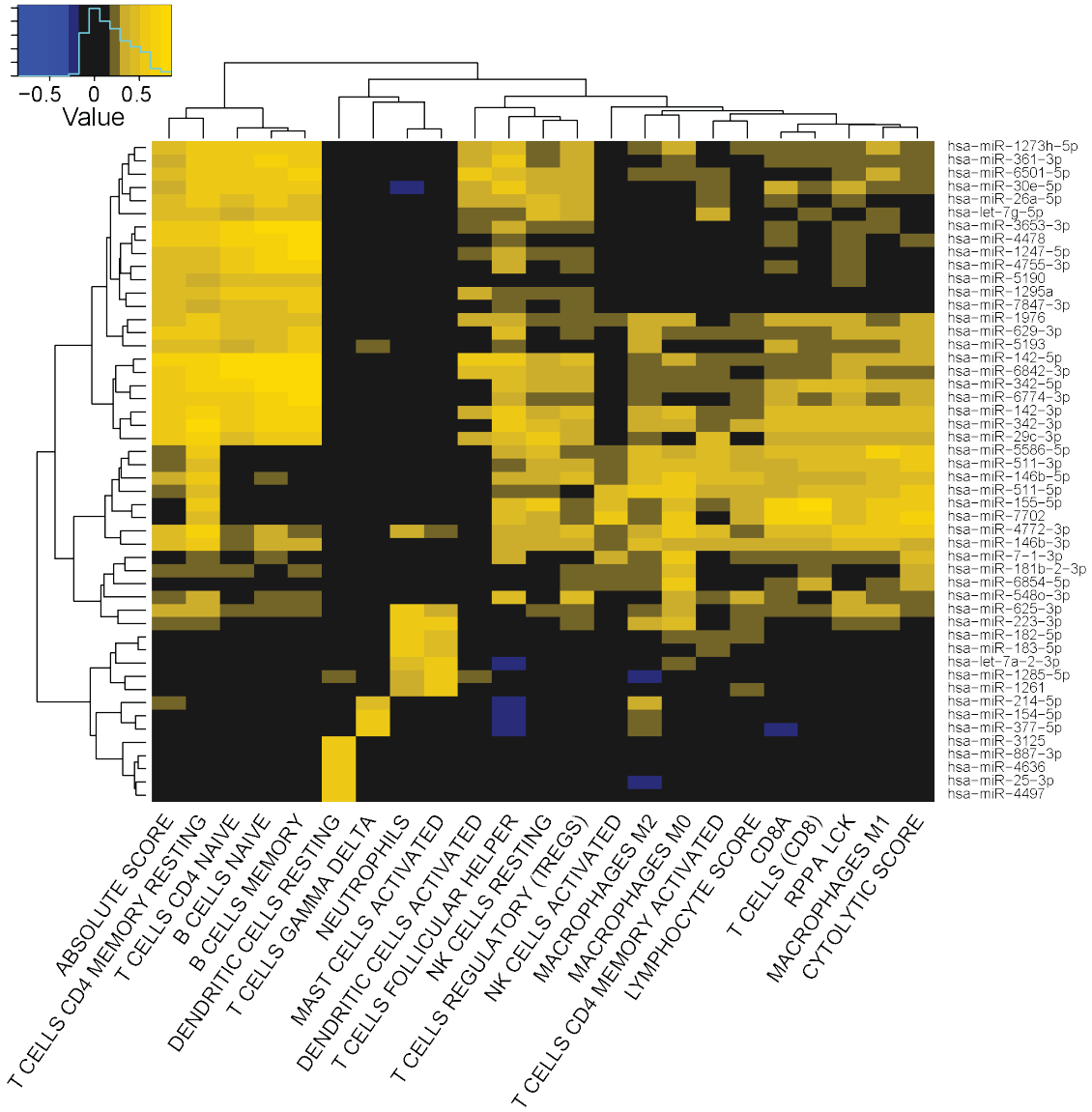

Figure 2.6. Identification of Immuno-MicroRNAs in Melanoma TCGA. We compared MicroRNA expression with 24 transcriptomic, protein and histopathological markers of immune infiltration and activation in 123 high purity regional lymph node biopsies from the melanoma TCGA. (**a**) A clustered heatmap representing 50 microRNAs with a significant association (Spearman correlation coefficient > 0.5, FDR adjusted P-value <0.1) with at least one immune marker.

twenty-three high purity, metastatic melanomas with the strongest positive and negative associations with immune markers tor additional survival analysis (Figure 2.5). Using this approach, we classified 50 out of 817 microRNAs (Spearman's rho <-0.4, >0.4, FDR adjusted p<0.1) as 'Immune- Associated MicroRNAs' (Figure 2.6). We then performed survival analysis on the 'immune-associated microRNAs using Cox's proportional hazards and Kaplan Meier survival analysis (Figure 2.7). Five out of fifteen (10%) microRNAs had a statistically significant association (log-rank p<0.05) with overall survival in regional lymph node TCGA melanoma samples. Of these, the microRNA with the strongest association with overall survival was miR-146b-3p (hazard ratio = 0.22 (95% CI = 0.1-0.46), log-rank p-value <0.0001), which is a stronger prognostic power than the best immune marker (LCK hazard ratio = 0.28). The other four microRNAs were miR-155-5p, miR-1976, miR-361-3p, miR-142-3p (Hazard ratio, log-rank p-value; 0.39, 0.0017; 0.32, 0.0059; 0.35, 0.04; 0.44, 0.047 respectively).

Identification of Validated Targets of Immune-MicroRNAs with Known Roles in Melanoma Immuno-Biology

To identify rational and testable mechanisms that could potentially explain the association of our microRNAs with immune infiltration or exclusion, we first filtered microRNAs based on their expression in a panel of 62 melanoma cell lines followed by searching for previously experimentally validated targets with known roles in melanoma immune-biology. Having identified fifty 'immune-associated' microRNAs we stratified them based on their expression in melanoma cell lines versus melanoma tissue. The rationale for this was the hypothesis that melanoma-specific microRNA regulation of gene expression could modulate immune infiltration, for example through cytokine secretion, and we wanted to

Figure 2.7 TCGA SKCM IMMUNE MICRORNA : KAPLAN MEIER & HAZARD RATIOS

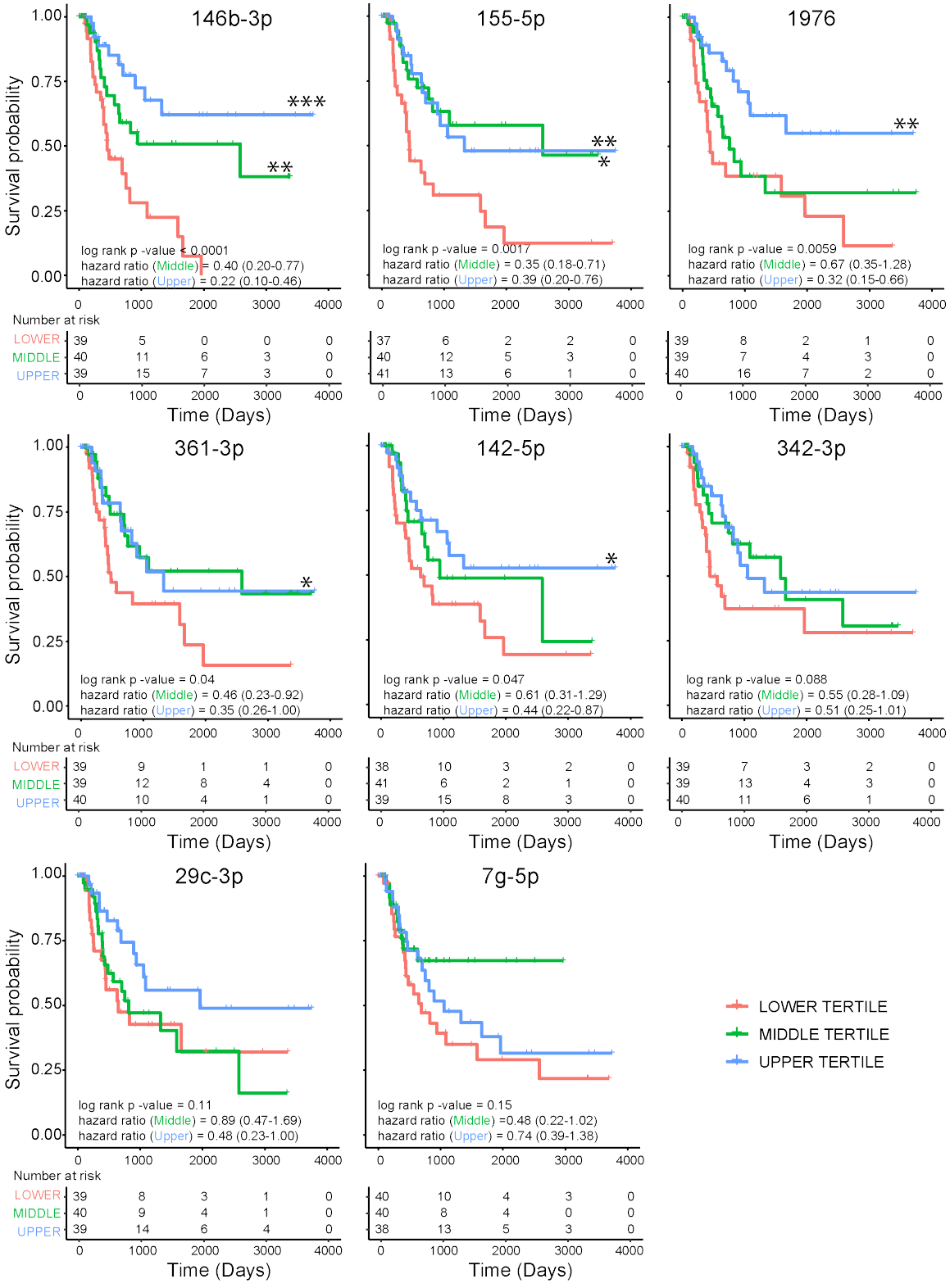

Figure 2.7 Immuno-MicroRNA Expression Associated with Improved Overall Survival in TCGA Melanoma Patients. We measured survival outcomes in TCGA melanoma patients based on the expression of immune-associated microRNAs in their tumours. (**a**) Kaplan Meier curves for each microRNA displaying curves for samples divided into tertiles based on expression of each microRNA, using time to death as the event value. Log rank p-value and hazard ratios ± 95% confidence intervals are shown for upper and middle tertiles compared to lower tertile in each plot. * represents P-value < 0.05, ** represents P-value < 0.01, *** represents P-value <0.001, compared to the lowest tertitle in each plot.

separate these microRNAs from the microRNAs that are predominantly expressed in the infiltrating immune cells that arise as a consequence rather than a cause of inflammation (Figure 2.3 b-d). Using this approach we identified fourteen microRNAs with 1 or more experimentally validated immune targets, among these there were 9 microRNAs with 1 or more experimentally validated immune target that had been directly implicated or had a rational connection to mechanisms of melanoma immune evasion (Table 2.1).

MiR-508-3p Regulation of NF-kB and Downstream Immune Modulatory Genes

Of the microRNAs with validated immune targets, the first that we investigated was miR-508-3p, which was associated with lower immune infiltration and lower scores of immune cytotoxicity in the TCGA SKCM dataset, suggesting an immunosuppressive effect on the tumor microenvironment. The interaction between hsa-miR-508-3p and the NF-κB genes NFKB1 and RELA has been described previously in gastric carcinoma, including the modulation of downstream NF-κB target genes [155]. NF-κB signaling regulates a large number of immunomodulatory genes and is the leading candidate to explain the immunosuppressive phenotype associated with hsa-miR-508-3p. Our first experiment to test if miR-508-3p regulated NF-kB activity was an in-silico analysis of miR-508-3p correlation with NF-kB target genes, using the target genes of non miR-508-3p targeted transcription factors STAT1 and MYC as negative controls (Figure 2.8 a). In this analysis we observed a slight but statistically significant ($p=0.0009$) inverse correlation of NF-kB target genes compared to negative controls, indicating that melanomas with higher miR-508-3p expression have less NF-kB activity. To test if the reported miR-508-3p repression of NF-kB existed in melanoma, we measured NF-kB protein expression by Western blot after transient transfection of a melanoma cell line (MDA 2333) with a miR-508-3p mimic

miR name	Validated targets	Immune genes	Notable genes
hsa-miR-17-5p	3335	51	TNF, CCL1, TGFB1, VEGFA, STAT3
hsa-miR-20a-5p	3067	42	CCL1, VEGFA
hsa-miR-92a-3p	3345	43	CCL8, HLA-E, NFKB1
hsa-miR-93-5p	2501	76	CCL1, HLA-A, VEGFA, TGFB1
hsa-miR-29a-3p	1394	53	VEGFA, TGFB2, RELA
hsa-miR-29b-3p	1292	24	VEGFA, TGFB1, TGFB2, IFNG
hsa-miR-29c-3p	1255	6	
hsa-miR-506-3p	221	4	
hsa-miR-508-3p	59	1	NFKB1, RELA
hsa-miR-509-3p	82	2	HLA-A
hsa-miR-513b-5p	248	2	
hsa-miR-514a-3p	105	2	
hsa-miR-155-5p	1395	68	IL6, IL10, IL2, TNF, CCL2
hsa-miR-342-3p	837	31	

Table 2.1 Identification of Validated Targets of 'Immuno-MicroRNAs' With Known Roles in Melanoma Immuno-Biology. We compared the validated targets of microRNAs identified in Figure 2.6 in MiRTarBase. The number of validated targets with an immune ontology are counted and specific genes with published roles in melanoma immunity are listed.

Figure 2.8 MiR-508 is Associated with Reduced Expression of NFkB Target Genes and Inhibits Secretion of IL-6 in Melanoma Cell Lines

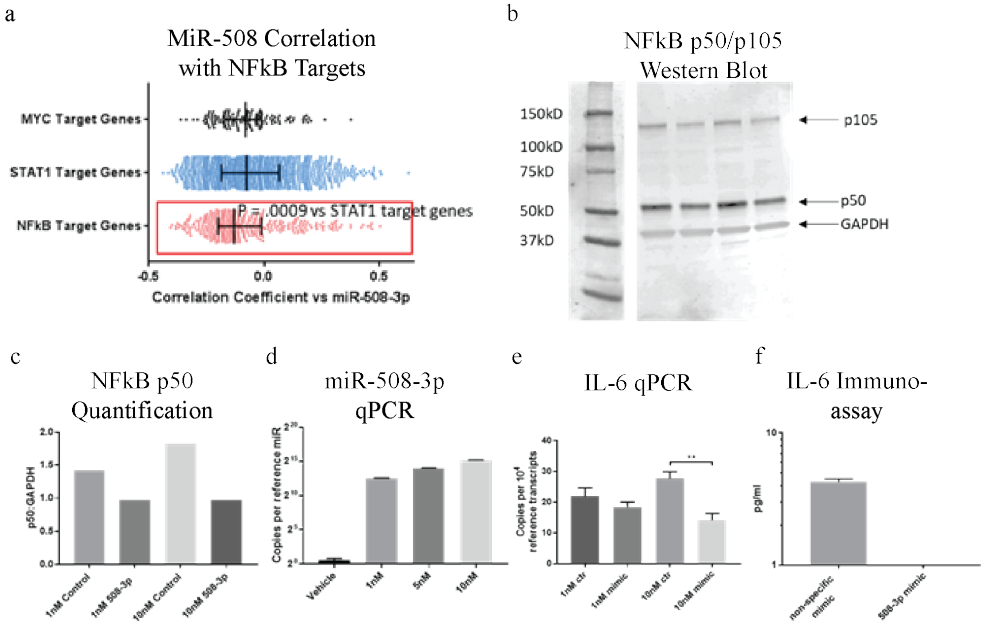

Figure 2.8 MiR-508 is Associated with Reduced Expression of NFkB Target Genes and Inhibits Secretion of IL-6 in Melanoma Cell Lines. We tested the effect of miR-508-3p expression on NFkB and NFkB target gene expression in melanoma. (**a**) Dotplot representing Spearman's correlation coefficients of miR-508-3p with curated gene-sets representing the transcription targets of the NFkB, MYC and STAT1 in TCGA melanoma. (**b**) Western blot showing NFkB p50/p105 staining and GAPDH loading control. Samples from left to right are 1nM non-specific miR mimic, 1nM miR-508-3p mimic, 10nM non-specific miR mimic, 10nm miR-508-3p mimic. (**c**) Barplot representing intensity of NFkB p50 staining relative to GAPDH in each sample. (**d**) Barplot representing copies of miR-508-3p relative to reference miR in MDA2333 melanoma cells measured by qPCR after transfection with different doses of miR-508-3p mimic. (**e**) Barplot representing copies of IL-6 mRNA transcripts relative to reference gene in MDA2333 melanoma cells after transfection with different doses of miR-508-3p mimic. (**f**) Barplot representing levels of secreted IL-6 from conditioned media from MDA2333 cell line cultures after transfection with non-specific microRNA mimic and miR-508-3p mimic.

(Figure 2.8 b,c). When we quantified NF-kB protein levels we observed reduced NF-kB p50:GAPDH ratios with both 1nM and 10nM doses of miR-508-3p mimics compared to non-specific mimic controls (0.94 vs 1.41, 0.97 vs 1.76 respectively). Of the many NF-kB targets, we selected IL-6 as a strong candidate for melanoma regulation of the immune microenvironment. We subsequently tested our melanoma cell line for IL-6 mRNA expression by qPCR and found a significant reduction after transfection with 10nM miR-508-3p mimic compared to 10nM non-specific mimic treated cells ($p<0.01$) (Figure 2.8 e). In addition we tested IL-6 protein secretion in conditioned media from melanoma cell lines under the same transfection conditions (Figure 2.8 f). Taken together these data suggest that miR-508-3p negatively regulates NF-kB expression and function in melanoma, and protein expression of downstream NF-kB transcription targets such as IL-6 can be regulated by miR-508-3p modulation.

MiR-509-3p Modulates Expression of HLA Expression in Melanoma

The next microRNA of interest that we investigated *in vitro* was miR-509-3p. Similarly to miR-508-3p, miR-509-3p was inversely correlated with expression of immune markers in melanoma, and in HLA had a feasible mechanism of action to elicit an immunosuppressive phenotype. For this microRNA we measured HLA-ABC expression by flow cytometry in a panel of four melanoma cell lines after transient transfection with miR-509-3p mimic (Figure 2.9). We observed significant repression of HLA expression in two out of four miR-509-3p mimic treated cell lines compared to non-specific mimic treated cells ($p<0.001$).

Multiple Immune-Associated MicroRNAs Modulate Cytokine Secretion In Vitro

Figure 2.9 Exogenous Expression of MiR-509 Downregulates HLA Expression in 2/4 Melanoma Cell Lines.

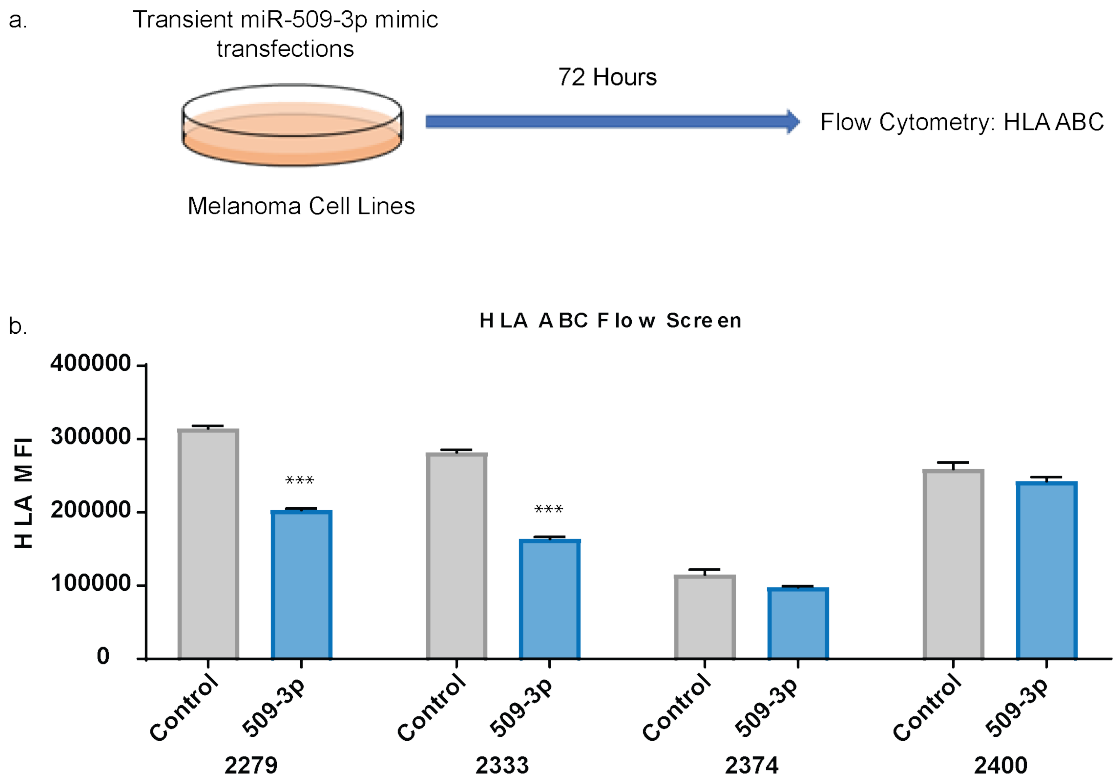

Figure 2.9 Exogenous Expression of MiR-509 Downregulates HLA Expression in 2/4 Melanoma Cell Lines. We transiently transfected the melanoma cell line MDA 2333 with miR-509-3p to test it's effect on HLA expression, previously validated as a miR-509-3p target. (**a**) Schematic of experimental design, transfected cells allowed 72 hours for exogenous microRNA effects to manifest. (**b**) Boxplot representing median fluorescence intensity of HLA-ABC antibody staining in multiple melanoma cell lines after transient transfection with either a non-specific microRNA mimic or miR-509-3p mimic. *** represents p-value < 0.001

Figure 2.10 Exogenous Expression of Immune Associated Melanoma MicroRNAs Regulate Secretion of Immuno-regulatory Cytokines

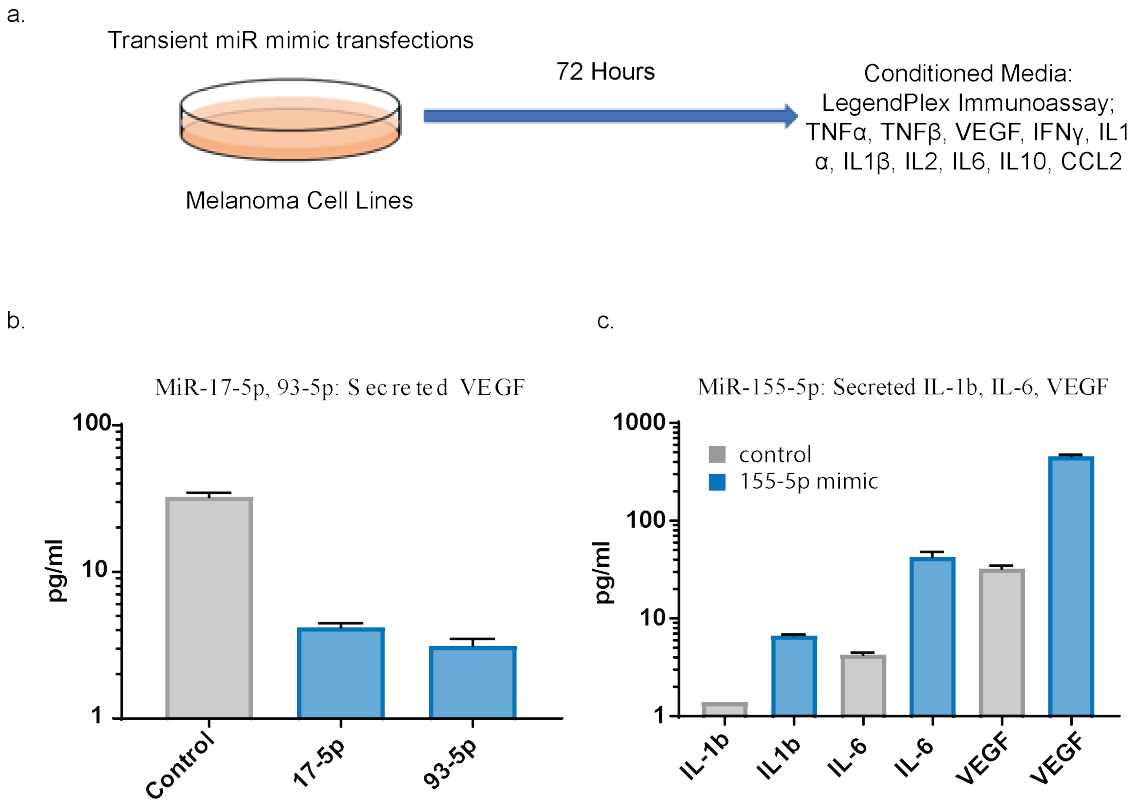

Figure 2.10 Exogenous Expression of Immune Associated Melanoma MicroRNAs Regulate Secretion of Immuno-regulatory Cytokines. We transiently transfected the melanoma cell line MDA 2333 with immune-associated microRNAs miR-17-5p, 93-5p and 155-5p to test their effects on secretion of previously validated cytokine targets. (**a**) Schematic of experimental design, transfected cells allowed 72 hours for exogenous microRNA effects to manifest. (**b**) Boxplot representing duplicate immunoassay quantification of secreted VEGF in conditioned media from transiently transfected cells with either a non-specific microRNA mimic or miR-17-5p or miR-93-5p mimic. (**c**) Boxplot representing duplicate immunoassay quantification of secreted IL-1b, IL-6 and VEGF in conditioned media from transiently transfected cells with either a non-specific microRNA mimic or miR-155-5p.

Having demonstrated the potential for immune associated microRNAs to modulate immunomodulatory genes in vitro we tested three additional microRNAs with experimentally validated cytokine targets. We selected miR-17-5p, miR-93-5p which are both reported to target VEGF and miR-155-5p which is reported to target Suppressor of Cytokine Signaling 1 (SOCS1) and measured cytokine release by multiplex immunoassay (Figure 2.10) In both miR-17-5p and miR-93-5p mimic treated melanoma cell culture we observed reduced secretion of VEGF compared to non-specific mimic transfected cells. In miR-155-5p mimic treated cells we observed a dramatic increase in secretion of IL-1b, IL-6 and VEGF.

MiR-155 Regulates Melanoma Cell Sensitivity to T-cell Killing In Vitro

Finally, we selected miR-155-5p, due to its dramatic in vitro effect on cytokine secretion, for further immune analysis. We used a chromium release assay to measure melanoma cell death after co-culture with MART-1 specific T-cells to measure specific T-cell killing of melanoma cells (Figure 2.11). We demonstrated specificity for MART-1 positive, HLA-matched cell lines, with cell death only observed in cell lines that were MART-1 positive and HLA-02 positive. Cell lines that were either MART-1 negative or HLA mismatched were not affected. We tested four MART-1, HLA-02 positive melanoma cell lines, either transfected with a miR-155-5p mimic or inhibitor compared to non-specific mimics and inhibitors and found a significant protective effect i.e. reduced cell death when cells were treated with miR-155-5p mimics, in Mel526, MDA2333, MDA2400 and MDA2508 ($p=0.01$, <0.0001, <0.0001, <0.0001 respectively).

Figure 2.11 Exogenous Expression of miR-155-5p Regulates Melanoma Cell Sensitivity to T-Cell Killing In-Vitro

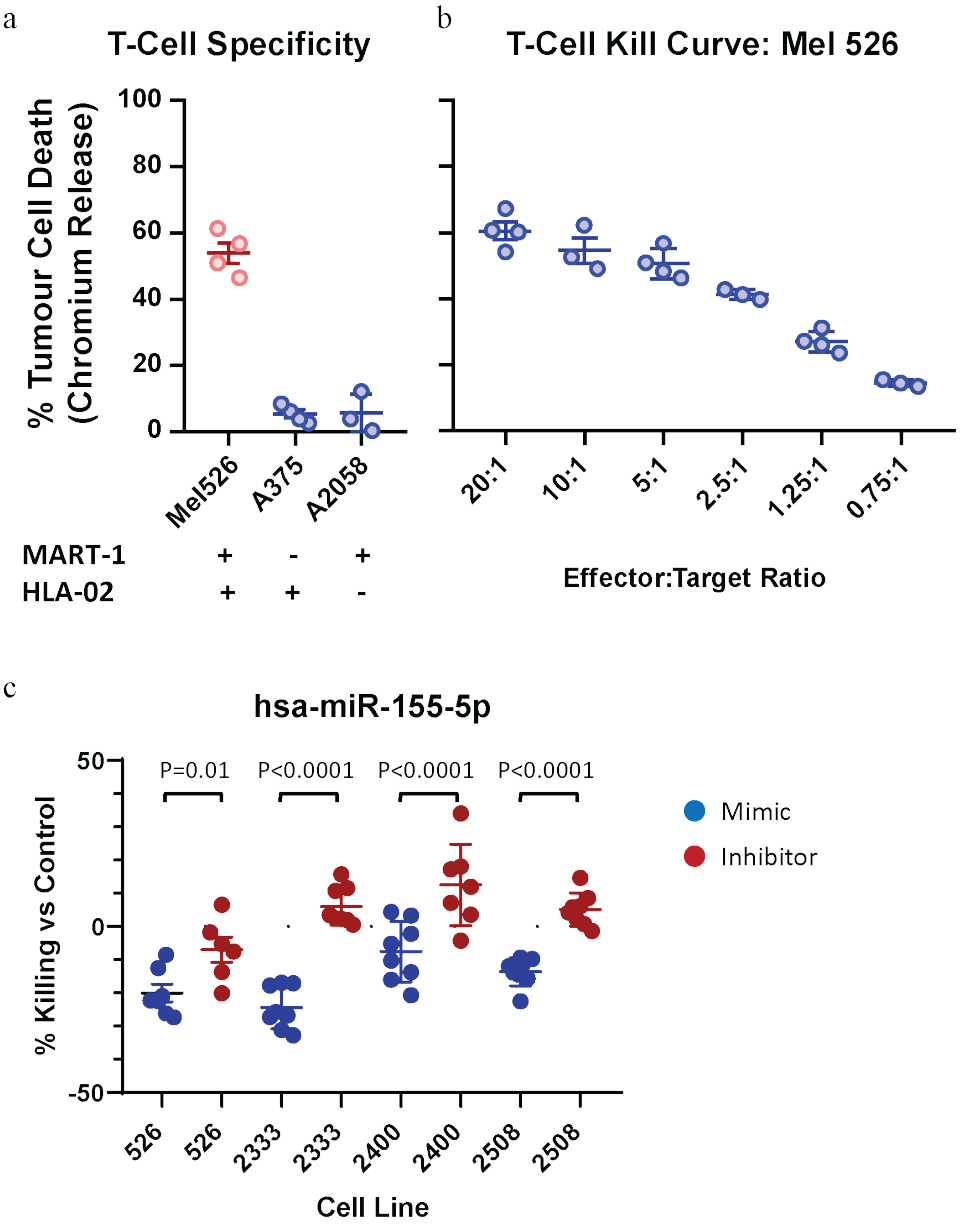

Figure 2.11 Exogenous Expression of Immune Associated Melanoma MicroRNAs regulate Melanoma Cell Sensitivity to T-Cell Killing In-Vitro. We performed T-cell killing assays on a panel of 4 melanoma cell lines with transient transfection of miR-155-5p mimic and inhibitor to determine the effect of miR-155-5p expression on sensitivity of melanoma cells to T-cell killing. (**a**) Dotplots representing % tumor cell death of positive controls, Mel256 (HLA matched and positive for T-cell cognate antigen – MART1), and negative controls, A375 and A2058 (MART-1 negative or HLA mismatched) (**b**) Dotplot representing % mel526 cell death under different effector : target cell ratios (**c**) Dotplot representing relative % melanoma cell death versus transfection control for each cell line when transfected with either miR-155-5p mimic or inhibitor.

SUMMARY

We have completed a detailed description of the immune composition of metastatic melanoma tissue using a selection of bioinformatics tools based on mRNA sequencing data. We showed that the proportions of different immune populations as estimated by CIBERSORT were relatively stable across disease sites, although absolute immune content was increased in lymph node biopsies. Expression of certain transcriptomic markers including the cytolytic score and total CIBERSORT scores were shown to have prognostic value when measuring overall survival of melanoma patients, although this was not as powerful as LCK protein expression.

We were able to identify 50 microRNAs whose expression were significantly correlated with the abundance of at least one measured immune feature of melanoma tumors. Amongst these 50 immune-associated microRNAs we identified 5 that had significant prognostic value, including miR-146b-3p which outperformed LCK protein expression based on a univariate Cox's-proportional hazard model. There are limitations of this model including the assumption of proportional hazard over time but also making direct comparisons of hazard ratios determined in separate univariate models. Additional statistical analysis including multivariate Cox's proportional hazard models and also parametric survival models would be desirable for a more robust validation of these markers as prognostic biomarkers.

We then sought to elucidate any immune-modulatory mechanisms that these microRNAs may regulate in melanoma. We identified 14 microRNAs with previously validated immune targets. Of these we selected miR-508-3p (Targets NF-kB), miR-509-3p (Targets HLA-A), miR-17-5p (Targets VEGF), miR-93-5p (Targets VEGF), miR-155 (Targets

SOCS1) for further investigation. In each case we were able to show microRNA regulation of their respective targets. In the case of miR-155-5p we were able to dramatically increase secretion of IL-1b, IL-6 and VEGF *in vitro* through exogenous expression of miR-155-5p. Exogenous expression of miR-155-5p also had a profound protective effect against T-cell killing.

CHAPTER THREE

MICRORNA AND mRNA PROFILING OF PRE-PD1 INHIBITOR TREATED MELANOMA BIOPSIES

ABSTRACT

Immunotherapy has dramatically improved the outcome for many melanoma patients, however, approximately half of patients do not receive durable responses. The mechanisms of resistance to immunotherapy are only partly understood and effective therapies to overcome them are urgently required.

MicroRNAs are major post-transcriptional regulators of gene expression and the aberrant expression and activity of microRNAs is involved in multiple oncogenic processes. In melanoma, these processes include proliferation, resisting cell death and activation of invasion and metastasis. There is also evidence that microRNAs can also regulate the tumor microenvironment and response to immunotherapy. To date, this has not been extensively studied in humans and could reveal important mechanisms of immune evasion that could be targeted therapeutically.

In this chapter we performed a genomic analysis of pre-PD1 treated melanoma biopsies to identify transcriptomic profiles associated with response. We also quantified microRNA expression from the same biopsies to identify microRNA profiles associated with response to therapy and also their relationship with transcriptomic profiles of response.

INTRODUCTION

Response to anti-PD-1 immunotherapy is determined by a complex relationship between tumor cells, the tumor microenvironment (TME) and the host immune system. Several transcriptomic studies of PD-1 treated melanoma patients have already been published and have revealed distinct gene expression profiles associated with patients who responded to therapy [90, 92, 156-160]. Transcriptomic analyses of melanoma tumors prior to anti-PD-1 treatment have identified gene expression signatures that predict responder and non-responder patients with better accuracy than single biomarkers. Understanding the mechanisms that regulate response-associated transcriptomic profiles are therefore of significant clinical interest, as they may offer novel biomarker and therapeutic approaches to overcoming resistance.

MicroRNAs are key regulators of gene expression and are associated with disease progression and drug resistance in multiple cancer types including melanoma. We therefore hypothesized that microRNAs may be associated with immune evasion via their regulation of gene expression and that this would be measurable in melanoma biopsies from patients undergoing anti-PD-1 immunotherapy.

In this study, we performed genomic analysis of pre-treatment tumor samples from patients treated with anti-PD-1 immunotherapy and identified two transcriptionally distinct subgroups associated with clinical response. Further characterization of the two groups using miRNA sequencing revealed novel miRNAs associated with response. Additionally,

we also performed analyses mapping mRNA:microRNA interactions in the TME and their associations with response to PD-1 treatment.

RESULTS

Patient Cohort:

Twenty-nine patients with AJCCv8 stage III or IV melanoma undergoing PD-1 immune checkpoint blockade at the University of Texas MD Anderson Cancer Center were included in this study (Table 3.1). All patients had cutaneous-type or unknown primary melanoma. Twenty (67%) patients were male, nine (31%) patients were female. Seventeen (59%) patients had progressed on prior ipilimumab treatment. Pre-treatment biopsies were consented and collected under institutional-review-board-approved protocols [2012-0846 and LAB00-063] no more than 6 months prior to commencement of pembrolizumab or nivolumab therapy and with no intervening therapy or documented continuous progression during a brief period of intervening therapy. Best Overall Response (BOR) was calculated using RECIST 1.1 criteria. Fourteen (48%) patients were classified as receiving clinical benefit (BOR; stable disease >6months, complete or partial response), while Fifteen (52%) patients were classified as not receiving clinical benefit (BOR; progressive disease). Measured Median Progression-Free Survival (PFS) in the non-responder group was 83 days (range; 20-NA), median PFS was not reached in the responder group (range; 257-NA). Lesion specific responses were available for thirteen (45%) patients where incisional biopsies were performed (Figure 3.1, Table 3.1).

Unsupervised Clustering Identifies Response-Associated Transcriptomic Profiles

Figure 3.1. Schema of Pre-PD1 Treatment Melanoma Cohort

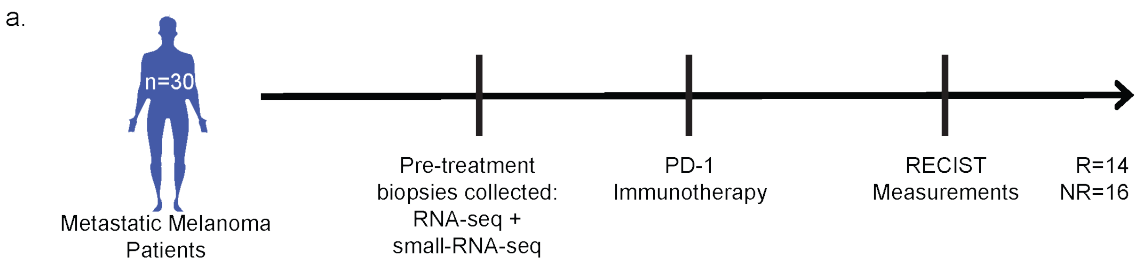

Figure 3.1. Schema of Pre-PD1 Treatment Melanoma Cohort. We collected melanoma specimens from 30 patients before they started anti-PD-1 checkpoint blockade for molecular analysis. (a) Schema showing the study design, with collections and RNA-sequencing of pre-treatment biopsies prior to treatment with anti-PD1 checkpoint blockade.

Table 3.1 Pre-PD1-Treated Melanoma Patient Characteristics

Characteristic	PD-1i No Clinical Benefit	PD-1i Clinical Benefit
RNA sequencing	14	15
Small RNA sequencing	9	13
Sex		
Male	12 (86%)	9 (56%)
Female	2 (14%)	7 (44%)
Melanoma Type		
In situ	-	-
Cutaneous unspecified	6 (43%)	7 (44%)
Superficial spreading	1 (7%)	2 (13%)
Lentigo malignant melanoma	-	-
Nodular	1 (7%)	2 (13%)
Acral lentiginous	1 (7%)	1 (6%)
Mucosal	-	-
Unknown primary	5 (36%)	2 (13%)
Disease stage (AJCCv8)		
IIIa/b	1 (7%)	-
IIIc/d	3 (21%)	2 (13%)
IVa	-	2 (13%)
IVb	-	1 (6%)
IVc	10 (71%)	11 (69%)
IVd	-	-
Serum LDH (U/L; Median, Range)	528.5 (349-1786)	432 (78-1090)
Prior ipilumumab		
Yes	7 (50%)	11 (69%)
No	7 (50%)	5 (31%)
Best Overall Response (BOR, RECIST 1.1)		
CR	6 (43%)	-
PR	6 (43%)	-
SD	2 (14%)	-
PD	-	16 (100%)
PFS (median, range; days)	1205 (257-1644)	80.5 (20-90)

We first sought to identify transcriptomic profiles associated with response to anti-PD-1 treatment using RNA-sequencing (RNA-seq) on biopsies from pre-PD1-treatment melanoma patients. We first used consensus clustering to determine optimum unsupervised clustering of all samples, based on expression of the 1500 most variable genes (Figure 3.2). We generated consensus clustering matrices for a range of cluster solutions (k=2-6) to find the optimum number of mRNA clusters in the dataset (Figure 3.2 a-e). To quantify the accuracy of the different clustering solutions we measured cumulative distribution functions (CDF) of each consensus matrix (Figure 3.2 f-g). It is apparent that each increase in the number of clusters incrementally increases the CDF of the consensus matrix although there are diminishing returns with each additional cluster, there is still no obvious inflection point that would definitively guide our choice of an optimal clustering solution. Indeed with the 6 cluster solution two of the clusters only include individual samples, indicating the granularity that is resolved by the consensus clustering is to the level of inter sample variability rather than shared transcriptomic characteristics of multiple samples. This paradigm is highlighted in the tracking plot indicating cluster membership of each sample across clustering solutions (Figure 3.2 h). The two-cluster model using this method effectively separated responding and non-responding patients: Cluster 1 containing 12/14 clinical benefit patients and cluster 2 containing 11/15 non-clinical benefit patients (Figure 3.3, Notably, these samples clustered independently of melanoma subtype (p=0.825), gender (p=0.688) and receipt of previous immunotherapy (p=0.13) (Table 3.1) Increasing the number of clusters increased the Area Under the Curve (AUC) of the Cumulative Distribution Function (CDF) curves (K2 = ~0.5, K4 = ~0.9) but the additional clusters did not further separate samples by response or melanoma subtype and due to low numbers

Figure 3.2 Consensus clustering of RNA-sequencing data

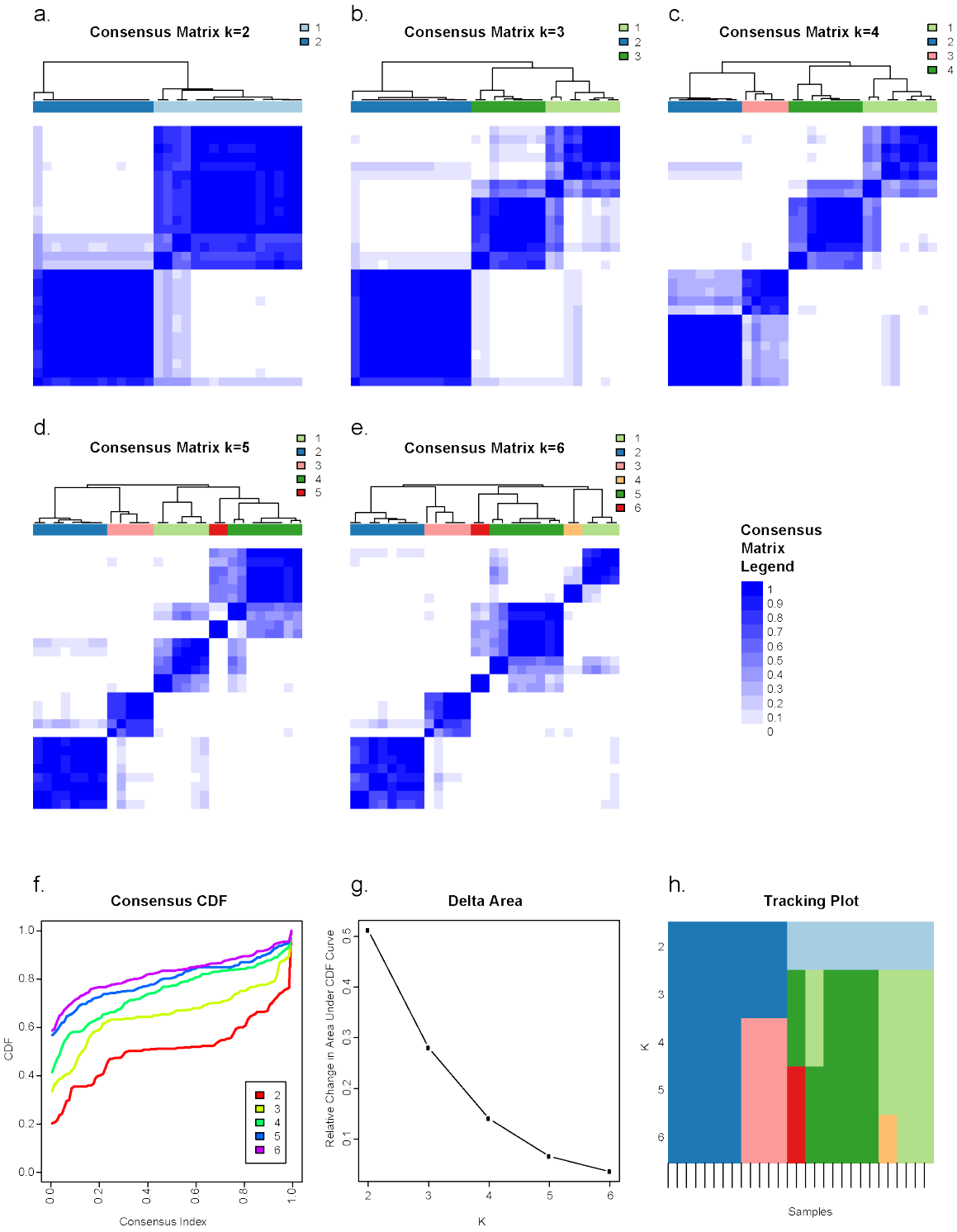

Figure 3.2. Consensus Non-Negative Matrix Factorization Clustering of Pre-PD-1 Treated Melanoma RNA-seq Samples. We used non-negative matrix factorization to identify unsupervised transcriptomic subsets within our RNA-seq dataset. (**a-e**) cNMF clustering of all samples using the 1500 genes with highest standard deviation for k=2 to k=6. (**f**) Plot of the cumulative distribution function (CDF) curves or each clustering solution k2:k6. (**g**) Plot representing the change in the area under the curve of each CDF curve in f, with each additional k. (**h**) Tracking plot showing the cluster membership of each sample (x-axis) for each k clustering solution (y-axis).

Figure 3.3 Characterisation of pre-PD1 Treatment Biopsies

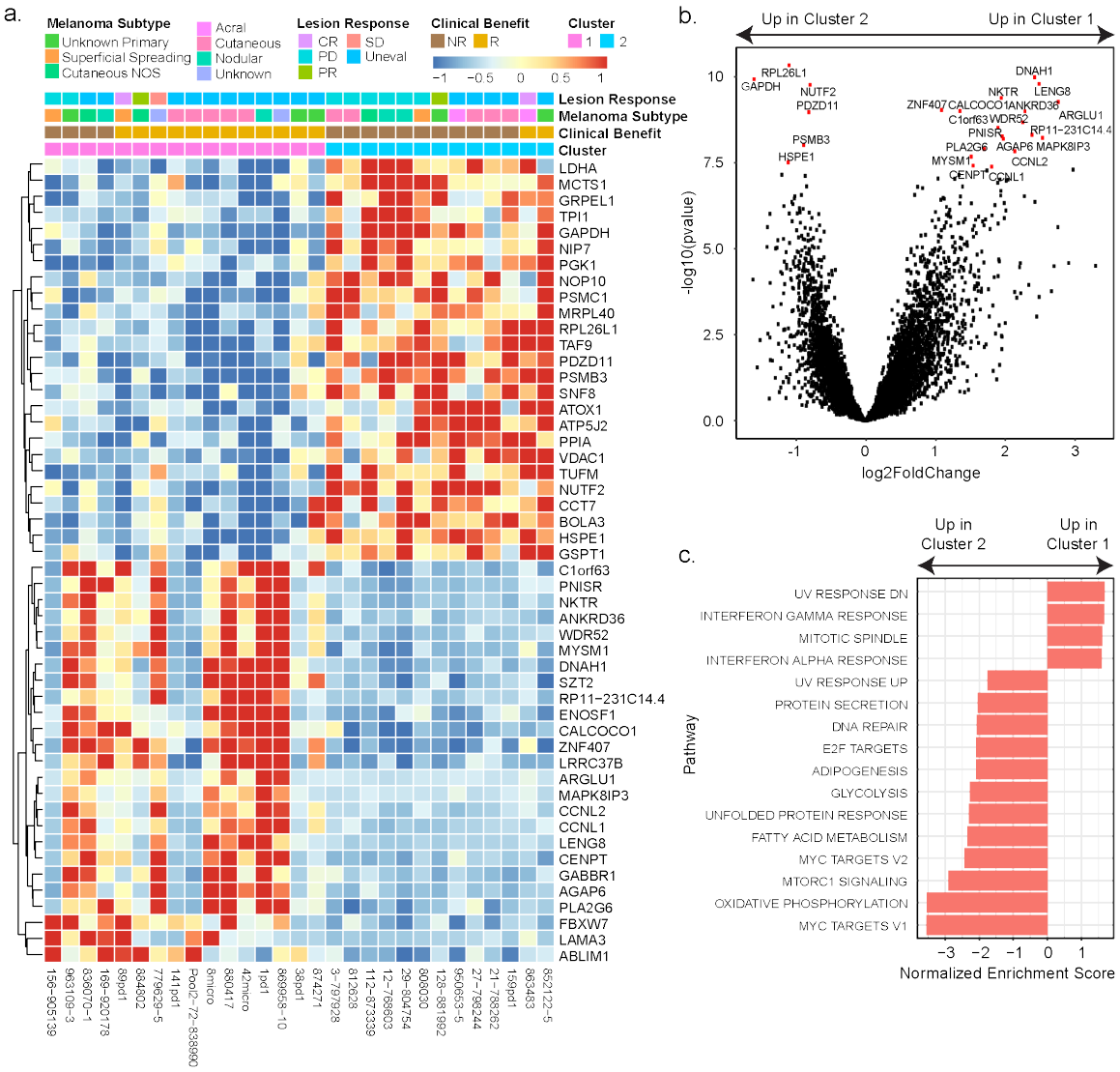

Figure 3.3 Characterisation of pre-PD1 Treatment Melanoma Biopsies. We collected melanoma biopsies from 30 pre-PD1 treated melanoma patients. (**a**) A clustered heatmap representing the 50 genes with the most significant differential gene expression differences between mRNA 'Cluster 1' and 'Cluster 2' as identified by consensus non-negative matrix factorisation (25 highest in 'Cluster 1' and 25 highest in 'Cluster 2'). Values displayed are gene-normalized Z-scores. Tracks above heatmap display sample information including the mRNA cluster memebership, clinical benefit, lesion-specific response and melanoma subtype. (**b**) A volcano plot displaying all DESEQ2 differential expression results from mRNA sequencing, plotting log2-foldchange against negative log10 p-values. Top differentially expressed genes are coloured red and labeled with gene names. (**c**) Hallmark Gene-Set Enrichment Analysis (GSEA) of differentially expressed genes identified by DESEQ2 with a normalized enrichment score >1.5 identifies enrichment of 4 genesets in mRNA cluster 1 (associated with improved clinical benefit) and 12 genesets in mRNA cluster 2 (associated with reduced clinical benefit).

would reduce the power of additional analysis. We were able to measure lesion specific-responses for 13 incisional biopsies. Since response to immunotherapy can be heterogeneous and sampling from individual lesions may not be representative of the whole disease, we compared the lesion specific response with the overall response and plotted those with our heatmap of gene expression analysis (Figure 3.3 a). Of the lesion specific-responses these only one had a mismatched classification where the lesion responded differently to the overall disease course. In order to further explore the biological significance of the two clusters we had identified we compared differential gene expression between the clinical benefit and non-clinical benefit clusters, identifying 641 genes with an FDR adjusted p-value <0.1. To explore the biological significance of the differential gene expression we performed Gene set enrichment analysis (GSEA) of these 641 significantly differentially expressed genes. This identified 4 gene sets enriched in the Responder cluster (FDR<0.001), including Interferon Gamma Response and Interferon Alpha Response, indicative of a functioning host immune reponse, while the Non-Responder cluster was enriched for 12 gene sets (FDR <0.001), including MYC and E2F transcription factor targets, Oxidative Phosphorylation and DNA repair genes (Figure 3.3 c).

Response-Associated Clusters Enriched for Immune Markers

As response to immunotherapy is closely related to pre-existing immune features of the TME, we measured the levels of immune markers in our samples and compared expression across our response-associated clusters. We calculated the cytolytic score, the immune-predictive score (IMPRES), and estimates of the cellular composition of our samples from transcriptome data using MCP counter (Figure 3.4 a -d)[153, 160, 161]. Of these markers,

Figure 3.4 Immune Features of pre-PD1 Treatment Biopsies

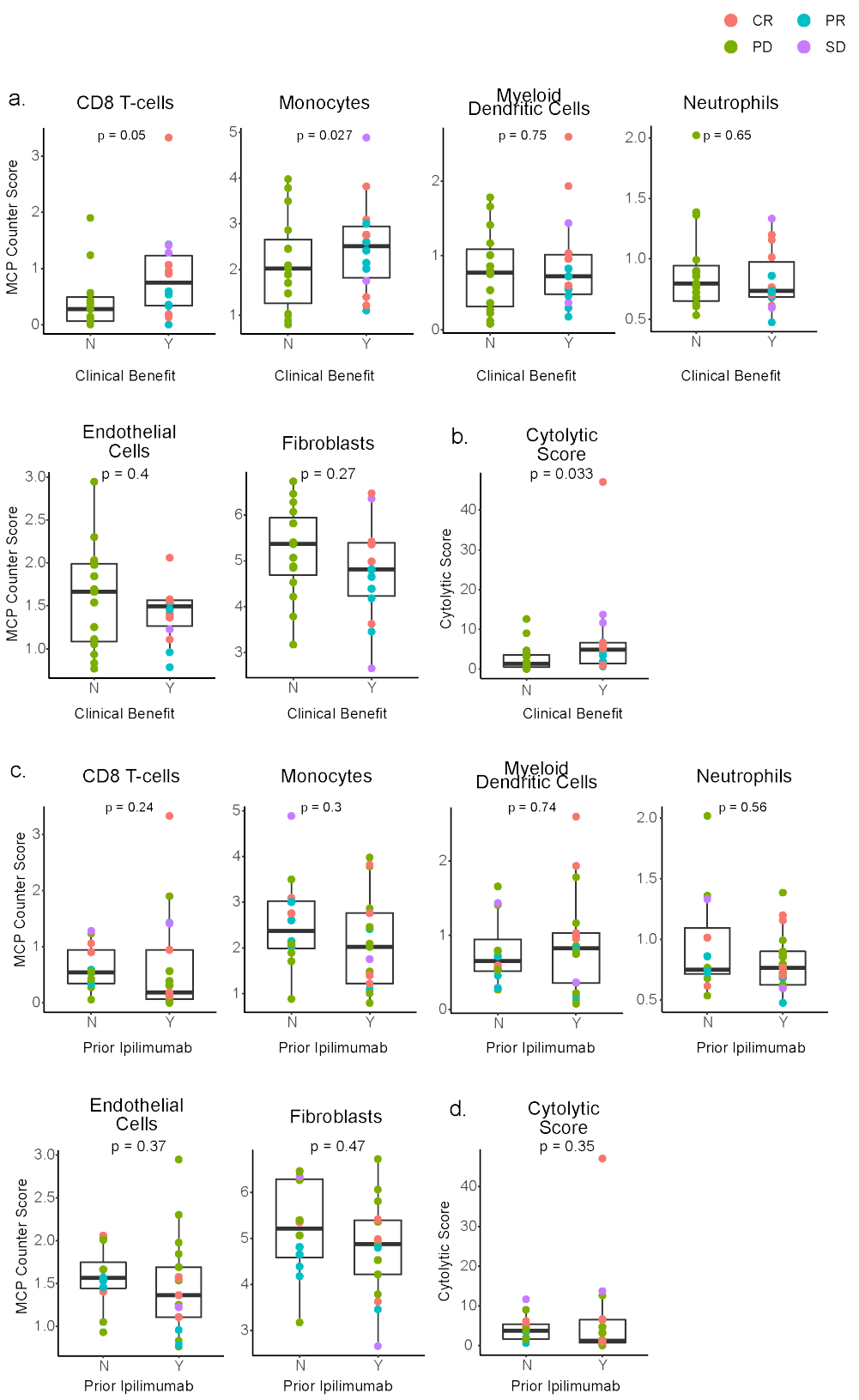

Figure 3.4 Immune Characterisation of Pre-PD-1 Treated Melanoma Biopsies. We calculated immune scores based on transcriptomic expression data for each sample with MCP counter and cytolytic scores based on Perforin 1 and Granzyme A expression. (**a**) Expression of MCP counter microenvironment cell composition estimates compared between biopsies from patients who did or did not receive clinical benefit from anti-PD-1 checkpoint blockade. (**b**) Expression of tumour cytolytic scores compared between patients who did and did not receive clinical benefit from anti-PD-1 checkpoint blockade. We also compared MCP counter scores (**c**) and cytolytic scores (**d**) between patients who had or had not received prior ipilimumab therapy to test the effect of a prior immunotherapy on the composition of the immune microenvironment.

Data points are colour coded by individual patient response and groups are compared using Wilcoxon's rank-sum test.

there was significant enrichment of T-cells (p=0.01), cytotoxic lymphocytes (p=0.02), B-cells (p=0.05) and neutrophils (p=0.04), as estimated by MCP counter, in the clinical benefit cluster. The cytolytic, IMPRES and MCP-counter-CD8-T-cell score also trended higher in the clinical benefit cluster but did not reach statistical significance. A similar pattern of immune-marker enrichment was observed when comparing samples strictly by RECIST response. In this comparison T-cells (p=0.02), cytotoxic lymphocytes (p=0.04) and B cells (p=0.02) were again higher in responding samples, as were CD8 T-cells (p=0.05), NK cells (p=0.05), cytolytic score (p=0.03) and IMPRES (p=0.01). The higher neutrophil signature that we observed in the responder-cluster was not seen in this comparison (p=0.65). To test if prior immunotherapy with Ipilimumab had an effect on responses or to the composition of the tumour microenvironment, we repeated our response and immune microenvironment analysis with prior ipilimumab therapy as the predictor variable. We found that prior ipilimumab therapy was not associated with RECIST response (p=0.59) or the response associated clusters in this cohort. To test if prior Ipilimumab treatment had an impact on the immune microenvironment in our samples, we compared immune marker expression in 17 samples that had prior Ipilimumab exposure with the 12 samples that were immunotherapy naïve. Overall, only the NK cell signature was significantly differentially expressed, being lower in Ipilimumab treated samples compared to immunotherapy naïve samples (p=0.04) (Figure 3.4 c-d). The cytotoxic lymphocyte and IMPRES signatures also trended lower in Ipilimumab treated samples although this was not statistically significant (p=0.07 and p=0.06 respectively). It is difficult to determine in this study if these differences in immune markers are a direct result of Ipilimumab's biological activity on the tumour-immune infiltrate or whether Ipilimumab

treatment has selected for tumours with a specific immune microenvironment, however we did not observe any significant effect on outcome to subsequent PD-1 therapy in this cohort.

Transcriptomic Clusters Associated with Distinct MicroRNA Expression Profiles

Having identified two response-associated clusters from our transcriptomic data, we wanted to identify microRNAs that were associated with these clusters and to describe the relationship between microRNA and mRNA expression in our dataset. We first used DEseq2 to identify individual microRNAs that were differentially expressed in the responder and non-responder clusters. This analysis identified 5 microRNAs enriched in the responder cluster and 10 microRNAs enriched in the non-responder cluster (padj<0.1) (Figure 3.5a,c). Of these 15 microRNAs, miR-31-5p, 203a-3p and miR-205-5p were the top candidates for further analysis, with a log fold change (>2) between the responder and non-responder clusters and experimental evidence of biological activity (miRbase). Second, as microRNA family members exert co-operative regulation through shared sequence homology, we considered microRNA family members that individually may not have met the inclusion criteria for the individual microRNA analysis but cumulatively may be of biological significance. In this analysis we identified 3 microRNA families enriched in the responder cluster and 2 microRNA families enriched in the non-responder cluster (padj<0.1) (Figure 3b). These microRNA families included miR-31, miR-203 and miR-205 in concordance with our individual microRNA analysis. In addition, the miR-515 family was highly enriched in the responder cluster (lfc=7.8 padj<0.001), although no single miR-515 family members were detected in our initial microRNA analysis due to their low individual expression levels. As there was not 100% concordance between our

Figure 3.5 MicroRNA Differential Expression Analysis

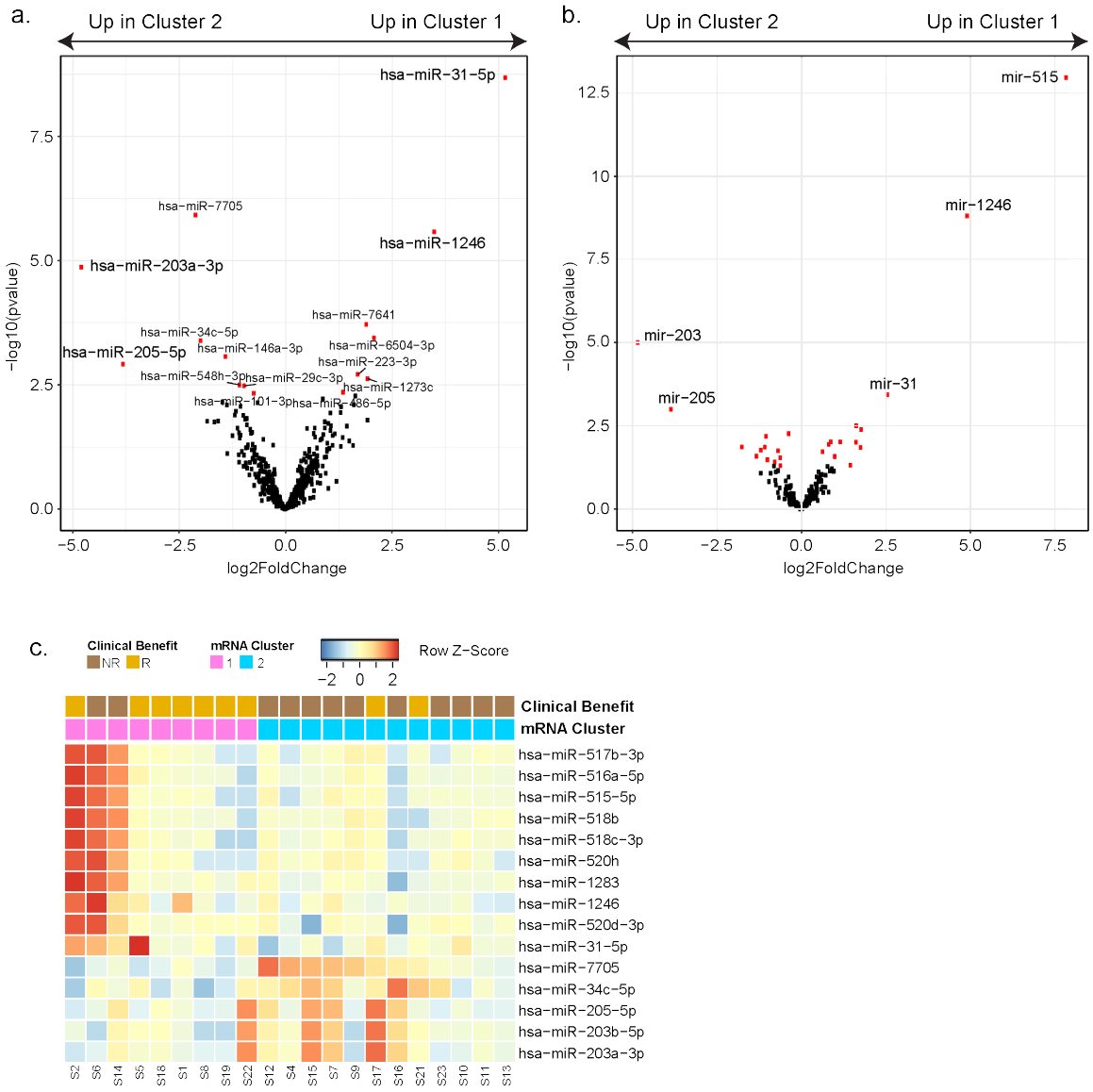

Figure 3.5 MicroRNA Differential Expression Analysis in Pre-PD-1 Treatment Melanoma Biopsies. We performed microRNA sequencing from RNA extracted from the biopsies of melanoma patients prior to treatment with anti-PD-1 checkpoint blockade. In this analysis we used DESEQ2 to compare the differential expression in microRNAs in samples that we had classified by their mRNA cluster membership, as above. (**a**) A volcano plot representing log2 fold changes and negative log 10 p-values for each microRNA compared using DESEQ2. Values on the left of the plot are enriched in samples belonging to mRNA cluster 2, associated with resistance to anti-PD-1 therapy, and values on the right are enriched in samples belonging to mRNA cluster 1, associated with sensitivity to anti-PD-1 therapy. (**b**) A volcano plot representing log2 fold changes and negative log 10 p-values for each microRNA family (sum of counts of each microRNA family member) compared using DESEQ2. Values on the left of the plot are enriched in samples belonging to mRNA cluster 2, associated with resistance to anti-PD-1 therapy, and values on the right are enriched in samples belonging to mRNA cluster 1, associated with sensitivity to anti-PD-1 therapy. (**c**) Heatmap representing per sample expression of the top differentially expressed microRNAs in samples from mRNA cluster 1 vs cluster 2. Values are row normalized z-scores from variance stabilized log2 transformed read counts. Sample cluster membership and clinical benefit is shown in the tracks above the heatmap.

transcriptomic clusters and clinical benefit, we also repeated this analysis with a direct comparison of samples from patients who did receive clinical benefit vs those that did not receive clinical benefit (Figure 3.6). Using this approach we confirmed some microRNAs that we previously identified as significantly differentially expressed between transcriptomic clusters, including miR-205-5p and miR-31-5p.

Experimental Validation of Response-Associated MicroRNAs

Although none of the microRNAs that we identified in our differential expression analysis had previously been implicated in tumour immunology, we sought to determine if they played a role in melanoma cell sensitivity to T-cell killing in-vitro. For these assays we first measured endogenous expression of miR-31-5p, miR-200b-3p and miR-205-5p in a panel of four melanoma cell lines (Mel-526, MDA-2333, MDA-2400 and MDA-2580). We found very low or undetectable levels of our microRNAs of interest in all four cell lines (figure 3.7 b). Transient transfection of microRNA mimics dramatically and consistently increased levels of specific microRNA in each cell line allowing us to compare the effect of increased microRNA expression on melanoma sensitivity to T-cell killing (figure 3.7 c). We measured melanoma cell death by chromium release assay after a 4 hour co-culture with MART-1 specific T-cells in our four melanoma cell lines (Figure 3.7 d). We observed no differences in melanoma cell death with miR-31-5p in any of the four cell lines we tested. With miR-200b-3p we noted one out of the four cell lines (MDA 2333) had a slight but statistically significant reduction level of cell death, indicating exogenous miR-200b-3p conferred some resistance to T-cell killing. However the remaining three cell lines had unchanged sensitivity to T-cell killing suggesting a cell specific effect. With miR-205-5p we also saw a slight but statistically significant protective effect against T-cell

Figure 3.6 MicroRNA Differential Expression Analysis Based on Clinical Benefit

a.

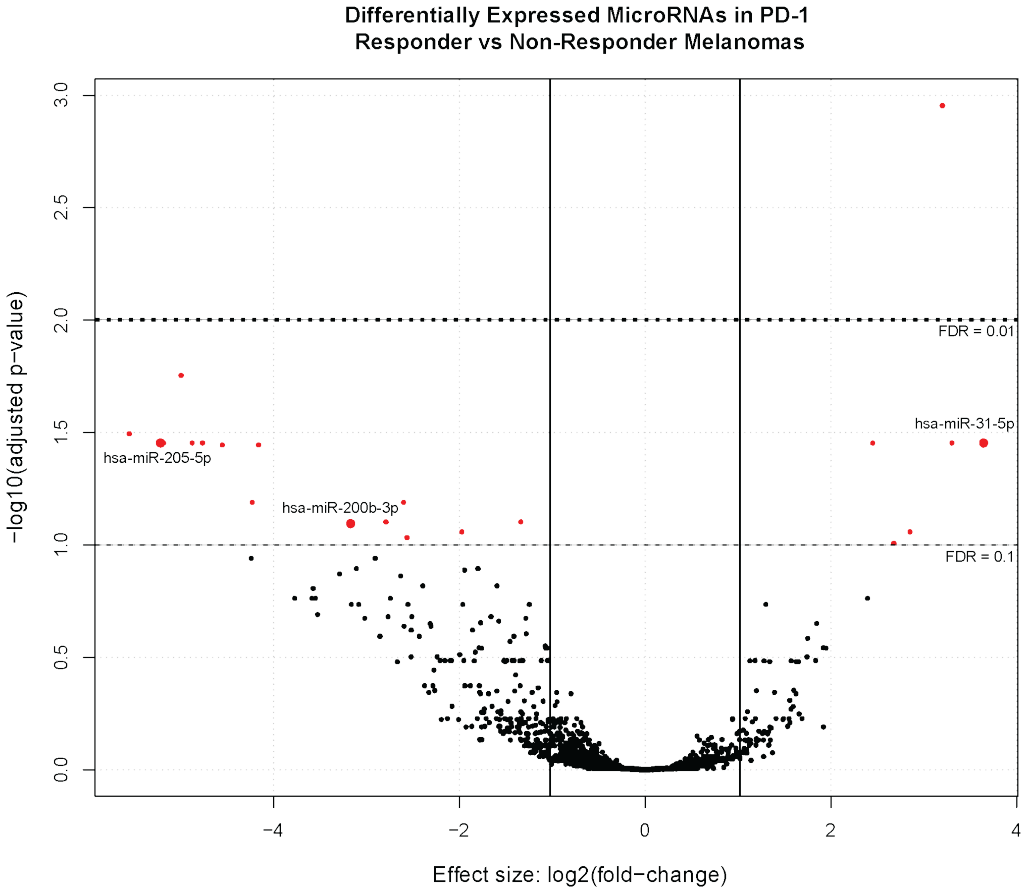

b.

	baseMean (RPM)	log2FoldChange	pvalue	FDR
hsa-miR-346	3.68	3.20	0.00	0.00
hsa-miR-1269b	20.88	-5.00	0.00	0.02
hsa-miR-520g-3p	34.33	-5.55	0.00	0.03
hsa-miR-205-5p	4665.67	-4.76	0.00	0.04
hsa-miR-31-3p	82.35	3.30	0.00	0.04
hsa-miR-31-5p	6353.58	3.65	0.00	0.04
hsa-miR-517b-3p	252.29	-4.76	0.00	0.04
hsa-miR-517c-3p	101.30	-5.22	0.00	0.04
hsa-miR-518f-3p	104.68	-4.88	0.00	0.04
hsa-miR-520f-3p	24.06	-5.18	0.00	0.04
hsa-miR-6782-5p	3.78	2.45	0.00	0.04
hsa-miR-516b-5p	57.72	-4.16	0.00	0.04
hsa-miR-517a-3p	18.83	-4.55	0.00	0.04
hsa-miR-1286	22.05	-2.60	0.00	0.06
hsa-miR-524-5p	16.43	-4.23	0.00	0.06
hsa-miR-200b-3p	583.25	-2.79	0.00	0.08
hsa-miR-4461	27.16	-1.34	0.00	0.08
hsa-miR-520h	32.77	-3.17	0.00	0.08
hsa-miR-7705	179.96	-1.97	0.00	0.09
hsa-miR-892a	18.76	2.85	0.00	0.09
hsa-miR-202-5p	61.22	-2.56	0.00	0.09
hsa-miR-891a-5p	42.65	2.68	0.00	0.10

Figure 3.6 MicroRNA Differential Expression Based on Clinical Benefit (**a**) A volcano plot representing log2 fold changes and negative log 10 p-values for each microRNA compared using DESEQ2. Values on the left of the plot are enriched in samples from patients who did not receive clinical benefit from anti-PD-1 immunotherapy and values on the right are enriched in samples from patients who did receive clinical benefit from anti-PD-1 therapy. (**b**) Summary statistics from top differentially expressed microRNAs from a, identifying three microRNAs with significantly high expression with large log2foldchanges (>2) and FDR <0.1)

Figure 3.7 Effect of Exogenous Expression of Response-Associated MicroRNAs on Melanoma Cell Line Sensitivity to T-Cell Killing

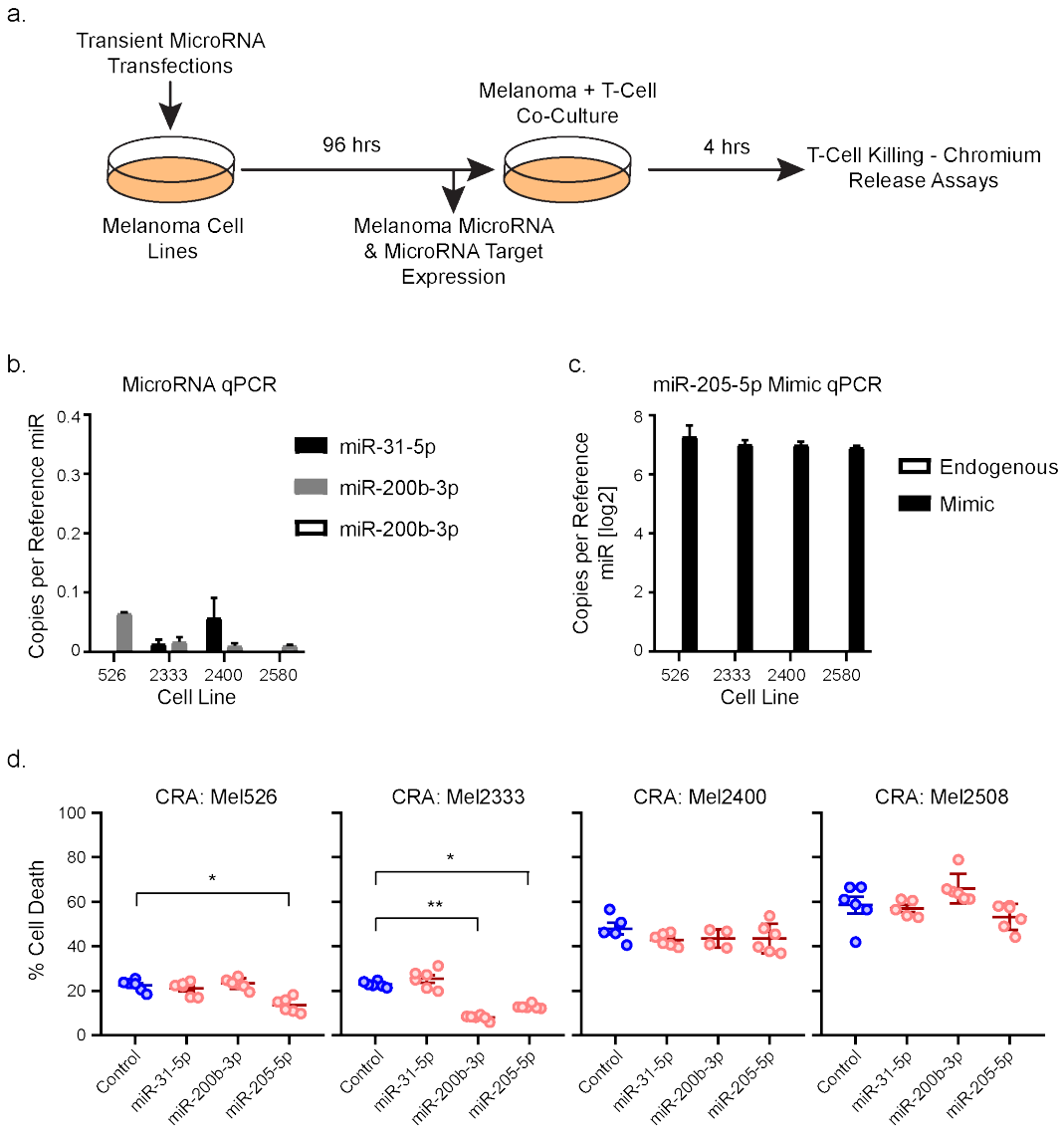

Figure 3.7 Effect of Exogenous Expression of Response-Associated MicroRNAs on Melanoma Cell Line Sensitivity to T-Cell Killing. We performed T-cell killing assays on a panel of 4 melanoma cell lines with transient transfection of microRNAs of interest to measure the effect of increased microRNA expression on sensitivity of melanoma cells to T-cell killing. (**a**) Schema. (**b**) Barplots representing endogenous expression of each microRNA of interest in each cell line relative to stably expressed reference microRNAs. (**c**) Barplots representing levels of exogenous miR-205-5p 72hrs post transfection in a panel of melanoma cell lines relative to stably expressed reference microRNAs. (**d**) Dotplots displaying percentage cell death from each cell line under each microRNA condition after 4hr co-culture with T-cells. Significant differences vs control are depicted by a black bar.

killing in two of the four cell lines tested (Mel526 and MDA2333). In this case the remaining two cell lines also had an unchanged sensitivity to T-cell killing.

Summary

In this chapter we used RNA and microRNA sequencing to profile the tumors of a cohort of twenty-nine pre-PD1 inhibitor treated melanoma patients. Using an unsupervised approach to classifying tumors based on their mRNA expression we were able to identify two transcriptomic groups that closely aligned with responses to immunotherapy. Among these two groups we were able to identify enrichment of particular gene sets associated with response and resistance to therapy. These included an enrichment of genes involved in interferon gamma response in responding tumors and an enrichment of genes involved in oxidative phosphorylation in non-responding tumors. We also identified transcriptomic immune markers were also enriched in responding tumors, including a CD8 T-cell signature.

Having established transcriptomic groups of samples that corresponded to response, we identified microRNAs differentially expressed between the two groups, identifying eight differentially expressed microRNAs. Of these we selected three with the highest tissue expression for *in vitro* functional validation, miR-31-5p, miR-200b-3p and miR-205-5p. We used a T-cell killing assay with melanoma cells transfected with these microRNAs to identify any effects on sensitivity to T-cell killing. Using this assay we found a modest protective effect of miR-205-5p in 2/4 melanoma cell lines indicating this microRNA may help melanomas evade immune destruction and resist PD1 immune checkpoint blockade.

CHAPTER FOUR

NETWORK ANALYSIS OF MELANOMA TISSUE AND CELL LINES REVEALS MICRORNA NETWORKS RELEVANT TO PD1 IMMUNOTHERAPY

This Chapter is based on the following work

- Robert Szczepaniak Sloane, Michael A. Davies, Scott E. Woodman, Miles C. Andrews, Jennifer A. Wargo. Identification of MicroRNA-mRNA Networks in Melanoma and Their Association with PD-1 Checkpoint Blockade Outcomes. Manuscript Submitted

ABSTRACT

Metastatic melanoma is a deadly malignancy with historically poor outcomes to therapy. Immuno-Oncology (IO) agents targeting immune checkpoint molecules such as Cytotoxic Lymphocyte Antigen-4 (CTLA-4) and Programmed Death-1 (PD-1) have revolutionized melanoma patient care, achieving significantly improved response rates and remarkable long-term survival. Despite the vast improvement in treatment options, roughly half of melanoma patients do not receive long-term clinical benefit from IO therapies and there is an urgent need to understand and mitigate mechanisms of resistance. MicroRNAs are key post-transcriptional regulators of gene expression and can regulate many aspects of cancer biology including immune evasion. In this study we used network analysis to define two core microRNA-mRNA networks in melanoma tissues and cell lines corresponding to 'MITF-low' and 'keratin' transcriptomic subsets of melanoma. We then compared expression of these core microRNAs in pre-PD-1 inhibitor treated melanoma patients and

observed that higher expression of miR-100-5p and miR-125b-5p were associated with significantly longer overall survival compared to low expressing tumors. These findings suggest that miR-100-5p and 125b-5p are potential markers of response to PD-1 inhibitors and further experimental investigation of these microRNA-mRNA interactions may yield further insight into melanoma resistance to PD-1 inhibitors.

INTRODUCTION

Immune checkpoint inhibitors targeting Cytotoxic T-lymphocyte associated protein 4 (CTLA-4) and Programmed cell death 1 (PD-1) have radically improved survival outcomes for metastatic melanoma patients. Treatment with PD-1 inhibitors result in long-term survival for ~40% of patients, compared to ~20% with CTLA-4 inhibition and just 5% with the prior standard of care, dacarbazine [26, 162-164]. However, a significant subset of melanoma patients do not receive clinical benefit from these treatments. Understanding the factors that influence response to immune checkpoint blockade is therefore necessary for new therapeutic strategies and to improve patient care.

Translational studies by our lab and others have identified several key determinants of response to PD-1 inhibition; intuitively these include the presence of PD-1 positive T-cells and the expression of programmed cell death 1 ligand 1 (PD-L1) in the tumor microenvironment (TME) and a high tumor mutation and immunogenic neoantigen burden [157, 165-167]. In addition, numerous cellular and genomic parameters have been associated with response including distinct transcriptomic profiles, PTEN status, composition of the gut microbiome and the composition of the TME including levels of B-cells, and fibroblasts [45, 156-158, 160, 168-171]. Despite these advances in our understanding, improvements in clinical practice are yet to be realized, and improved predictive biomarkers and therapeutic strategies are still required to improve patient care.

MicroRNAs are major post-transcriptional regulators of gene expression, directly binding and repressing translation of approximately 60% of human mRNAs [142]. MicroRNA regulation of gene expression has an established role in many of the hallmarks of cancer biology [172]. In melanoma this includes angiogenesis, EMT, invasion and resistance to

targeted therapy [173-176]. Furthermore, a comprehensive study of The Cancer Genome Atlas (TCGA) Skin and Cutaneous Melanoma (SKCM) dataset defined three transcriptomic subsets of melanoma ('Keratin', 'MITF-low' and 'Immune') each with a distinct microRNA expression profile [126]. Pre-clinical studies in multiple cancer types including melanoma have provided evidence of microRNA-mediated immune regulation that can affect sensitivity to immune surveillance [134, 135, 137]. However, melanoma microRNA expression has not been extensively studied in the context of clinical immunotherapy responses. We therefore sought to map the landscape of microRNA expression in melanoma and identify relationships with immunotherapy outcomes.

In this study we used a network analysis approach to identify a core set of microRNAs, in TCGA tumors and patient derived melanoma cell lines, with strong associations with melanoma gene expression [177]. Using this approach we identified two distinct microRNA networks, broadly similar to previously identified patterns of microRNA expression in melanoma. We subsequently examined the relationship of these microRNAs with survival outcomes in pre-PD-1-treatment melanoma biopsies and identified miR-100-5p and miR-125b-5p, from the same microRNA network, were associated with survival benefit in PD-1 treated patients.

RESULTS

Landscape of microRNA-mRNA associations in TCGA Melanomas

To build a network of relationships between the miRnome and the transcriptome we first comparing Spearman's correlation coefficients of all microRNAs and all mRNAs reads from the TCGA melanoma datasets. All microRNAs with at least one mRNA correlation (Spearman's rho <-0.4, >0.4) were plotted with hierarchical clustering in a heatmap to explore groups of microRNAs with common patterns of gene expression (Figure 4.1a). Using this approach we can identify two main clusters of microRNA-mRNA correlations, each with two major sub-clusters. On the left, the larger cluster contains 14 microRNAs all of which were previously identified as associated with the 'keratin' melanoma transcriptomic subset and includes the canonical 'keratin' melanoma microRNA, miR-211-5p, On the right of the heatmap with ten microRNAs, we observed microRNAs associated with the 'MITF'low' (miR-125b-5p, miR-100-5p) and 'Immune' (miR-146b-3p, miR-146b-5p, miR29b-3p, miR-223-3p) melanoma transcriptomic subsets. When comparing these subsets, it is easy to identify subclusters with almost perfectly opposite gene expression associations, most notably the 'keratin' microRNAs, including miR-211-5p which appears to mirror the 'MITF-low' microRNAs, miR-100-5p and miR-125b-5p. Similarly, the 'Keratin' microRNAs miR-17-3p, miR-17-5p and miR-92a-3p mirror the 'Immune' microRNAs. It is interesting to note that we can identify relationships between the existing three-transcriptomic subset classification of melanomas that may not have been predicted. For example while the dichotomy between 'keratin' and 'MITF-low' microRNA is established, it is interesting to note that the 'keratin' microRNAs separate into two sub-clusters, one of which more closely mirrors

Figure 4.1: Network Analysis of Global MicroRNA:mRNA Associations in TCGA Melanoma Samples.

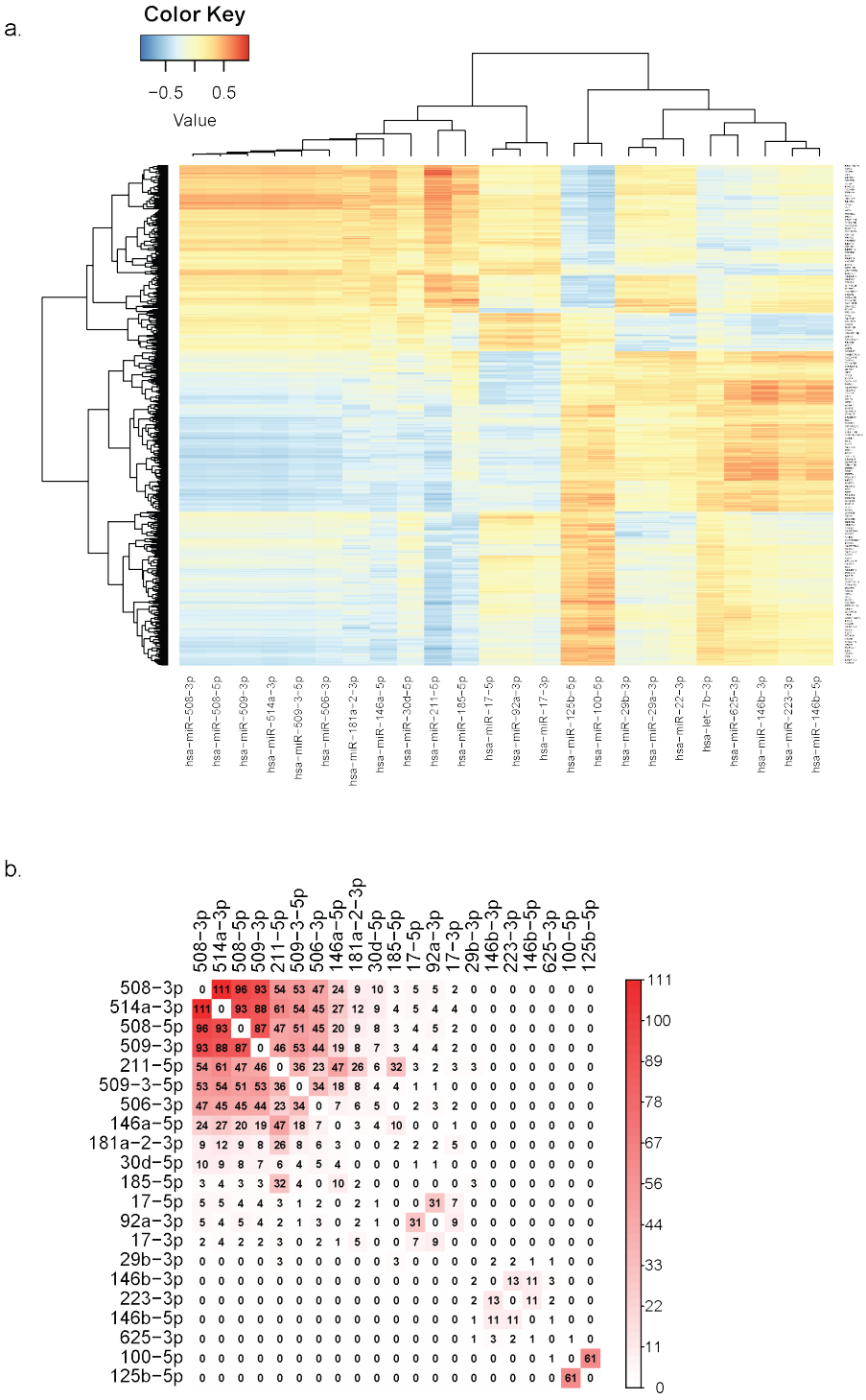

Figure 4.1: Network Analysis of Global MicroRNA:mRNA Associations in TCGA Melanoma Samples. (**a**) Clustered heatmap representing Spearman's rho values of all microRNA:mRNA correlations observed in TCGA melanoma samples where each microRNA has an inverse correlation (Spearman's rho <-0.4) with expression of at least 1 mRNA. (**b**) Adjacency matrix representing the number of mRNA inverse correlations shared by each microRNA in the TCGA microRNA:mRNA network.

‘MITF-low’ microRNAs while the other subset more closely mirrors the ‘Immune’ subset of microRNAs. It is tempting to speculate that the one subset of ‘keratin’ microRNAs including miR-211-5p is central to maintaining the ‘keratin’ phenotype while the other subset is involved in other biological processes that may associate with immune infiltration or exclusion.

To further investigate the cluster relationships from the heatmap we plotted the number of inverse correlations shared between each microRNA identified in Figure 4.1a in an adjacency matrix (Figure 4.1b). In this analysis it is easy to identify the same cluster membership described in the heatmap, with the ‘keratin’ microRNAs forming the largest cluster with an apparent tiered membership, with miR-508-3p, miR-508-5p, miR-509-3p and miR-514a-3p sharing the most number of mRNA associations (87-111 shared associations) while three of the ‘keratin’ microRNAs, miR-17-5p, miR-92a-3p, miR-17-3p, form a distinct subcluster with relatively few shared associations with any other ‘keratin’ microRNAs (0-5 shared associations). The remaining ‘keratin’ microRNAs have significant overlap with the miR-508-3p cluster although with fewer overall shared mRNA associations with other ‘keratin’ microRNAs (0-61 shared associations). The remaining ‘MITF-low’ and ‘Immune’ melanoma subset microRNAs again form separate and distinct clusters.

We then used a network analysis approach to quantify inverse correlations of microRNA and mRNA expression in the TCGA melanoma dataset. We identified 1739 microRNA-mRNA associations comprising 74 microRNAs inversely correlated with expression of at least 1 mRNA (Spearman’s rho <-0.4). Of these 74 microRNAs, 19 were associated with >20 mRNAs each, accounting for 1521/1739(87%) of the total microRNA-mRNA inverse

correlations. Bipartite and unipartite network projections of the top 19 microRNAs identifies three distinct network hubs corresponding to the 'Keratin', 'MITF-low' and 'Immune' transcriptomic-subset-associated-microRNAs previously identified in this TCGA cohort and, unsurprisingly due to the overlapping methodology, shares similarities to the data represented in Figure 4.1 (Figure 4.2). The largest of these hubs consists of the TCGA 'Keratin' associated microRNAs; miR-211-5p, 146a-5p, 181a-2-3p, 506-3p, 508-3p, 508-5p, 509-5p, 509-3-5p, 514a-3p, 17-3p, 17-5p, 92a-3p and 185-5p (Fig 1a, b, Table S2). This network hub accounts for 1153/1739 (66%) of all observed microRNA-mRNA inverse correlations and also contains the microRNAs with the highest degree centrality (miR-211-5p - 293), betweenness centrality (miR-29b-3p, 17-3p, 211-5p, 185-5p - 42.5, 25.5, 24.5, 23.5, respectively), and eigenvector centrality (miR-508-3p, 514a-3p, 508-5p, 509-3p [1, 1, 0.93, 0.92, respectively]). The second largest network hub, by number of microRNA-mRNA associations (266/1739, 15%), consists of the TCGA 'MITF-low' microRNAs; miR-100-5p and 125b-5p. This hub is separate from the rest of network, with zero shared mRNA associations with other microRNAs and therefore scores low (<0.01) on eigen, betweeness and closeness network centrality. We also observed that MITF was among the inversely correlated mRNAs within this network, consistent with the previous characterization of these microRNAs in the TCGA. The third largest network hub, by number of microRNA-mRNA associations (102/1739, 6%) consists of the TCGA 'Immune' microRNAs; miR-29b-3p, 146b-3p, 146b-5p and 223-3p. This network hub only shares scores low for measures of network centrality

Figure 4.2. Network Analysis of Global MicroRNA:mRNA Associations in TCGA Melanoma

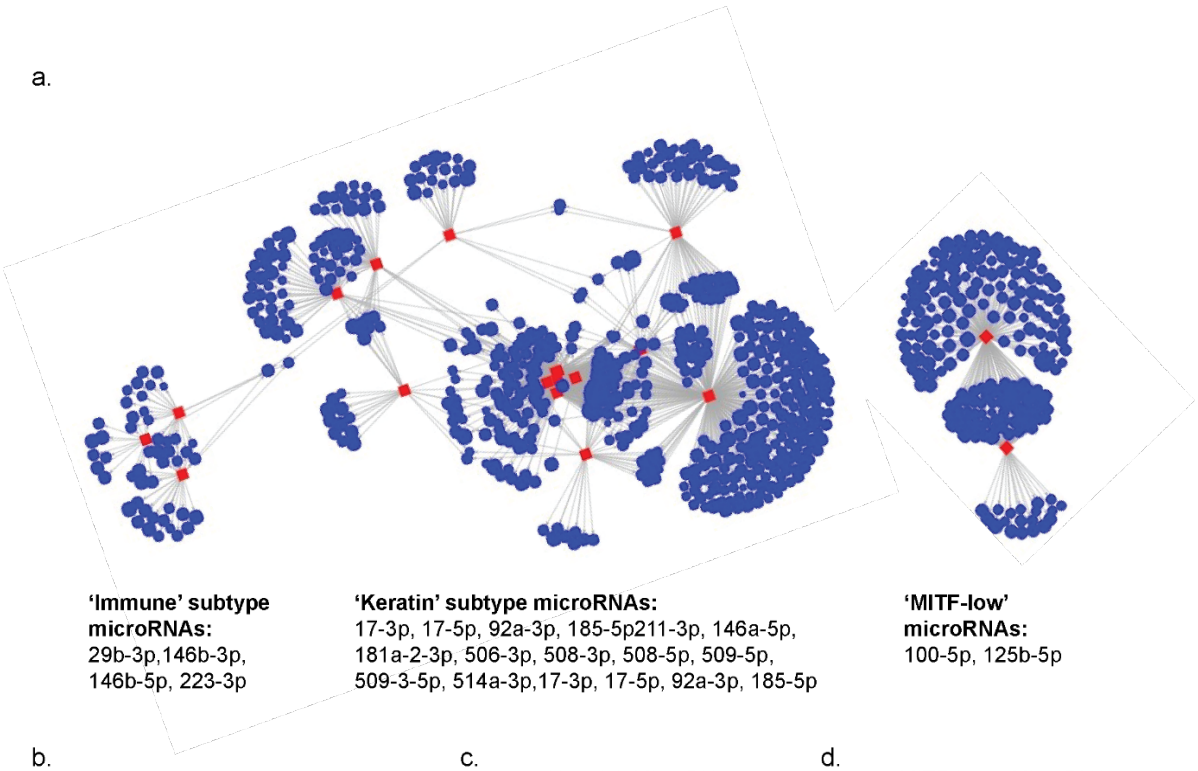

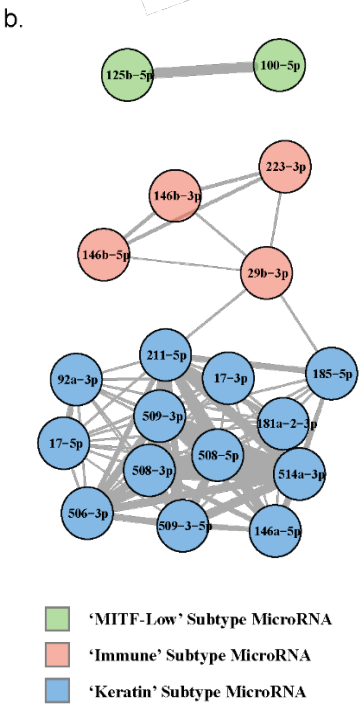

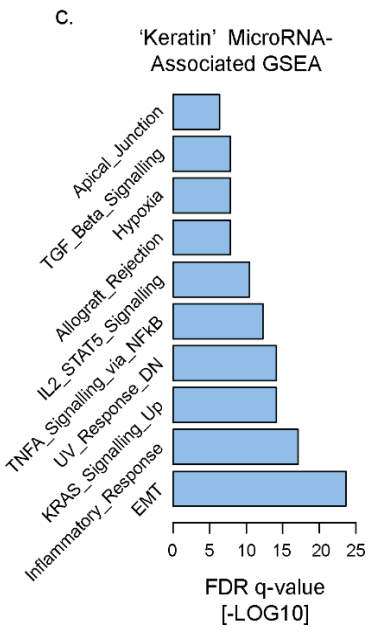

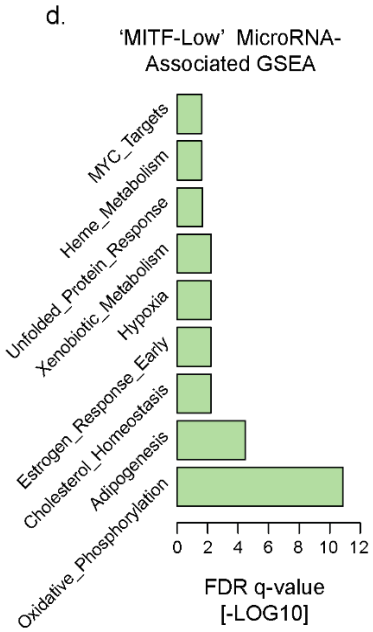

Figure 4.2: Network Analysis of Global MicroRNA:mRNA Associations in TCGA Melanoma. Inverse correlations of microRNA and mRNA pairs were calculated to identify potential microRNA regulated gene networks. (**a**) Bipartite network projection displaying the 19 microRNAs (red) with highest numbers (>20) of inversely correlated (Spearman's rho <-0.4) mRNAs (blue) within all TCGA melanoma samples, identifies three distinct microRNA:mRNA network hubs. (**b**) Unipartite network projection displaying the mRNA inverse correlations shared by each microRNA (higher number of correlations indicated by connecting line thickness). MicroRNAs are colour coded by their previous association with specific TCGA transcriptomic subsets. (**c**) Gene-Set Enrichment Analysis of all mRNAs inversely correlated with 'Keratin' transcriptomic subset associated microRNAs. (**d**) Gene-Set Enrichment Analysis of all mRNAs inversely correlated with 'MITF-Low' transcriptomic subset associated microRNAs.

(<0.1) indicating very few shared mRNA associations with other microRNAs in the network. To understand the biological significance of these networks we performed gene set enrichment analysis (GSEA) on the mRNAs that were inversely correlated with each network (Fig 4.2 c, d). The most significant enrichment of genes in the 'keratin' microRNA cluster was in the epithelial to mesenchymal transition (EMT) gene set (33 genes, FDR q = 2.36E-24), consistent with prior experimental evidence of miR-211-5p inhibition of EMT in melanoma. The most significant enrichment of genes in the 'MITF-low' microRNA cluster was in oxidative phosphorylation (15 genes, FDR q = 1.39E-11). In parallel with the findings of individual mRNA associations, there was also no overlap of gene set enrichment between the 'keratin' and 'MITF-low' microRNA associated genes, indicating that these networks represent functionally distinct regulatory networks. Genes that were inversely correlated with the 'Immune' microRNAs were not found to be enriched in any gene-sets.

Landscape of microRNA-mRNA Associations in Patient Derived Melanoma Cell Lines

To verify our findings from the TCGA samples, we repeated our analysis in a panel of 61 early passage melanoma cell lines obtained from melanoma TIL harvests performed at The University of Texas MD Anderson Cancer Center. Our first observation from this analysis was the far stronger correlation of microRNA and mRNA expression in melanoma cell lines compared to melanoma tissue, presumably due to the reduced complexity of cell culture conditions allowing greater resolution of melanoma specific transcription. This allowed us to increase our correlation coefficient threshold to 0.6 from 0.4 in the TCGA melanoma analysis. We identified 4489 unique microRNA-mRNA associations comprising 81 microRNAs inversely correlated with expression of at least 1 mRNA

(Spearman's rho <-0.6) (Figure 4.3). All microRNAs with at least one mRNA correlation (Spearman's rho <-0.6, >0.6) were plotted with hierarchical clustering in a heatmap to explore groups of microRNAs with common patterns of gene expression (Figure 4.3a). Although much larger than the heatmap generated with the TCGA data, the structure is relatively simple, with two main clusters of mRNAs and three clusters of microRNAs. On the left, the larger microRNA cluster contains fifty-nine microRNAs including the 'keratin' microRNAs that we identified in the TCGA. This large microRNA cluster has strong inverse correlations with the largest mRNA cluster indicating involvement in repression of a large subset of genes. The second prominent cluster on the right of the heatmap is a much smaller cluster of 14 microRNAs including the 'MITF-low' microRNAs miR-100-5p and miR-125b-5p identified in the TCGA analysis. This cluster of microRNAs has strong inverse correlations with the smaller mRNA cluster in contrast to the first microRNA cluster. This is a repeat of the 'keratin' and 'MITF-low' dichotomy that we observed in the TCGA dataset. The third cluster of consists of 35 microRNAs that seem to have an intermediate association with the two mRNA clusters. In total we observed 2/2 'MITF-low', 10/13 'Keratin' and 1/4 'Immune' associated microRNAs that we identified in the TCGA dataset. We further investigated the relationships between the microRNAs identified in this analysis using an adjacency matrix visualizing the number of inverse mRNA correlations shared by each microRNA, filtered to include the top 18 microRNAs with the highest individual mRNA associations (Figure 4.3b). This plot again highlights the dichotomy of 'keratin' and 'MITF-low' microRNAs in melanoma, with many of the same microRNAs identified in the TCGA analysis repeated here, including miR-211-5p, miR-100-5p and miR-125b-5p.

Figure 4.3. Global MicroRNA:mRNA Associations in Melanoma Cell Lines

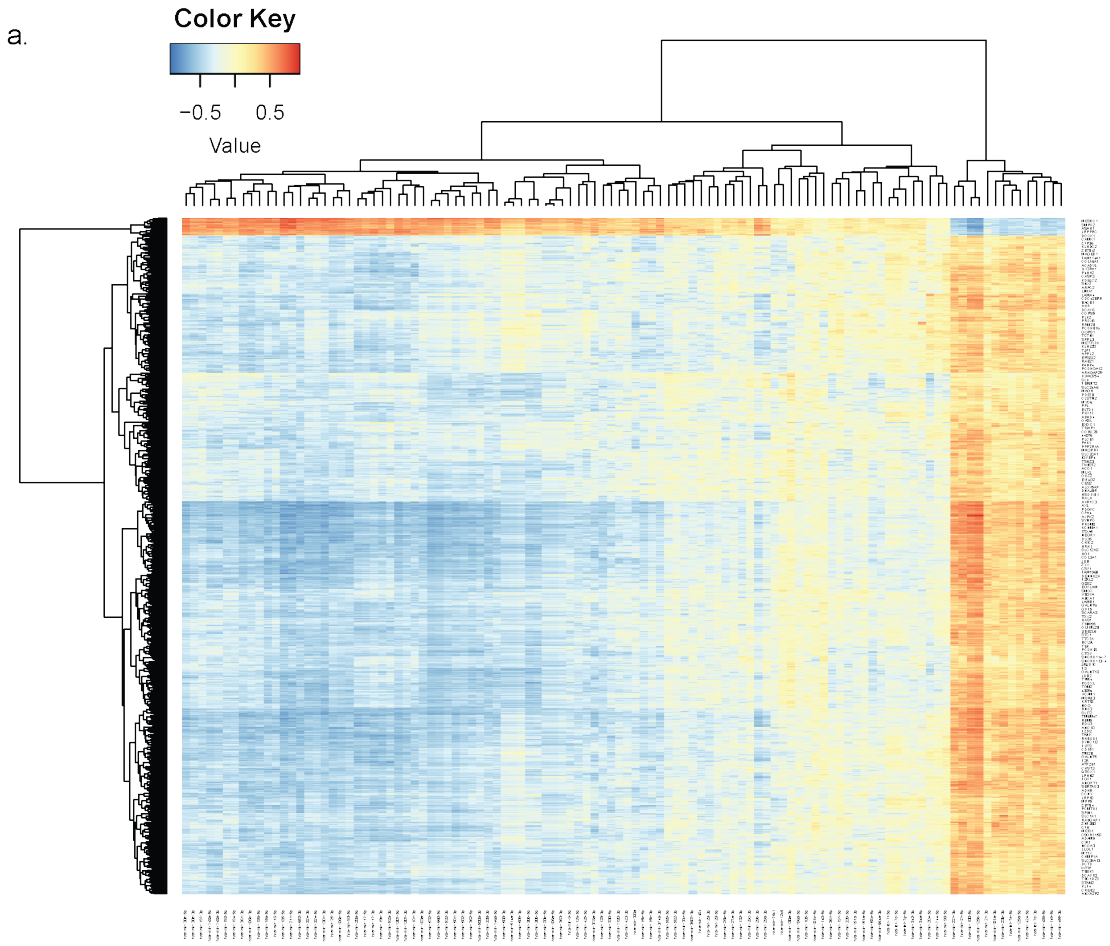

b.

	hsa-mir-185-5p	hsa-mir-1301-3p	hsa-mir-211-5p	hsa-mir-652-3p	hsa-mir-532-5p	hsa-mir-324-3p	hsa-mir-324-5p	hsa-mir-25-3p	hsa-mir-106b-5p	hsa-mir-660-5p	hsa-mir-15a-5p	hsa-mir-1307-5p	hsa-mir-93-5p	hsa-mir-361-3p	hsa-mir-20a-5p	hsa-mir-17-3p	hsa-mir-100-5p	hsa-mir-125b-5p
hsa-mir-185-5p	0	159	165	139	112	102	102	106	96	94	103	94	79	82	63	44	0	0
hsa-mir-1301-3p	159	0	139	112	107	116	110	82	78	90	85	80	76	60	41	29	0	0
hsa-mir-211-5p	165	139	0	115	92	96	98	78	75	81	88	68	62	59	47	24	0	0
hsa-mir-652-3p	139	112	115	0	94	84	90	102	89	80	94	80	67	73	45	33	0	0
hsa-mir-532-5p	112	107	92	94	0	77	77	63	67	117	66	60	60	49	42	26	0	0
hsa-mir-324-3p	102	116	96	84	77	0	107	70	71	71	69	65	64	49	28	22	0	0
hsa-mir-324-5p	102	110	98	90	77	107	0	64	66	70	64	58	64	46	25	18	0	0
hsa-mir-25-3p	106	82	78	102	63	70	64	0	104	54	71	72	75	77	28	32	0	0
hsa-mir-106b-5p	96	78	75	89	67	71	66	104	0	54	68	68	84	58	31	29	0	0
hsa-mir-660-5p	94	90	81	80	117	71	70	54	54	0	56	54	48	44	36	24	0	0
hsa-mir-15a-5p	103	85	88	94	66	69	64	71	68	56	0	43	49	53	26	17	0	0
hsa-mir-1307-5p	94	80	68	80	60	65	58	72	68	54	43	0	60	66	43	44	0	0
hsa-mir-93-5p	79	76	62	67	60	64	64	75	84	48	49	60	0	42	26	24	0	0
hsa-mir-361-3p	82	60	59	73	49	49	46	77	58	44	53	66	42	0	30	33	0	0
hsa-mir-20a-5p	63	41	47	45	42	28	25	28	31	36	26	43	26	30	0	60	0	0
hsa-mir-17-3p	44	29	24	33	26	22	18	32	29	24	17	44	24	33	60	0	0	0
hsa-mir-100-5p	0	0	0	0	0	0	0	0	0	0	0	0	0	0	0	0	0	128
hsa-mir-125b-5p	0	0	0	0	0	0	0	0	0	0	0	0	0	0	0	0	128	0

Figure 4.3: Network Analysis of Global MicroRNA:mRNA Associations in Melanoma Cell Lines. (**a**) Clustered heatmap representing Spearman's rho values of all microRNA:mRNA correlations observed in melanoma cell lines where each microRNA has an inverse correlation (Spearman's rho <-0.6) with expression of at least 1 mRNA. (**b**) Adjacency matrix representing the number of shared mRNA inverse correlations shared by each microRNA in the melanoma cell line microRNA:mRNA network.

For network analysis in the cell line dataset we repeated our filter of the initial 81 microRNAs used for the adjacency matrix. The top 18 microRNAs were associated with >100 mRNAs each, accounting for 2748/4489 (61%) of the total microRNA-mRNA inverse correlations. Bipartite and unipartite network projections of the top 18 microRNAs identified two distinct network hubs (4.4 a,b). These two network hubs shared common characteristics with the 'Keratin' and 'MITF-low' hubs identified in the TCGA dataset. The 'MITF-low' network hub comprised the same two microRNAs, miR-100-5p and miR-125b-5p and accounted for 308/4489 (7%) of the total microRNA-mRNA inverse correlations in this dataset. In agreement with our TCGA analysis, we observed that MITF was among the inversely correlated mRNAs within this network. This hub is again completely separate from the rest of the network, with zero shared mRNA associations with other microRNAs and therefore scores low (<0.01) on eigen, betweeness and closeness network centrality. The larger hub accounted for 2440/4489 (50%) of the total microRNA-mRNA inverse correlations in this dataset and shared some similarities with the 'keratin' hub from the TCGA analysis, including the presence of miR-17-3p, 185-5p and 211-5p, but did not exclusively contain microRNAs from the TCGA 'Keratin' transcriptomic subset (6/16 'Keratin', 2/16 'Immune' and 8/16 unaffiliated to any TCGA transcriptomic subset). We again performed GSEA on the mRNAs inversely correlated with each network. In the larger network we identified striking similarities with the 'keratin' network in the TCGA analysis, sharing 6 of the top 10 enriched gene sets, including EMT, UV_Response_DN, Apical_Junction, TNFA_Signalling_via_NFkB, Hypoxia and TGF_Beta_Signalling (Table S6). The GSEA of mRNAs inversely correlated with the 'MITF-low' microRNA

Figure 4.4. Network Analysis of Global MicroRNA:mRNA Associations in Melanoma Cell Lines

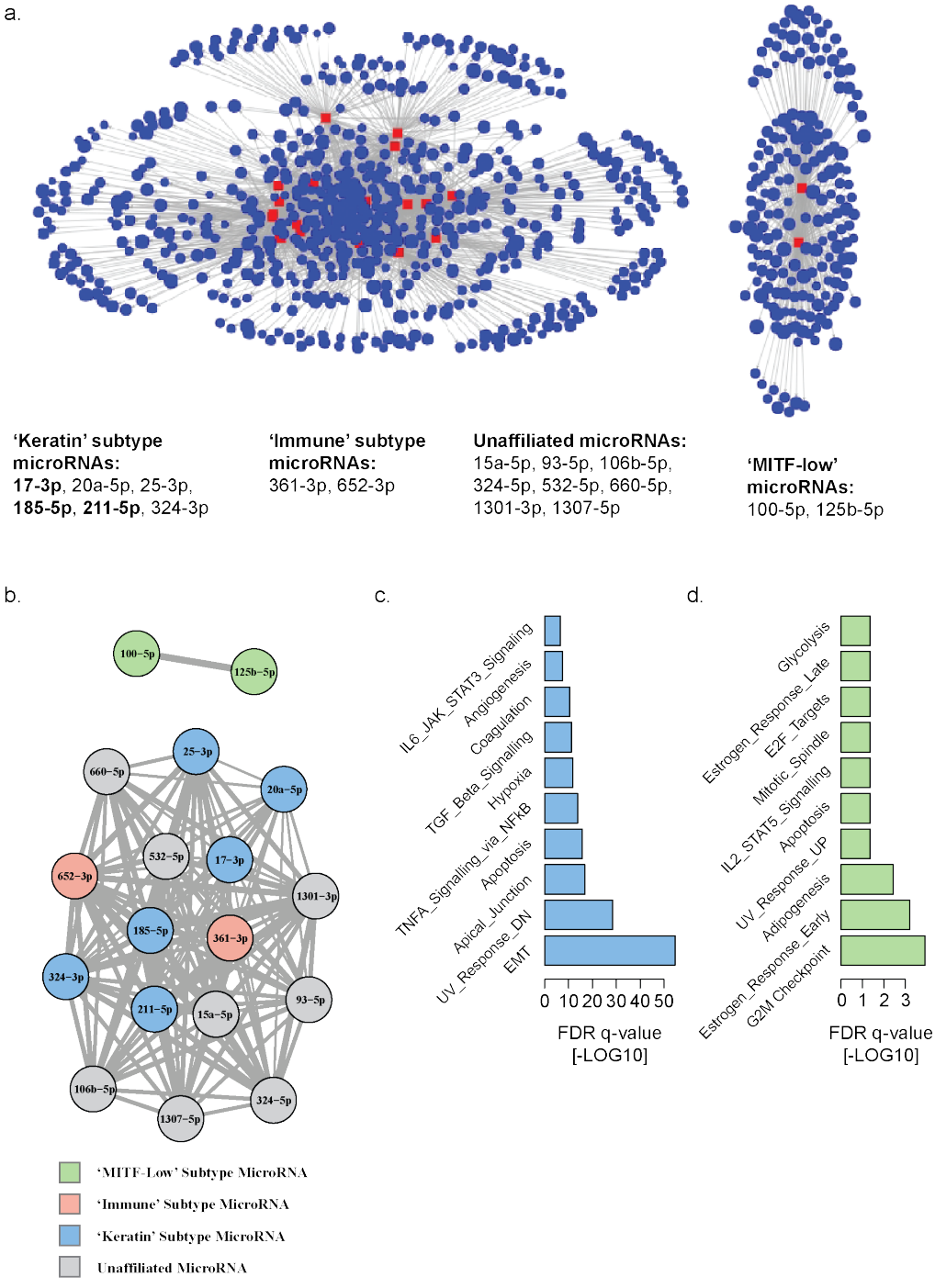

Figure 4.4: Network Analysis of Global MicroRNA:mRNA Associations in Melanoma Cell Lines. Inverse correlations of microRNA and mRNA pairs were calculated to identify potential microRNA regulated gene networks. (**a**) Bipartite network projection displaying the 18 microRNAs (red) with highest numbers (>100) of inversely correlated (Spearman's rho <-0.6) mRNAs (blue) within all TCGA melanoma samples, identifies two distinct microRNA:mRNA network hubs. (**b**) Unipartite network projection displaying the mRNA inverse correlations shared by each microRNA (higher number of correlations indicated by connecting line thickness). MicroRNAs are colour coded by their previous association with specific TCGA transcriptomic subsets. (**c**) Gene-Set Enrichment Analysis of all mRNAs inversely correlated with 'Keratin' transcriptomic subset associated microRNAs. (**d**) Gene-Set Enrichment Analysis of all mRNAs inversely correlated with 'MITF-Low' transcriptomic subset associated microRNAs.

network also shared 2/10 enriched genesets with the TCGA 'MITF-low' network including Estrogen_Response_Early and Adipogenesis.

PD-1 Treated Patient Cohort

Having identified prominent microRNA-mRNA networks in melanoma tumors and cell lines, we asked if any of the microRNAs from these networks were related to immunotherapy outcomes in pre-PD1 treated melanomas. We compared expression of the 19 microRNAs with the highest degree centrality in the TCGA bipartite network analysis in the pre-PD-1-treatment biopsies of 22 stage III/IV melanoma patients, of whom 10 received clinical benefit and 12 did not. We observed significantly higher expression of both miR-100-5p (median log2 counts: 12.48 vs 11.25, p-value = 0.036) and miR-125b-5p (median log2 counts: 17.35 vs 15.49, p-value = 0.025) in the tumors of patients who received clinical benefit compared to those who did not receive clinical benefit (p=0.025, p=0.36, respectively) (Figure 4.5, Table 4.1). Although no other microRNAs were significantly differentially expressed, we did note that miR-146a-5p, which has been implicated as a negative regulator of immune activation *in vivo*, was slightly elevated in the tumors of patients who did not receive clinical benefit (median log2 counts: 19.05 vs 18.13, p-value = 0.28) [30425059]. We then performed survival analysis using Cox's proportional hazard model and Kaplan Meier analysis (Figure 4.5 a, d-g). The survival analysis showed low hazard ratios for both miR-100-5p (HR (95%CI): 0.5 (0.3-0.85) p=0.01) and miR-125b-5p (HR (95%CI):0.51 (0.29-0.9) p=0.02) (Figure 4.5 a). High melanoma expression of miR-100-5p and miR-125b-5p were both shown to predict improved progression-free survival (log-rank test p=0.02, p=0.01, respectively) and overall survival (log-rank test p=0.05, p=0.05, respectively).

Table 4.1 Melanoma Pre-PD1 Treated Patient Characteristics

Characteristic	PD1-I No Clinical Benefit (n=13)	PD1-I Clinical Benefit (n=9)
Sex		
Male	8 (62%)	8 (89%)
Female	5 (38%)	1 (11%)
Melanoma Type		
Cutaneous unspecified	5 (38%)	4 (44%)
Superficial spreading	2 (15%)	-
Nodular	4 (31%)	-
Acral lentiginous	1 (8%)	1 (11%)
Unknown primary	1 (8%)	4 (44%)
Disease state (AJCCv8)		
IIIa/b	-	-
IIIc/d	2 (15%)	3 (33%)
IVa	2 (15%)	-
IVb	1 (8%)	-
IVc	8 (62%)	6 (67%)
IVd	-	-
Serum LDH (U/L; median, range)	456.5 (349-1789)	454.5 (385-1090)
Prior Ipilimumab		
Yes	9 (69%)	4 (44%)
No	4 (31%)	5 (56%)
Best Overall Response (BOR, RECIST 1.1)		
CR	-	3 (33%)
PR	-	4 (44%)
SD	-	2 (22%)
PD	13 (100%)	-
PFS (median, range ; days)	78 (20-87)	538 (321-NA)

Figure 4.5. Identification of MicroRNAs Associated with PD1 Treatment Outcomes

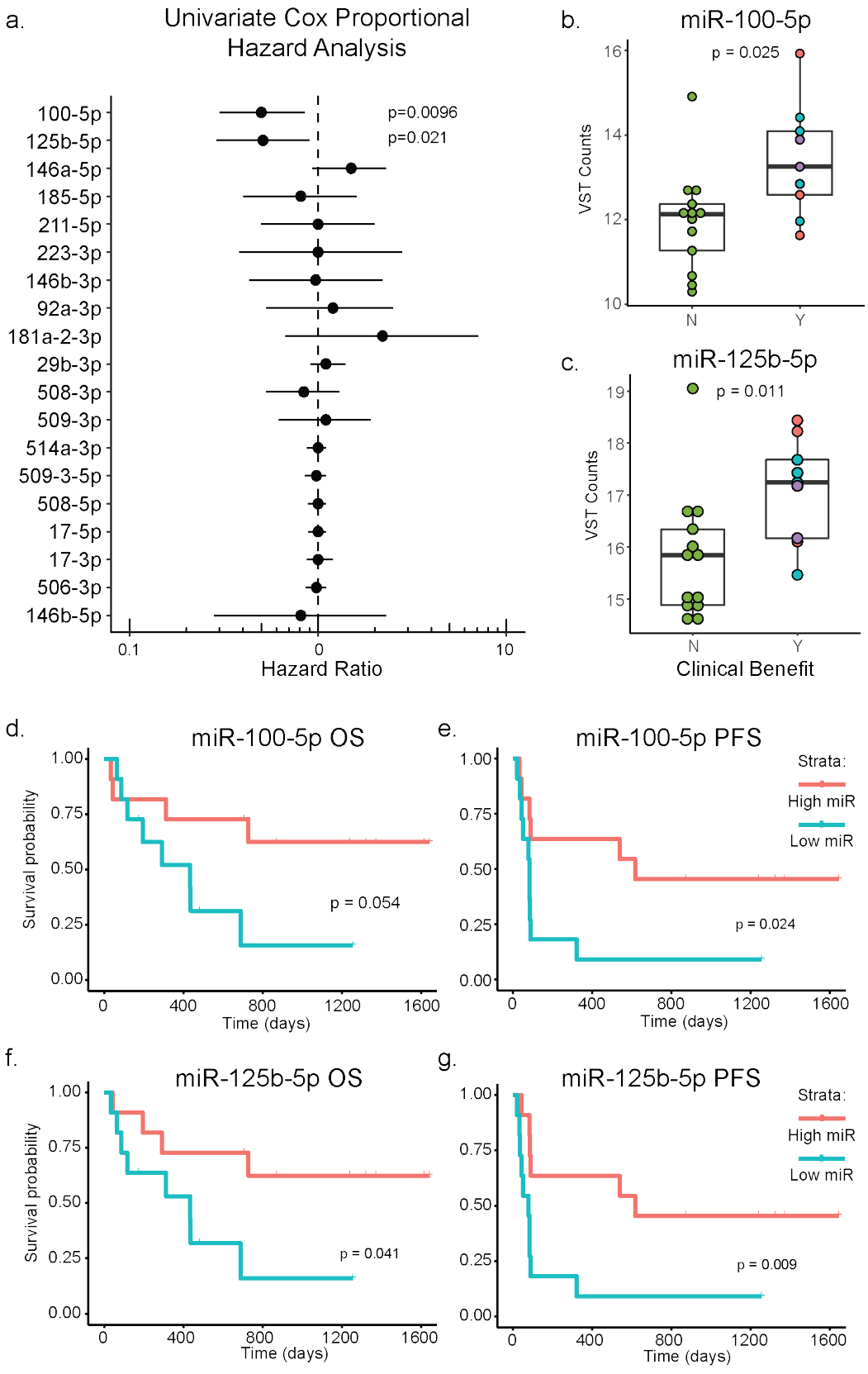

Figure 4.5: Survival Analysis of Melanoma MicroRNAs in Pre-PD-1-Treated Melanoma Biopsies. MicroRNA **s**equencing was performed on 22 Pre-PD-1-treated melanoma biopsies, variance-stabilised-log2-transformed counts were generated using DESEq2. (**a**) A forest plot displaying hazard ratios ± 95% confidence intervals from univatiate Cox's proportional hazard analysis of each of the 19 microRNAs with the highest degree centrality in bipartite network analysis of TCGA microRNA:mRNA expression. (**b-c**) Boxplots comparing variance-stabilised-log2-transformed counts of miR-100-5p and miR-125b-5p in melanoma biopsies from patients who did not receive clinical benefit from anti-PD-1 immunotherapy versus those who did receive clinical benefit. Boxplots display median, interquartile range and whiskers representing 1.5 x the interquartile range. (**d-g**) Kaplan Meier curves displaying the time to PFS or OS for patients with biopsies with high (above median) compared to low (below median) expression of miR-100-5p or miR-125b-5p.

Discussion

We identified three core microRNA-mRNA networks in melanoma tumors that broadly corresponded with previous observations of 'Keratin', 'MITF-low' and 'Immune' transcriptomic subsets in the TCGA SKCM dataset [126]. Further investigation of these networks confirmed previous findings about the roles of these microRNAs, including the prominence of miR-211-5p within the 'keratin' transcriptomic subset of melanoma and a strong enrichment of epithelial to mesenchymal genes, including AXL and ZEB1, which were inversely correlated with miR-211-5p expression. This supports previous evidence for the regulatory role of miR-211 in EMT-like processes in melanoma [174]. Similarly we found miR-100-5p and miR-125b-5p formed an independent network hub and were inversely correlated with MITF expression, mirroring the association of these microRNAs with 'MITF-low' melanomas from previous TCGA analysis [126]. The strong depletion of OXPHOS genes associated with the MITF-low network is also supported by prior evidence for the role of miR-125b and MITF as regulators of mitochondrial metabolism [178, 179].

The correlation analysis within the melanoma cell line dataset resulted in a substantially higher number of microRNA-mRNA pairs allowing us to increase the correlation coefficient threshold (<-0.6) and also the number of inverse correlations (>100) required for inclusion in our network analysis. The increased sensitivity to microRNA-mRNA interactions is likely due to the sampling of high purity cell lines with consistent culture conditions compared to the variability inherent in whole tumors with unpredictable stromal, immune and metabolic variation.

The network analysis in the melanoma cell lines shared broad similarities with the TCGA network with a high degree of overlap in terms of individual microRNA-mRNA

associations and also in GSEA of those mRNAs. The most obvious agreement between datasets occurred with miR-125b and miR-100-5p network, with no overlap with other microRNA-mRNA pairs and inverse correlation with MITF expression. One notable difference in this network was the absence of enrichment of OXPHOS genes inversely correlated with miR-100-5p and miR-125b-5p. It is possible that this difference is due to the significant differences in metabolic requirements between cell culture and the TME, but it is also possible that these metabolic differences are attributable to other components of the TME such as monocytes [178, 180, 181] . The larger microRNA-mRNA network identified in cell lines shared many characteristics with the 'keratin' microRNA network identified in the TCGA analysis, with a core of the same 'keratin' melanoma-subset-associated microRNAs including miR-211-5p. This network also shared enrichment of 6/10 gene sets with the 'keratin' TCGA network including EMT genes such as AXL and ZEB1.

To identify microRNAs associated with PD-1 checkpoint blockade outcomes, we compared microRNA expression in pre-treatment melanoma biopsies from patients who did or did not receive clinical benefit from therapy. We focused on those microRNAs that had the strongest degree centrality scores from our TCGA network analysis, hypothesizing that microRNAs associated with specific gene expression profiles would most likely be associated with differential responses. Using Cox's univariate proportional hazard model we found both 'MITF-low' microRNAs from our network analysis, miR-100-5p and miR-125b-5p, were associated with clinical benefit in this cohort. Interestingly previous research has implicated expression of these microRNAs, in a panel of others, with myeloid derived suppressor cell (MDSC) mediated resistance to immune checkpoint inhibitors. It

is unclear from their methodology and published data what the individual predictive power of each microRNA within the panel was. It is important to note that this microRNA data was obtained through peripheral plasma sampling and is therefore unclear how comparable it is with tumor expression data [182]. Although there is limited experimental evidence for the role of these microRNAs in melanoma immunity, it should be noted that OXPHOS was the most significantly inversely correlated gene set identified in the 'MITF-low' microRNA-mRNA. There is some recent evidence for the role of OXPHOS and melanoma immune evasion [183-185]. In this study, melanoma brain metastases with lower OXPHOS gene expression were associated with higher immune infiltration. We can therefore speculate that 'MITF-low' microRNAs and associated inverse correlation of OXPHOS gene expression may influence melanoma immunity, although this would require further investigation.

Beyond the 'MITF-low' microRNAs, we found a trend towards higher miR-146a-5p expression in melanomas that did not receive clinical benefit, although this result did not reach statistical significance, possibly due to the small cohort size. This aligns with a pre-clinical model of miR-146a-5p in melanoma association with resistance to immunotherapy and also highlights a potential dichotomy between 'keratin' and 'MITF-low' associated microRNAs and immunotherapy responses [137].

CHAPTER FIVE

DISCUSSION AND FUTURE DIRECTIONS

DISCUSSION

Summary of all MicroRNA Analyses

We undertook parallel and partially overlapping approaches to identification of microRNAs implicated in melanoma immunity and resistance to anti PD-1 immunotherapy. We were able to identify multiple microRNAs by each method, however not every microRNA was included in every analysis. To summarize the data we collected for each microRNA, I have included a table (Table 5.1). There are few microRNAs that we were able to collect comprehensive experimental and clinical data from because they were primarily identified by different aims within this project and we did not have time to cross-validate each microRNA, particularly experimentally with cytokine secretion and T-cell killing assays. Below is a discussion of our findings for each methodology used and the microRNAs subsequently identified. Briefly these can be classified into three categories; 1- MicroRNAs with strong prognostic value in TCGA data and experimental evidence for roles in regulating immune pathways and processes but no evidence of differential expression in clinical specimens (miR-155-5p). I discuss below the reasons why miR-155-5p may not be identified as predictive in anti-PD-1 treated patients due to opposite effects in different cell types in the tumour microenvironment and further analysis and experiments that could resolve this 2. MicroRNAs with evidence of differential expression in clinical specimens and some experimental evidence of immune modulation but little association with survival and no association with immune markers or prognostic value in

TCGA (miR-205-5p, miR-200b). 3. MicroRNAs with strong associations with survival in anti-PD-1 treated melanoma patients but with no association with immune markers or prognosis in TCGA (miR-100-5p, miR-125b-5p). These microRNAs are of great interest as discussed below as they may represent a subtype of melanoma with a distinct phenotype with as-yet undescribed sensitivity to anti-PD-1 immunotherapy and/or a potential predictive biomarker in this setting. I describe in the future directions section experiments that could be performed to elucidate this.

Identification of Immune-Associated MicroRNAs in TCGA Melanoma Samples

A comprehensive analysis of TCGA melanoma tissue identified 5 microRNAs with strong associations with immune infiltration and rational validated immune targets that may explain these associations. We were able to demonstrate in melanoma cell lines that these microRNAs can regulate their predicted immune targets in this disease and may offer potential mechanisms for modulating the melanoma tumor microenvironment. Of these microRNAs miR-155-5p had the most profound biological effects *in vitro*.

Table 5.1 Summary of MicroRNA Analyses

MicroRNA	TCGA Microenvironment Cluster Association	Melanoma Cell Line Expression	Immune Cell Expression (DICE)	Prognostic Association (TCGA)	Regulates Cytokine Secretion *in vitro*	Alters Sensitivity to T-Cell Killing *in vitro*	Associated With PD-1 Inhibitor Response	Associated with prolonged survival with PD-1
146b-5p	Immune	Yes	No	Positive	N/A	N/A	No	No
155-5p	Immune	Yes	Yes	Positive	Yes Increase	Desensitization 4/4 Cell Lines	No	No (Negative trend)
1976	Immune	Yes	No	Positive	N/A	N/A	No	No
361-3p	Intermediate Immune	Yes	No	Positive	N/A	N/A	No	No
142-5p	Immune	Yes	Yes	Positive	N/A	N/A	No	No
31-5p	N/A	No	No	No	N/A	No Effect	Yes Positive	No

1246	Intermediate Melanoma	Yes	N/A	No	N/A	N/A	Yes Positive	No
34c-5p	N/A	No	No	No	N/A	N/A	Yes Negative	No
203a-3p	Intermediate Melanoma	Yes	No	No	N/A	N/A	Yes Positive	No
203b-5p	N/A	No	No	N/A No	N/A	N/A	Yes Positive	No
205-5p	Intermediate Melanoma	Yes	No	No	N/A	Desensitisation 2/4 Cell Lines	Yes Negative	No
200b-3p	Intermediate Immune	No	No	No	N/A	Desensitization ¼ Cell Lines	Yes Negative	No
7705	N/A	No	N/A	N/A	N/A	N/A	Yes Negative	No
125b-5p	Stromal / MITF low	Yes	No	No	N/A	N/A	Yes Positive	Yes Positive

100-5p	Stromal / MITF low	Yes	No	No	N/A	N/A	Yes Positive	Yes Positive

MiR-155-5p

High expression of miR-155-5p was correlated with immune markers in TCGA melanoma samples and was associated with improved OS in those patients. Sequencing data from melanoma and immune cell lines showed that miR-155 was expressed in melanoma cells and in activated T-cells. While there is abundant evidence for the activating role of 155-5p in T-cells, its immune role in melanoma cells is poorly defined. The data from this assay suggests that miR-155-5p in tumor cells could contribute to immune evasion which would contradict the survival benefit associated with miR-155-5p expression in the TCGA. Based on this data I would reason that improved OS survival associated with miR-155-5p in TCGA patients is due to a) miR-155-5p expression and activity in immune cells and/or b) a tumor suppressor role in melanoma that is more significant than its effect on immune evasion. Further investigation of the differential effects of miR-155-5p is required to determine the cell-specific effects in the tumor microenvironment (see future directions)

Identification of MicroRNAs Associated with Clinical Response to PD1 Inhibitors

Using RNA and small RNA sequencing we were able to identify 8 microRNAs with significant differential expression between melanoma patients who did or did not receive clinical benefit from PD1 inhibitors, furthermore we were able to experimentally validate these microRNAs in a T-cell-melanoma co-culture assay: miR-31-5p was overexpressed in responding lesions and therefore hypothesized that is would sensitize melanoma cells to

T-cell killing. With this assay I did not observe any effect of miR-31-5p on sensitivity to T-cell killing in any of the 4 cell lines tested. This data suggests that miR-31-5p expression in melanoma cells does not affect direct interactions with cytotoxic T-cells and its association with response to immunotherapy may be through a separate mechanism such as mediating immune infiltration or through activity in other cell types such as immune cells. miR-200b-3p was overexpressed in non-responding lesions to PD-1 checkpoint blockade and therefore I hypothesized miR-200b-3p would protect melanoma cells from T-cell killing. This was the case in 2/4 cell lines. miR-205-5p, like miR-200b-3p, was overexpressed in non-responding lesions to PD-1 checkpoint blockade. Again I hypothesized this microRNA would protect melanoma cells from T-cell killing and this was the case in 3/4 cell lines. The data from miR-200b-3p and miR-205-5p suggests that individually they can regulate sensitivity to T-cell killing in some but not all melanomas. Interestingly, while miR-200b-3p shows activity in 2/4 and miR-205-5p shows activity in 3/4 cell lines, every cell line tested was affected by at least one of these two microRNAs. Further investigation of the mechanism of action for both of these microRNAs may reveal important immunoregulatory pathways that could be exploited for melanoma immunotherapy. Since only a modest effect on sensitivity to T-cell killing was observed it is important to identify the cell type or types within the tumor microenvironment that these microRNAs are expressed in and therefore biologically active in as described in the future directions section below. The T-cell killing assay we used was a reductive experiment with only a fraction of the factors present in the tumor microenvironment and it is therefore necessary to use a more complete model of tumor immunity. With this information we can design syngeneic mouse models with conditional expression of our

microRNAs of interest in the relevant cell types. Using this model it would be possible to identify how the tumor microenvironment is altered depending on expression of each microRNA by measuring tumor, immune and stromal cell populations in models with high or low target microRNA both with and without immunotherapy intervention. Furthermore, specific effects on gene expression could be measured with microRNA-mRNA reporter assays and downstream protein quantification by western blot or a multiplex method such as RPPA. Measuring the dependence of any phenotype on the expression of specific proteins targeted by our microRNAs of interest may reveal the mechanisms that these microRNAs can regulate immunotherapy responses.

After extensive analysis of the microRNA sequencing data in our melanoma patient cohort, we recognized that using the binary clinical benefit endpoint was very sensitive to changes in sample classification. For example, when we included lesion specific responses we changed the definition of one sample between clinical benefit and non-clinical benefit. In a cohort of 22 patients, this had significant effects on the differential expression analysis. We also noted significant differences in differential expression analysis when we compared samples based on their membership of transcriptomic groups or strictly by RECIST response. We therefore determined that identifying microRNAs associated with PFS and OS outcomes after anti-PD-1 therapy was a more robust method than associations with response. This is regarded as the gold standard for immunotherapy due to the atypical kinetics of immunotherapy with regard to tumor responses as traditionally measured by RECIST. Furthermore, we reasoned that we should limit our model to microRNAs that we know are significantly associated with gene expression in melanoma to improve the

statistical power of our analysis, considering the small cohort of PD1 inhibitor treated patients.

To this end I used network analysis to identify microRNA-mRNA associations in melanoma tumors (SKCM TCGA) and in melanoma cell lines (MD Anderson Melanoma Cell Line Cohort). I then used Cox's proportional hazard model to identify associations with PFS and OS in our pre-PD1 treated melanoma patient samples from the top 18 microRNAs identified in the network analysis. This approach determined that miR-100-5p and miR-125b-5p were significantly associated with improved OS and PFS in patients treated with anti-PD-1 therapy. Furthermore these two microRNAs represent a distinct microRNA-mRNA network that does not overlap with other microRNA-mRNA networks identified in our samples.

Further clinical and experimental validation of these targets are warranted to translate these findings into potential clinically useful targets.

FUTURE DIRECTIONS

Although we have extensively studied expression of microRNA and their associations with immune features in melanoma and identified several specific microRNAs with statistical associations with response and survival outcomes to PD-1 checkpoint blockade, the mechanisms that underlie these associations remain poorly defined and warrant further investigation. Here I will discuss the research that I think is the logical continuation of this project to address the questions we have raised and demonstrate clinical relevance.

Resolution of Tissue Level Sequencing

One of the challenges of RNA sequencing of RNA extracted from homogenized tumor is the inability to attribute the signal we see to specific components of the tumor microenvironment. We know that different cell lineages present in the tumor microenvironment have distinct RNA and microRNA expression profiles and the data we receive from whole tumor sequencing is an average of the values across multiple cell types including immune, stromal and tumor cells. Further complicating the data we see is the variation in tumor microenvironment composition between patients and even in tumors from the same patient and even in different locations within the same tumor. We are therefore unable to definitively attribute the source of differential expression of any of the genes we identify; do they represent a genuine biological difference within melanocytes, stromal cells or immune cells between responding or non-responding lesions or are they merely acting as biomarkers for the abundance of these different cell types which also governs response?

To answer this question we need to separately sequence the different constituents of the tumor microenvironment. Single cell sequencing would provide the highest resolution although the current technical and financial constraints on this technology may prohibit a significant study [186, 187]. For the purposes of resolving expression between cell types, single cell resolution is likely not required and could be achieved by FACS enumeration and sorting cells by expression of lineage markers and sequencing the resulting populations. Other in situ gene expression methods may also be useful to study intra tumoral heterogeneity [188].

As we have shown here, the activity of certain genes can lead to competing phenotypes within the tumour microenvironment. For example miR-155-5p is an established marker

of immune activation and expressed in high levels in cytotoxic T-cells. Conversely, we have shown that expression of miR-155-5p in melanoma tumour cells has an immune-protective effect. Tissue level resolution of miR-155-5p is therefore unable to differentiate potentially beneficial expression in T-cells compared to possible detrimental expression in melanoma cells. Thus, the absence of miR-155-5p enrichment in either responding or non-responding melanoma tumours is inconclusive and requires further investigation.

Additionally, I believe this would help improve the power of the statistical analysis of other microRNAs including miR-100-5p and miR-125b-5p which are both known to be expressed in tumour and stromal cell populations such as fibroblasts, which may be immunosuppressive, in contrast to our dataset which shows that tissue expression of miR-100-5p and miR-125b-5p is associated with improved overall survival, indicating contrasting immune effects in different components of the tumor microenvironment [182]. Identifying the source of each microRNA will allow us to investigate the mechanism of that microRNA in the appropriate cell type.

Experimental Validation of Clinically Relevant MicroRNAs

While we were able to identify numerous microRNAs associated with different immune features and with PD-1 inhibitor responses in melanoma, we have only been able to perform limited functional validation of these genes, particularly those that were identified in the clinical cohort, which took longer to identify. Future experiments using miR-100-5p and miR-125b-5p conditional knockout cell lines *in vitro* and *in vivo* models of tumor immunity will be required to elucidate the role these microRNAs have in melanoma immunity.

There are several outstanding questions concerning the role of miR-100-5o and miR-125b-5p in melanoma immunity: Primarily, are miR-100-5p and miR-125b-5p directly regulating genes that are mediating resistance/sensitivity to immunotherapy or are they biomarkers of a differential immune phenotype i.e. are these microRNA associations with PD-1 response correlative or causative. We could initially test the effect of these microRNAs on gene expression and determine if these microRNAs are key regulators of this gene expression profile or a dependent covariate incidentally associated with the observed transcriptomic profile. Although we performed comprehensive correlation analysis of these microRNAs with mRNA expression in melanoma and tissue, it is not sufficient to conclude that these genes are directly regulated, indeed there was no enrichment for predicted miR-100-5p or miR-125b-5p targets within the inversely correlated mRNA network that we identified, suggesting any association with these specific genes is indirect. To test this we must show that miR-100-5p and miR-125b-5p expression regulates target gene expression in melanoma (either in melanoma cell lines or other microenvironment populations). This can be tested using reporter assays for microRNA-mRNA binding which can empirically measure the mRNAs that are bound in melanoma by these microRNAs. Measuring downstream protein expression as described above could provide further evidence for actual miR-100-5p / miR-125b-5p regulation of specific protein expression in melanoma. Further, if as suspected these microRNAs do not directly regulate the target genes, we can focus on their interaction with other regulators of gene expression such as transcription factors. Functional validation of these microRNAs with an immune endpoint should also be investigated. This can initially be the assays we have established during this project such as multiplex cytokine secretion and or T-cell

killing assays *in vitro*. Additional in vivo experimental models as described above would also be of use, testing the role of these microRNAs in melanoma cells and also in stromal cell populations in a more complete model of tumor immunity.

Furthermore in the event that specific modulation of these microRNAs does not affect tumour immunity, it would be of interest to address if the phenotype they are associated with i.e. a mesenchymal like melanoma had experimental differences to immune therapy. These experiments could be wide ranging, including screening a large panel of melanoma cell lines with melanocytic vs mesenchymal-like properties for their immune phenotypes i.e. MHC expression, cytokine secretion and T-cell killing sensitivity. Experimentally induced epithelial to mesenchymal transition in a syngeneic mouse model of melanoma would also be a powerful tool to measure the contribution of this phenotype to immune evasion. Proliferation, migration and other metabolic features could also be tested which could test potential non-immune specific mechanisms of better outcomes.

In Vitro MicroRNA Gain of Function Screening

Lentiviral gain of function screens are powerful genetic screening tools that allow us to identify genes that regulate specific phenotypes. Before the laboratory shutdown and restrictions on on-campus movement between research buildings we were part-way through a gain of function pooled microRNA screen testing the effect of each human microRNA on the sensitivity of melanoma cell lines to T-cell killing. The aim of this experiment was to use an unbiased screening approach to identify microRNAs that can mediate melanoma sensitivity to T-cell killing**.** We planned to identify candidate microRNAs by transfecting melanoma cell lines with a pooled-gain-of-function-lentiviral-library covering all annotated human microRNAs and measuring enrichment and depletion

of specific microRNAs after a T-cell killing assay described above. We would then identify the mechanism of immune-associated microRNA activity in melanoma by identification of differentially expressed proteins by RPPA in microRNA-transfected cell lines vs control. We can then test if the candidate microRNA directly or indirectly targets the mRNA of that protein and if targeting that protein using an independent method reproduces the immune phenotype induced by exogenous expression of the microRNA of interest.

Completion of these experiments will identify microRNAs that could regulate melanoma immunity and resistance to immunotherapy, providing important new therapeutic targets.

CHAPTER SIX
MATERIALS AND METHODS

TCGA Melanoma (SKCM) Dataset:

Normalized mRNA (FPKM) and microRNA (RPM) counts from 368 metastatic melanoma tumors were downloaded from http://gdac.broadinstitute.org/. We applied a purity filter removing samples with <80% tumor nuclei leaving 322 samples for further analysis.

Melanoma Cell Line dataset:

Normalized mRNA (FPKM) and microRNA (RPM) counts were generated from a cohort of metastatic melanoma patients at The University of Texas MD Anderson Cancer Center as previously described [189, 190]. Genomic data are available from the European Genome-Phenome Archive (EGA) under accession EGAS00001004536 upon valid request to the applicable Data Access Committee as indicated via the EGA.

Pre-PD-1 Treated Cohort of Melanoma Patients

Twenty-nine patients with AJCCv8 stage III or IV melanoma undergoing PD-1 immune checkpoint blockade at the University of Texas MD Anderson Cancer Center were included in this study (Table 1). All patients had cutaneous-type or unknown primary melanoma. \ Twenty (67%) patients were male, nine (31%) patients were female. Seventeen (59%) patients had prior ipilimumab treatment. Pre-treatment biopsies were consented and collected under institutional-review-board-approved no more than 6 months prior to commencement of pembrolizumab or nivolumab therapy and with no intervening therapy. Best Overall Response (BOR) was calculated using RECIST 1.1 criteria Fourteen

(48%) patients were classified as receiving clinical benefit (BOR; stable disease >6months, complete or partial response), while Fifteen (52%) patients were classified as not receiving clinical benefit (BOR; progressive disease). Survival statistics were calculated from the start date of PD-1 inhibitor treatment. Median Progression-Free Survival (PFS) in the non-clinical benefit group was 83 days (range; 20-NA), median PFS was not reached in the responder group (range; 257-NA). Lesion specific responses were available for thirteen (45%) patients where incisional biopsies were performed.

mRNA & MicroRNA Expression Analysis in clinical samples: Total RNA was extracted from snap-frozen macrodissected melanoma tumors using the AllPrep DNA/RNA/miRNA Universal Kit (Qiagen) and quality assessed using the Agilent 2100 Bioanalyzer. 40-80ng of total RNA was used as input for library preparation with the Illumina TruSeq RNA Access library prep kit following the manufacturer's instructions. 12-plex sequencing pools were sequenced using one high-output run of 76bp paired-end reads on an Illumina NextSeq 500 system at the University of Texas MD Anderson Cancer Center Sequencing and Microarray Facility (SMF). Fastq files underwent quality control using FastQC (v0.11.5) and removal of reads containing 15 contiguous low-quality bases (phred score <20) prior to STAR 2-pass alignment (v2.5.2b) to Gencode v19 with default parameters followed by post-alignment quality assessment using RNASeQC (v1.1.8). After sample-level merging of BAM files removing one pool having poor Spearman correlation to a duplicate pool from the same sample, reads were quantified using htseq-count (v0.6.1) and normalized into fragments per kilobase of transcript per million mapped reads (FPKM). For microRNA sequencing, total RNA samples was used as input for small RNA sequencing library preparation using the unique molecular identifier enabled QIAseq

miRNA Library Kit (Qiagen). Samples were sequenced using 76bp single end reads on an Illumina NextSeq 500 and raw UMI count data generated using the QIAseq miRNA analysis pipeline available at geneglobe.qiagen.com. Secondary analysis was performed in R using the DESeq2 package for differential expression analysis and count normalisation using the variance stabilizing transformation (vst) method.

MCP Counter

We used MCP counter to estimate relative and absolute abundance of the component cell types of the tumour microenvironment, including various immune and stromal cell populations from RNA sequencing data. We used the 'MCPCounter' R package (https://github.com/ebecht/MCPcounter) as previously described [161].

Cox Proportional Hazard Model

Samples were stratified either into two groups, either above or below the median expression of the predictor variable, or into tertiles. The survival variable of each group, either time to a progression event (Progression free survival analysis) or a death event (Overall survival analysis), was then tested using Cox's proportional hazard model using the R function 'coxph' from the R package 'survival' (https://cran.r-project.org/web/packages/survival/index.html) Hazard ratios are reported ±95% Confidence Intervals. R functions were used with default settings as described in the user guide.

Kaplan Meier Curves

Samples were stratified into two or three groups based on expression of the predictor variable as described for the cox-proportional hazard model. Kaplan Meier curves and log-

rank p-values comparing overall survival or progression free survival for each variable were generated using the R functions 'survfit' and 'ggsurvplot' from the R package 'Survminer' (https://cran.r-project.org/web/packages/survminer/index.html) R functions were used with default settings as described in the user guide.

Correlation Analysis

Correlation analysis of microRNA expression with other molecular features of melanoma samples was performed using Spearman correlation analysis using the R function 'rcorr()' in the 'Hmisc' package (https://cran.r-project.org/web/packages/Hmisc/index.html).

Bipartite Network Analysis

Input data for bipartite network analysis was Spearman's correlation coefficients from global correlation analysis of microRNA and mRNA expression, as described above, in TCGA melanoma samples and separately in the melanoma cell line cohort. Correlation data was formatted in three column dataframes for bipartite network analysis, with column 1 containing the microRNA name, column 2 containing the mRNA name and column 3 containing the correlation coefficient for each pair. MicroRNA-mRNA correlations were filtered to exclude all microRNA-mRNA pairs that did not show strong negative associations indicative of microRNA suppression of gene expression (Spearman's rho <-0.4, <-0.6 in TCGA and cell lines respectively). Igraph network objects were created from dataframes containing filtered correlation data using the R function 'graph_from_data_frame' in the 'igraph' package (https://cran.r-project.org/web/packages/igraph/index.html). Igraph objects were assigned bipartite mapping using the R function 'bipartite_mapping' in the 'igraph' package. The network

statistic ‘degree centrality’ was then called for each microRNA in the igraph object which was then used to filter the microRNAs with the fewest mRNA associations (<15, <100 in TCGA and cell line datasets respectively). Incidence matrices of all remaining microRNA:mRNA correlations were generated using the R function ‘as_incidence_matrix’ in the ‘igraph’ R package. Bipartite networks were then projected from the igraph objects using the R function ‘visIgraph’ with the ‘layout_nicely’ layout from the ‘visNetwork’ package (https://cran.r-project.org/web/packages/visNetwork/index.html).

Unipartite Network Analysis

Unipartite (one-mode network) igraph objects were generated from the igraph objects from bipartite network analysis described above using the R function ‘bipartite.projection’ from the ‘igraph’ package. Adjacency matrices for each dataset were generated using the R function ‘as_adjacency_matrix’ from the ‘igraph’ package. The following network statistics were calculated for each microRNA; Degree centrality, betweenness centrality, closeness centrality and eigen centrality. Unipartite networks were generated using the base R function ‘plot’ with the igraph layout ‘graphopt’. The thickness of edges between microRNA vertices were based on the edge weight.

Gene Set Enrichment Analysis

GSEA was performed through the Broad Institutes Molecular Signature Database website (https://www.gsea-msigdb.org/gsea/msigdb/annotate.jsp). Gene set overlaps were compared with the ‘H: Hallmark gene sets’. The top 10 gene sets with an FDR q-value <0.05 are reported.

Predicted and Validated MicroRNA Target Databases

The database of experimentally validated microRNA targets, miRTarBase v8, was downloaded (http://mirtarbase.cuhk.edu.cn/php/download.php). MicroRNA targets were filtered based on the strongest evidence of regulation (Reporter assays, Western blot and qPCR)

A database of predicted microRNA targets, TargetScan v7.2, was also downloaded (http://www.targetscan.org/cgi-bin/targetscan/data_download.vert72.cgi).

Cell Culture

For microRNA studies, human melanoma cell lines, from the adoptive T-cell therapy program described above, were cultured in complete media at 37ºC and 5% CO2 for a maximum of 5 passages before experiments were performed. Cell lines were maintained in the logarithmic growth phase and were passaged when they reached 70-80% confluence at ratios optimised for each cell line used. For each passage, cells were washed x2 with ice cold PBS before incubation with 0.25% trypsin [GIBCO] until cells detached. Trypsin was immediately neutralized using complete media. Cells were then spun @180RCF for 5 minutes to pellet. Media was aspirated before cells were resuspended in 1ml ice cold PBS to wash. A 10ul aliquot was taken at this stage for cell counting by haemocytometer or cellometer using manufacturer's instructions. The washed cells were spun again at 180RCF for 5 minutes to pellet and PBS aspirated. Cells were then resuspended in complete media at 1*10^6 cells per ml for downstream applications. Cell lines were STR fingerprinted and regularly confirmed as mycoplasma negative as described above.

Transient MicroRNA Transfections

For Transient microRNA transfections cells were seeded in complete media at normal densities to maintain logarithmic growth in either 96 well, 12 well, 6 well or t25 flasks depending on the number of cells required per experiment. After 8 hours of culture for firm attachment to take place, complete media was aspirated and cells were gently washed in ice cold PBS x2.

Transient transfections were achieved by culturing target melanoma cell lines with the desired miRIDIAN microRNA mimics or inhibitors (Dharmacon) at a concentration of 10nm in serum-free OptiMEM media for 16 hours. We used a cationic lipid transfection reagent, Dharmafect (Dharmacon), at a concentration of 2µl/ml according to manufacturer's instructions to facilitate transfection. Concentration of transfection reagent was optimized per cell line by measuring transfection efficiency of a fluorescently labelled microRNA mimic control (Dharmacon) by fluorescent microscopy). After transfection, transfection media was aspirated and cells washed 1x with ice cold PBS before cells were returned to standard culture conditions for 72hrs for microRNA phenotypes to manifest before downstream applications.

RNA Extractions, cDNA & Mature microRNA preparations.

RNA Extractions from cell lines for downstream applications was performed using Norgen Total RNA Purification Kit (Norgen Biotek) using manufacturer's instructions. In short, cell lines were harvested from 6-well plate cultures at 80% confluency (0.5-1 x 106 cells). Culture media was then aspirated and cells were gently washed twice with ice cold PBS. PBS was aspirated and 350µl lysis buffer was added to each well of the plate for 5 minutes with gentle agitation. Lysate was transferred to a microfuge tube and mixed with 200µl 100% ethanol and samples were vortexed for 10 seconds. All lysate was then bound to

columns and centrifuged at 3500 RCF for 1 minute and flow through discarded. Columns were then washed x3 with 400µl and spun at 3500 RCF for 1 minute. Column was then dried by spinning for 2 minutes at 14,000 RCF. RNA was then eluted from the column using elution buffer supplied with the kit. 50µl elution buffer was added to each column and then spun for 2 minutes at 200 RCF and then 1 minute at 14,000 RCF. RNA quantity and quality was then assessed using Nano Drop One (ThermoFisher Scientific), using Norgen Biotek elution buffer as blank calibration samples. RNA samples with 260/280 ratios <1.9 were rejected and extraction repeated. Samples were stored at -20ºC for short-term storage (<1 week) prior to downstream applications or stored for up to 12 months at -80ºC if required.

cDNA was generated from total RNA using High-Capacity cDNA Reverse Transcription Kit (Applied Biosystems) using the manufacturer's instructions. In brief, 500ng total RNA was added to cDNA master mix including reverse-transcription buffer, dNTP mix, reverse-transcription random primers, MultiScribe reverse transcriptase and RNase inhibitor supplied with kit at recommended concentrations. Thermal cycling conditions were as follows: Step 1 at 25ºC for 10 minutes, step 2 at 37ºC for 120 minutes, step 3 at 85ºC for 5 minutes before sample returned to 4ºC for downstream use or freeze at -20ºC or -80ºC for short or long term storage respectively.

Mature microRNA cDNA was generated from total RNA using Taqman Advanced miRNA cDNA Synthesis Kit (ThermoFisher Scientific) and using manufacturers instructions. In brief, 10ng of total RNA was used per reaction. RNA was polyadenylated using polyA buffer, PolyA enzyme and ATP supplied with kit at recommended concentrations for 45 minutes at 37ºC before the reaction was stopped at 65ºC for 10 minutes and then returned

to 4ºC before ligation. The ligation was performed using RNA ligase, ligation adaptor, ligase buffer and PEG 8000 supplied with kit at recommended concentrations for 60 minutes at 16ºC and then returned to 4ºC before reverse transcription. Reverse transcription was performed using universal reverse transcription primer, reverse transcription enzyme, dNTP mix and reverse transcription buffer provided with the kit at recommended concentrations at 42ºC for 15 minutes before the reaction was stopped at 85ºC for 5 minutes and then returned to 4ºC before the miR-amplification reaction. The miR-amplification reaction was then performed using miR-amplification master mix and primer mix supplied with the kit at the recommended concentrations using the following cycling conditions: Enzyme activation at 95ºC for 5 minutes x1, denature at 95ºC for 3 seconds and anneal/extension at 60ºC for 30 seconds x14, stop reaction at 99ºC for 10 minutes, then return sample to 4ºC for downstream use or freeze at -20ºC or -80ºC for short or long term storage respectively.

All reactions were performed using a Mastercycler Nexus thermocycler (Eppendorf)

qPCR

qPCR reactions were performed in MicroAmp EnduraPlate Optical 96-Well Fast Celar Reaction plates (Applied Biosystems) on QuantStudio Flex analyser (Applied Biosystems). Data was analysed using QuantStudio 6 & 7 Flex Real Time PCR System Software v1.0 (Applied Biosystems).

MicroRNA PCR reactions were performed using 5 µl of 1:10 diluted template from advanced microRNA synthesis reaction described above. Assays were repeated with undiluted template if sample was below detection threshold. 1 µl Taqman advanced

miRNA assay (Applied Biosystems) corresponding to the desired target microRNA, 10 µl Taqman Fast Advanced Master Mix x2 (Applied Biosystems) and 4 µl PCR-grade water were added to each template for a 20 µl reaction. Thermal cycling conditions were set as follows:

Enzyme activation – 20 seconds @ 95 ºC x1.

Denature – 1 second @ 95 ºC, Anneal/Extend 20 seconds @ 60 ºC x40.

Number of target copies per reference gene was calculated by comparing CT values from duplicate reactions of target microRNAs compared to CT values from duplicate reactions of stably expressed microRNAs – miR-103a-3p, 423-3p, 26a-5p. Comparisons were made independently for each cell line used in the experiment.

For qPCR of cDNA synthesized from total RNA we used SYBR green reactions per manufacturer's instructions. Briefly, 0.3 µl of each forward and reverse primer (Sigma) for each target were added to 3.75 µl SensiMix SYBR No-Rox (meridian Bioscience) and 1.15 µl PCR-grade H2O. 2.5 µl of 1:10 diluted template from cDNA reaction described above was added to each reaction for a total volume of 8 µl. Thermal cycling conditions were as follows:

Denature template – 1 minute @ 94 ºC, anneal primers – 2 minutes @ 55 ºC, Extension – 3 minutes @ 72 ºC x40.

The number of target copies per reference gene was calculated as described above but using GAPDH as the reference gene.

Legendplex Cytokine Panel

To measure cytokine secretion from melanoma cell lines we quantified expression of a customized panel of melanoma and immune specific cytokines using a custom, multiplexed, flow cytrometry, bead-based, immuno-assay, LEGENDplex (Biolegend). The custom panel contained the following target cytokines: IL-1a, IL-1b, IL-2, IL-6, CCL2 (MCP1), IL-10, TNF-a, TNF-b, IFN-g and VEGF. All assays were performed according to manufacturer's instructions. In brief, cell lines were cultured until 70% confluent in normal culture conditions. Growth medium was replaced 24 hours before assay with fresh media with additional 10nM TNFa to stimulate cytokine secretion. Cell culture media was collected and centrifuged to remove cell debris and was assayed immediately without dilution. For cell lines that had undergone transient microRNA transfections (described above), cell culture supernatant was assayed 96hrs after transfection in the same manner i.e. fresh media was applied for the purpose of cytokine collection 72 hours post-transfection.

Standard curves for each analyte were generated by serially diluting each standard (supplied with kit) 1:4 with assay buffer (supplied with kit) six times to generate a 7 point dilution from undiluted to 1:4096 dilution and a blank standard consisting of only assay buffer.

Samples were assayed in duplicate on a 96-well v-bottomed plate. 25µl of standard or cell culture supernatant was added to 25µl assay buffer. Mixed assay beads were vortexed before adding 25µl to each sample and incubated for 2hrs with moderate shaking at room temperature protected from light. Plates were centrifuged at 250 RCF for 5 minutes to pellet beads. Supernatant was discarded and plate was washed with 200µl of wash buffer per well before pelleting beads and discarding wash buffer. 25µl of detection antibodies were then

added to each well before incubating for 1 hour at room temperature while shaking at 800rpm protected from light. 25µl of SA-PE was then added directly to each well and plate was returned to the plate shaker for an additional 30 minutes. Beads were then pelleted and washed as above before each sample was resuspended in 150µl of wash buffer ready for FACS acquisition.

For data collection plates were loaded onto a BD Accuri C6 cytometer (BD Biosciences). Samples were gated on size to count only LEGENDplex beads A&B. 20,000 beads per sample were acquired and data saved as FCS files. FCS files were analysed using LEGENDplex data analysis software which quantified cytokine levels per sample by comparing mean fluorescence intensity values from each bead population against standard curves from known cytokine concentrations.

HLA & PDL1 Flow Cytometry

To quantify surface HLA-ABC and PD-L1 expression on melanoma cell lines we harvested cells at 70% confluence by trypsinisation then washed in ice cold PBS twice. One million cells were resuspended in 1ml ice cold FACS buffer (PBS, 10% FBS, 1% sodium azide). 50µl of each sample (5*104 cells) was added to a round bottom 96-well plate in duplicate for staining. Samples were stained using directly conjugated anti PD-L1 (APC anti-human CD274/ B7-H1/ PD-L1, clone:29E.2A3, Biolegend) or anti HLA-ABC (HLA-ABC Monoclonal Antibody, W6/32, FITC, eBioscience) antibodies at a concentration of 1:100 in 50µl FACS buffer for 1 hour at room temperature in the dark. Samples were centrifuged at 400 RCF for 5 minutes and washed with 100µl FACS buffer twice. Live/Dead staining for cell viability was achieved by adding 5µl of propidium iodide (PI) staining solution (10µg/ml in PBS) to each sample immediately prior to acquisition.

Sample acquisition was performed using a BD Accuri C6 cytometer (BD Biosciences) and samples were gated based on cell size and negative PI staining. Mean Fluorescence intensity for PD-L1 and HLA was measured from 10,000 live cells.

T-Cell Co-Culture Experiments and Chromium Release Assay

Melanoma sensitivity to T-cell killing was quantified using a chromium (Cr-51) release assay performed on melanoma cells that had been co-cultured with MART-1-specific human cytotoxic T-cells.

MART-1-specific T-cells were generated and prepared for the killing assay as previously described [191, 192]. Melanoma cell lines were tested for MART-1 expression by flow cytometry and HLA matched prior to assay. Melanoma negative controls included MART-1 + / HLA mismatched cells, MART-1 - / HLA matched cells, MART-1 - / HLA mismatched cells cell line. For co-culture assay, melanoma cell lines were cultured until 70-80% confluency under normal cell culture conditions. Cell lines that had undergone transient microRNA transfections (as described above) were harvested 72hrs post-transfection. Cells were detached by trypsinisation, washed, counted and resuspended at 2*106 cells/ml in complete media. For Cr-51 pulsing, enough cells for 2000 per co-culture condition were transferred to a 15 ml conical and diluted to the nearest whole ml with complete media. In a radioactive material designated lab, 100µl of 0.1 mCi Cr-51 was added per ml of cells and incubated for 1 hour. Cells were thoroughly washed by centrifugation and resuspension in fresh complete media twice before resuspending cells at a concentration of 2*104 cells per ml in complete media. 100 µl of this cell suspension was then added to the appropriate wells of a u-bottomed 96-well plate for co-culture. 100 µl of T-cells were then added to each well at concentrations to achieve effector to target

(E:T) ratios between 5:1 to 20:1 as optimized per cell line. Negative controls consisted of wells containing only target cells with no effector cells to measure baseline Cr-51 release. Positive controls consisted of wells containing target cells and trypan lysis buffer to measure complete Cr-51 release. After a 4 hour incubation 30µl of supernatant from each condition was transferred to a LumaPlate-96 (PerkinElmer) and allowed to dry overnight. The LumaPlates were read the following day and Cr-51 release was calculated as a percentage of total Cr-51 (positive control) minus baseline Cr-51(negative control) release.

BIBLIOGRAPHY

1. Sosman, J.A., K.B. Kim, L. Schuchter, R. Gonzalez, A.C. Pavlick, J.S. Weber, G.A. McArthur, T.E. Hutson, S.J. Moschos, K.T. Flaherty, P. Hersey, R. Kefford, D. Lawrence, I. Puzanov, K.D. Lewis, R.K. Amaravadi, B. Chmielowski, H.J. Lawrence, Y. Shyr, F. Ye, J. Li, K.B. Nolop, R.J. Lee, A.K. Joe, and A. Ribas, *Survival in BRAF V600-mutant advanced melanoma treated with vemurafenib.* N Engl J Med, 2012. **366**(8): p. 707-14.
2. Davies, H., G.R. Bignell, C. Cox, P. Stephens, S. Edkins, S. Clegg, J. Teague, H. Woffendin, M.J. Garnett, W. Bottomley, N. Davis, E. Dicks, R. Ewing, Y. Floyd, K. Gray, S. Hall, R. Hawes, J. Hughes, V. Kosmidou, A. Menzies, C. Mould, A. Parker, C. Stevens, S. Watt, S. Hooper, R. Wilson, H. Jayatilake, B.A. Gusterson, C. Cooper, J. Shipley, D. Hargrave, K. Pritchard-Jones, N. Maitland, G. Chenevix-Trench, G.J. Riggins, D.D. Bigner, G. Palmieri, A. Cossu, A. Flanagan, A. Nicholson, J.W. Ho, S.Y. Leung, S.T. Yuen, B.L. Weber, H.F. Seigler, T.L. Darrow, H. Paterson, R. Marais, C.J. Marshall, R. Wooster, M.R. Stratton, and P.A. Futreal, *Mutations of the BRAF gene in human cancer.* Nature, 2002. **417**(6892): p. 949-54.
3. Chapman, P.B., A. Hauschild, C. Robert, J.B. Haanen, P. Ascierto, J. Larkin, R. Dummer, C. Garbe, A. Testori, M. Maio, D. Hogg, P. Lorigan, C. Lebbe, T. Jouary, D. Schadendorf, A. Ribas, S.J. O'Day, J.A. Sosman, J.M. Kirkwood, A.M. Eggermont, B. Dreno, K. Nolop, J. Li, B. Nelson, J. Hou, R.J. Lee, K.T. Flaherty,

G.A. McArthur, and B.-S. Group, *Improved survival with vemurafenib in melanoma with BRAF V600E mutation.* N Engl J Med, 2011. **364**(26): p. 2507-16.

4. Hauschild, A., J.J. Grob, L.V. Demidov, T. Jouary, R. Gutzmer, M. Millward, P. Rutkowski, C.U. Blank, W.H. Miller, E. Kaempgen, S. Martín-Algarra, B. Karaszewska, C. Mauch, V. Chiarion-Sileni, A.M. Martin, S. Swann, P. Haney, B. Mirakhur, M.E. Guckert, V. Goodman, and P.B. Chapman, *Dabrafenib in BRAF-mutated metastatic melanoma: a multicentre, open-label, phase 3 randomised controlled trial.* Lancet, 2012. **380**(9839): p. 358-65.
5. Long, G.V., C. Fung, A.M. Menzies, G.M. Pupo, M.S. Carlino, J. Hyman, H. Shahheydari, V. Tembe, J.F. Thompson, R.P. Saw, J. Howle, N.K. Hayward, P. Johansson, R.A. Scolyer, R.F. Kefford, and H. Rizos, *Increased MAPK reactivation in early resistance to dabrafenib/trametinib combination therapy of BRAF-mutant metastatic melanoma.* Nat Commun, 2014. **5**: p. 5694.
6. Kwong, L.N., G.M. Boland, D.T. Frederick, T.L. Helms, A.T. Akid, J.P. Miller, S. Jiang, Z.A. Cooper, X. Song, S. Seth, J. Kamara, A. Protopopov, G.B. Mills, K.T. Flaherty, J.A. Wargo, and L. Chin, *Co-clinical assessment identifies patterns of BRAF inhibitor resistance in melanoma.* J Clin Invest, 2015. **125**(4): p. 1459-70.
7. Montagut, C., S.V. Sharma, T. Shioda, U. McDermott, M. Ulman, L.E. Ulkus, D. Dias-Santagata, H. Stubbs, D.Y. Lee, A. Singh, L. Drew, D.A. Haber, and J. Settleman, *Elevated CRAF as a potential mechanism of acquired resistance to BRAF inhibition in melanoma.* Cancer Res, 2008. **68**(12): p. 4853-61.
8. Emery, C.M., K.G. Vijayendran, M.C. Zipser, A.M. Sawyer, L. Niu, J.J. Kim, C. Hatton, R. Chopra, P.A. Oberholzer, M.B. Karpova, L.E. MacConaill, J. Zhang,

N.S. Gray, W.R. Sellers, R. Dummer, and L.A. Garraway, *MEK1 mutations confer resistance to MEK and B-RAF inhibition.* Proc Natl Acad Sci U S A, 2009. **106**(48): p. 20411-6.

9. Nazarian, R., H. Shi, Q. Wang, X. Kong, R.C. Koya, H. Lee, Z. Chen, M.K. Lee, N. Attar, H. Sazegar, T. Chodon, S.F. Nelson, G. McArthur, J.A. Sosman, A. Ribas, and R.S. Lo, *Melanomas acquire resistance to B-RAF(V600E) inhibition by RTK or N-RAS upregulation.* Nature, 2010. **468**(7326): p. 973-7.

10. Johannessen, C.M., J.S. Boehm, S.Y. Kim, S.R. Thomas, L. Wardwell, L.A. Johnson, C.M. Emery, N. Stransky, A.P. Cogdill, J. Barretina, G. Caponigro, H. Hieronymus, R.R. Murray, K. Salehi-Ashtiani, D.E. Hill, M. Vidal, J.J. Zhao, X. Yang, O. Alkan, S. Kim, J.L. Harris, C.J. Wilson, V.E. Myer, P.M. Finan, D.E. Root, T.M. Roberts, T. Golub, K.T. Flaherty, R. Dummer, B.L. Weber, W.R. Sellers, R. Schlegel, J.A. Wargo, W.C. Hahn, and L.A. Garraway, *COT drives resistance to RAF inhibition through MAP kinase pathway reactivation.* Nature, 2010. **468**(7326): p. 968-72.

11. Poulikakos, P.I., Y. Persaud, M. Janakiraman, X. Kong, C. Ng, G. Moriceau, H. Shi, M. Atefi, B. Titz, M.T. Gabay, M. Salton, K.B. Dahlman, M. Tadi, J.A. Wargo, K.T. Flaherty, M.C. Kelley, T. Misteli, P.B. Chapman, J.A. Sosman, T.G. Graeber, A. Ribas, R.S. Lo, N. Rosen, and D.B. Solit, *RAF inhibitor resistance is mediated by dimerization of aberrantly spliced BRAF(V600E).* Nature, 2011. **480**(7377): p. 387-90.

12. Straussman, R., T. Morikawa, K. Shee, M. Barzily-Rokni, Z.R. Qian, J. Du, A. Davis, M.M. Mongare, J. Gould, D.T. Frederick, Z.A. Cooper, P.B. Chapman, D.B.

Solit, A. Ribas, R.S. Lo, K.T. Flaherty, S. Ogino, J.A. Wargo, and T.R. Golub, *Tumour micro-environment elicits innate resistance to RAF inhibitors through HGF secretion.* Nature, 2012. **487**(7408): p. 500-4.

13. Jiang, X., J. Zhou, A. Giobbie-Hurder, J. Wargo, and F.S. Hodi, *The activation of MAPK in melanoma cells resistant to BRAF inhibition promotes PD-L1 expression that is reversible by MEK and PI3K inhibition.* Clin Cancer Res, 2013. **19**(3): p. 598-609.

14. Sullivan, R.J. and K.T. Flaherty, *Resistance to BRAF-targeted therapy in melanoma.* Eur J Cancer, 2013. **49**(6): p. 1297-304.

15. Larkin, J., P.A. Ascierto, B. Dréno, V. Atkinson, G. Liszkay, M. Maio, M. Mandalà, L. Demidov, D. Stroyakovskiy, L. Thomas, L. de la Cruz-Merino, C. Dutriaux, C. Garbe, M.A. Sovak, I. Chang, N. Choong, S.P. Hack, G.A. McArthur, and A. Ribas, *Combined vemurafenib and cobimetinib in BRAF-mutated melanoma.* N Engl J Med, 2014. **371**(20): p. 1867-76.

16. Long, G.V., D. Stroyakovskiy, H. Gogas, E. Levchenko, F. de Braud, J. Larkin, C. Garbe, T. Jouary, A. Hauschild, J.J. Grob, V. Chiarion-Sileni, C. Lebbe, M. Mandalà, M. Millward, A. Arance, I. Bondarenko, J.B. Haanen, J. Hansson, J. Utikal, V. Ferraresi, N. Kovalenko, P. Mohr, V. Probachai, D. Schadendorf, P. Nathan, C. Robert, A. Ribas, D.J. DeMarini, J.G. Irani, S. Swann, J.J. Legos, F. Jin, B. Mookerjee, and K. Flaherty, *Dabrafenib and trametinib versus dabrafenib and placebo for Val600 BRAF-mutant melanoma: a multicentre, double-blind, phase 3 randomised controlled trial.* Lancet, 2015. **386**(9992): p. 444-51.

17. Long, G.V., J.S. Weber, J.R. Infante, K.B. Kim, A. Daud, R. Gonzalez, J.A. Sosman, O. Hamid, L. Schuchter, J. Cebon, R.F. Kefford, D. Lawrence, R. Kudchadkar, H.A. Burris, G.S. Falchook, A. Algazi, K. Lewis, I. Puzanov, N. Ibrahim, P. Sun, E. Cunningham, A.S. Kline, H. Del Buono, D.O. McDowell, K. Patel, and K.T. Flaherty, *Overall Survival and Durable Responses in Patients With BRAF V600-Mutant Metastatic Melanoma Receiving Dabrafenib Combined With Trametinib.* J Clin Oncol, 2016. **34**(8): p. 871-8.

18. Flaherty, K.T., J.R. Infante, A. Daud, R. Gonzalez, R.F. Kefford, J. Sosman, O. Hamid, L. Schuchter, J. Cebon, N. Ibrahim, R. Kudchadkar, H.A. Burris, G. Falchook, A. Algazi, K. Lewis, G.V. Long, I. Puzanov, P. Lebowitz, A. Singh, S. Little, P. Sun, A. Allred, D. Ouellet, K.B. Kim, K. Patel, and J. Weber, *Combined BRAF and MEK inhibition in melanoma with BRAF V600 mutations.* N Engl J Med, 2012. **367**(18): p. 1694-703.

19. Flaherty, K.T., C. Robert, P. Hersey, P. Nathan, C. Garbe, M. Milhem, L.V. Demidov, J.C. Hassel, P. Rutkowski, P. Mohr, R. Dummer, U. Trefzer, J.M. Larkin, J. Utikal, B. Dreno, M. Nyakas, M.R. Middleton, J.C. Becker, M. Casey, L.J. Sherman, F.S. Wu, D. Ouellet, A.M. Martin, K. Patel, D. Schadendorf, and M.S. Group, *Improved survival with MEK inhibition in BRAF-mutated melanoma.* N Engl J Med, 2012. **367**(2): p. 107-14.

20. Krummel, M.F. and J.P. Allison, *CD28 and CTLA-4 have opposing effects on the response of T cells to stimulation.* J Exp Med, 1995. **182**(2): p. 459-65.

21. Leach, D.R., M.F. Krummel, and J.P. Allison, *Enhancement of antitumor immunity by CTLA-4 blockade.* Science, 1996. **271**(5256): p. 1734-6.

22. Qureshi, O.S., Y. Zheng, K. Nakamura, K. Attridge, C. Manzotti, E.M. Schmidt, J. Baker, L.E. Jeffery, S. Kaur, Z. Briggs, T.Z. Hou, C.E. Futter, G. Anderson, L.S. Walker, and D.M. Sansom, *Trans-endocytosis of CD80 and CD86: a molecular basis for the cell-extrinsic function of CTLA-4.* Science, 2011. **332**(6029): p. 600-3.

23. Romano, E., M. Kusio-Kobialka, P.G. Foukas, P. Baumgaertner, C. Meyer, P. Ballabeni, O. Michielin, B. Weide, P. Romero, and D.E. Speiser, *Ipilimumab-dependent cell-mediated cytotoxicity of regulatory T cells ex vivo by nonclassical monocytes in melanoma patients.* Proc Natl Acad Sci U S A, 2015. **112**(19): p. 6140-5.

24. Quezada, S.A., K.S. Peggs, M.A. Curran, and J.P. Allison, *CTLA4 blockade and GM-CSF combination immunotherapy alters the intratumor balance of effector and regulatory T cells.* J Clin Invest, 2006. **116**(7): p. 1935-45.

25. Hodi, F.S., S.J. O'Day, D.F. McDermott, R.W. Weber, J.A. Sosman, J.B. Haanen, R. Gonzalez, C. Robert, D. Schadendorf, J.C. Hassel, W. Akerley, A.J. van den Eertwegh, J. Lutzky, P. Lorigan, J.M. Vaubel, G.P. Linette, D. Hogg, C.H. Ottensmeier, C. Lebbé, C. Peschel, I. Quirt, J.I. Clark, J.D. Wolchok, J.S. Weber, J. Tian, M.J. Yellin, G.M. Nichol, A. Hoos, and W.J. Urba, *Improved survival with ipilimumab in patients with metastatic melanoma.* N Engl J Med, 2010. **363**(8): p. 711-23.

26. Schadendorf, D., F.S. Hodi, C. Robert, J.S. Weber, K. Margolin, O. Hamid, D. Patt, T.T. Chen, D.M. Berman, and J.D. Wolchok, *Pooled Analysis of Long-Term*

Survival Data From Phase II and Phase III Trials of Ipilimumab in Unresectable or Metastatic Melanoma. J Clin Oncol, 2015. **33**(17): p. 1889-94.

27. Prieto, P.A., J.C. Yang, R.M. Sherry, M.S. Hughes, U.S. Kammula, D.E. White, C.L. Levy, S.A. Rosenberg, and G.Q. Phan, *CTLA-4 blockade with ipilimumab: long-term follow-up of 177 patients with metastatic melanoma.* Clin Cancer Res, 2012. **18**(7): p. 2039-47.

28. Sharma, P. and J.P. Allison, *The future of immune checkpoint therapy.* Science, 2015. **348**(6230): p. 56-61.

29. Gros, A., P.F. Robbins, X. Yao, Y.F. Li, S. Turcotte, E. Tran, J.R. Wunderlich, A. Mixon, S. Farid, M.E. Dudley, K. Hanada, J.R. Almeida, S. Darko, D.C. Douek, J.C. Yang, and S.A. Rosenberg, *PD-1 identifies the patient-specific CD8$^+$ tumor-reactive repertoire infiltrating human tumors.* J Clin Invest, 2014. **124**(5): p. 2246-59.

30. Topalian, S.L., F.S. Hodi, J.R. Brahmer, S.N. Gettinger, D.C. Smith, D.F. McDermott, J.D. Powderly, R.D. Carvajal, J.A. Sosman, M.B. Atkins, P.D. Leming, D.R. Spigel, S.J. Antonia, L. Horn, C.G. Drake, D.M. Pardoll, L. Chen, W.H. Sharfman, R.A. Anders, J.M. Taube, T.L. McMiller, H. Xu, A.J. Korman, M. Jure-Kunkel, S. Agrawal, D. McDonald, G.D. Kollia, A. Gupta, J.M. Wigginton, and M. Sznol, *Safety, activity, and immune correlates of anti-PD-1 antibody in cancer.* N Engl J Med, 2012. **366**(26): p. 2443-54.

31. Brahmer, J.R., S.S. Tykodi, L.Q. Chow, W.J. Hwu, S.L. Topalian, P. Hwu, C.G. Drake, L.H. Camacho, J. Kauh, K. Odunsi, H.C. Pitot, O. Hamid, S. Bhatia, R. Martins, K. Eaton, S. Chen, T.M. Salay, S. Alaparthy, J.F. Grosso, A.J. Korman,

S.M. Parker, S. Agrawal, S.M. Goldberg, D.M. Pardoll, A. Gupta, and J.M. Wigginton, *Safety and activity of anti-PD-L1 antibody in patients with advanced cancer.* N Engl J Med, 2012. **366**(26): p. 2455-65.

32. Ribas, A., I. Puzanov, R. Dummer, D. Schadendorf, O. Hamid, C. Robert, F.S. Hodi, J. Schachter, A.C. Pavlick, K.D. Lewis, L.D. Cranmer, C.U. Blank, S.J. O'Day, P.A. Ascierto, A.K. Salama, K.A. Margolin, C. Loquai, T.K. Eigentler, T.C. Gangadhar, M.S. Carlino, S.S. Agarwala, S.J. Moschos, J.A. Sosman, S.M. Goldinger, R. Shapira-Frommer, R. Gonzalez, J.M. Kirkwood, J.D. Wolchok, A. Eggermont, X.N. Li, W. Zhou, A.M. Zernhelt, J. Lis, S. Ebbinghaus, S.P. Kang, and A. Daud, *Pembrolizumab versus investigator-choice chemotherapy for ipilimumab-refractory melanoma (KEYNOTE-002): a randomised, controlled, phase 2 trial.* Lancet Oncol, 2015. **16**(8): p. 908-18.

33. Robert, C., J. Schachter, G.V. Long, A. Arance, J.J. Grob, L. Mortier, A. Daud, M.S. Carlino, C. McNeil, M. Lotem, J. Larkin, P. Lorigan, B. Neyns, C.U. Blank, O. Hamid, C. Mateus, R. Shapira-Frommer, M. Kosh, H. Zhou, N. Ibrahim, S. Ebbinghaus, A. Ribas, and K.-. investigators, *Pembrolizumab versus Ipilimumab in Advanced Melanoma.* N Engl J Med, 2015. **372**(26): p. 2521-32.

34. Topalian, S.L., M. Sznol, D.F. McDermott, H.M. Kluger, R.D. Carvajal, W.H. Sharfman, J.R. Brahmer, D.P. Lawrence, M.B. Atkins, J.D. Powderly, P.D. Leming, E.J. Lipson, I. Puzanov, D.C. Smith, J.M. Taube, J.M. Wigginton, G.D. Kollia, A. Gupta, D.M. Pardoll, J.A. Sosman, and F.S. Hodi, *Survival, durable tumor remission, and long-term safety in patients with advanced melanoma receiving nivolumab.* J Clin Oncol, 2014. **32**(10): p. 1020-30.

35. Hamid, O., C. Robert, A. Daud, F.S. Hodi, W.J. Hwu, R. Kefford, J.D. Wolchok, P. Hersey, R.W. Joseph, J.S. Weber, R. Dronca, T.C. Gangadhar, A. Patnaik, H. Zarour, A.M. Joshua, K. Gergich, J. Elassaiss-Schaap, A. Algazi, C. Mateus, P. Boasberg, P.C. Tumeh, B. Chmielowski, S.W. Ebbinghaus, X.N. Li, S.P. Kang, and A. Ribas, *Safety and tumor responses with lambrolizumab (anti-PD-1) in melanoma.* N Engl J Med, 2013. **369**(2): p. 134-44.

36. Larkin, J., F.S. Hodi, and J.D. Wolchok, *Combined Nivolumab and Ipilimumab or Monotherapy in Untreated Melanoma.* N Engl J Med, 2015. **373**(13): p. 1270-1.

37. Postow, M.A., J. Chesney, A.C. Pavlick, C. Robert, K. Grossmann, D. McDermott, G.P. Linette, N. Meyer, J.K. Giguere, S.S. Agarwala, M. Shaheen, M.S. Ernstoff, D. Minor, A.K. Salama, M. Taylor, P.A. Ott, L.M. Rollin, C. Horak, P. Gagnier, J.D. Wolchok, and F.S. Hodi, *Nivolumab and ipilimumab versus ipilimumab in untreated melanoma.* N Engl J Med, 2015. **372**(21): p. 2006-17.

38. Johnson, D.B., I. Puzanov, and M.C. Kelley, *Talimogene laherparepvec (T-VEC) for the treatment of advanced melanoma.* Immunotherapy, 2015. **7**(6): p. 611-9.

39. Mach, N., S. Gillessen, S.B. Wilson, C. Sheehan, M. Mihm, and G. Dranoff, *Differences in dendritic cells stimulated in vivo by tumors engineered to secrete granulocyte-macrophage colony-stimulating factor or Flt3-ligand.* Cancer Res, 2000. **60**(12): p. 3239-46.

40. Broz, M.L., M. Binnewies, B. Boldajipour, A.E. Nelson, J.L. Pollack, D.J. Erle, A. Barczak, M.D. Rosenblum, A. Daud, D.L. Barber, S. Amigorena, L.J. Van't Veer, A.I. Sperling, D.M. Wolf, and M.F. Krummel, *Dissecting the tumor myeloid*

compartment reveals rare activating antigen-presenting cells critical for T cell immunity. Cancer Cell, 2014. **26**(5): p. 638-52.

41. Hercus, T.R., D. Thomas, M.A. Guthridge, P.G. Ekert, J. King-Scott, M.W. Parker, and A.F. Lopez, *The granulocyte-macrophage colony-stimulating factor receptor: linking its structure to cell signaling and its role in disease.* Blood, 2009. **114**(7): p. 1289-98.

42. Andtbacka, R.H., H.L. Kaufman, F. Collichio, T. Amatruda, N. Senzer, J. Chesney, K.A. Delman, L.E. Spitler, I. Puzanov, S.S. Agarwala, M. Milhem, L. Cranmer, B. Curti, K. Lewis, M. Ross, T. Guthrie, G.P. Linette, G.A. Daniels, K. Harrington, M.R. Middleton, W.H. Miller, J.S. Zager, Y. Ye, B. Yao, A. Li, S. Doleman, A. VanderWalde, J. Gansert, and R.S. Coffin, *Talimogene Laherparepvec Improves Durable Response Rate in Patients With Advanced Melanoma.* J Clin Oncol, 2015. **33**(25): p. 2780-8.

43. Puzanov, I., M.M. Milhem, D. Minor, O. Hamid, A. Li, L. Chen, M. Chastain, K.S. Gorski, A. Anderson, J. Chou, H.L. Kaufman, and R.H. Andtbacka, *Talimogene Laherparepvec in Combination With Ipilimumab in Previously Untreated, Unresectable Stage IIIB-IV Melanoma.* J Clin Oncol, 2016. **34**(22): p. 2619-26.

44. Long, G.V., R. Dummer, A. Ribas, I. Puzanov, O. Michielin, A. VanderWalde, R.H.I. Andtbacka, J. Cebon, E. Fernandez, J. Malvehy, A.J. Olszanski, T.F. Gajewski, J.M. Kirkwood, O. Kuznetsova, L. Chen, D.R. Kaufman, J. Chou, and F.S. Hodi, *A Phase I/III, multicenter, open-label trial of talimogene laherparepvec (T-VEC) in combination with pembrolizumab for the treatment of unresected, stage*

IIIb-IV melanoma (MASTERKEY-265). Journal for Immunotherapy of Cancer, 2015. **3**(Suppl 2): p. P181-P181.

45. Peng, W., J.Q. Chen, C. Liu, S. Malu, C. Creasy, M.T. Tetzlaff, C. Xu, J.A. McKenzie, C. Zhang, X. Liang, L.J. Williams, W. Deng, G. Chen, R. Mbofung, A.J. Lazar, C.A. Torres-Cabala, Z.A. Cooper, P.L. Chen, T.N. Tieu, S. Spranger, X. Yu, C. Bernatchez, M.A. Forget, C. Haymaker, R. Amaria, J.L. McQuade, I.C. Glitza, T. Cascone, H.S. Li, L.N. Kwong, T.P. Heffernan, J. Hu, R.L. Bassett, M.W. Bosenberg, S.E. Woodman, W.W. Overwijk, G. Lizée, J. Roszik, T.F. Gajewski, J.A. Wargo, J.E. Gershenwald, L. Radvanyi, M.A. Davies, and P. Hwu, *Loss of PTEN Promotes Resistance to T Cell-Mediated Immunotherapy.* Cancer Discov, 2016. **6**(2): p. 202-16.

46. Whittaker, S.R., J.P. Theurillat, E. Van Allen, N. Wagle, J. Hsiao, G.S. Cowley, D. Schadendorf, D.E. Root, and L.A. Garraway, *A genome-scale RNA interference screen implicates NF1 loss in resistance to RAF inhibition.* Cancer Discov, 2013. **3**(3): p. 350-62.

47. Alexandrov, L.B., S. Nik-Zainal, D.C. Wedge, S.A. Aparicio, S. Behjati, A.V. Biankin, G.R. Bignell, N. Bolli, A. Borg, A.L. Børresen-Dale, S. Boyault, B. Burkhardt, A.P. Butler, C. Caldas, H.R. Davies, C. Desmedt, R. Eils, J.E. Eyfjörd, J.A. Foekens, M. Greaves, F. Hosoda, B. Hutter, T. Ilicic, S. Imbeaud, M. Imielinski, M. Imielinsk, N. Jäger, D.T. Jones, D. Jones, S. Knappskog, M. Kool, S.R. Lakhani, C. López-Otín, S. Martin, N.C. Munshi, H. Nakamura, P.A. Northcott, M. Pajic, E. Papaemmanuil, A. Paradiso, J.V. Pearson, X.S. Puente, K. Raine, M. Ramakrishna, A.L. Richardson, J. Richter, P. Rosenstiel, M. Schlesner,

T.N. Schumacher, P.N. Span, J.W. Teague, Y. Totoki, A.N. Tutt, R. Valdés-Mas, M.M. van Buuren, L. van 't Veer, A. Vincent-Salomon, N. Waddell, L.R. Yates, J. Zucman-Rossi, P.A. Futreal, U. McDermott, P. Lichter, M. Meyerson, S.M. Grimmond, R. Siebert, E. Campo, T. Shibata, S.M. Pfister, P.J. Campbell, M.R. Stratton, A.P.C.G. Initiative, I.B.C. Consortium, I.M.-S. Consortium, and I. PedBrain, *Signatures of mutational processes in human cancer.* Nature, 2013. **500**(7463): p. 415-21.

48. Boni, A., A.P. Cogdill, P. Dang, D. Udayakumar, C.N. Njauw, C.M. Sloss, C.R. Ferrone, K.T. Flaherty, D.P. Lawrence, D.E. Fisher, H. Tsao, and J.A. Wargo, *Selective BRAFV600E inhibition enhances T-cell recognition of melanoma without affecting lymphocyte function.* Cancer Res, 2010. **70**(13): p. 5213-9.

49. Frederick, D.T., A. Piris, A.P. Cogdill, Z.A. Cooper, C. Lezcano, C.R. Ferrone, D. Mitra, A. Boni, L.P. Newton, C. Liu, W. Peng, R.J. Sullivan, D.P. Lawrence, F.S. Hodi, W.W. Overwijk, G. Lizée, G.F. Murphy, P. Hwu, K.T. Flaherty, D.E. Fisher, and J.A. Wargo, *BRAF inhibition is associated with enhanced melanoma antigen expression and a more favorable tumor microenvironment in patients with metastatic melanoma.* Clin Cancer Res, 2013. **19**(5): p. 1225-31.

50. Cantwell-Dorris, E.R., J.J. O'Leary, and O.M. Sheils, *BRAFV600E: implications for carcinogenesis and molecular therapy.* Mol Cancer Ther, 2011. **10**(3): p. 385-94.

51. Sumimoto, H., F. Imabayashi, T. Iwata, and Y. Kawakami, *The BRAF-MAPK signaling pathway is essential for cancer-immune evasion in human melanoma cells.* J Exp Med, 2006. **203**(7): p. 1651-6.

52. Kono, M., I.S. Dunn, P.J. Durda, D. Butera, L.B. Rose, T.J. Haggerty, E.M. Benson, and J.T. Kurnick, *Role of the mitogen-activated protein kinase signaling pathway in the regulation of human melanocytic antigen expression.* Mol Cancer Res, 2006. **4**(10): p. 779-92.

53. Liu, C., W. Peng, C. Xu, Y. Lou, M. Zhang, J.A. Wargo, J.Q. Chen, H.S. Li, S.S. Watowich, Y. Yang, D. Tompers Frederick, Z.A. Cooper, R.M. Mbofung, M. Whittington, K.T. Flaherty, S.E. Woodman, M.A. Davies, L.G. Radvanyi, W.W. Overwijk, G. Lizée, and P. Hwu, *BRAF inhibition increases tumor infiltration by T cells and enhances the antitumor activity of adoptive immunotherapy in mice.* Clin Cancer Res, 2013. **19**(2): p. 393-403.

54. Khalili, J.S., S. Liu, T.G. Rodríguez-Cruz, M. Whittington, S. Wardell, C. Liu, M. Zhang, Z.A. Cooper, D.T. Frederick, Y. Li, R.W. Joseph, C. Bernatchez, S. Ekmekcioglu, E. Grimm, L.G. Radvanyi, R.E. Davis, M.A. Davies, J.A. Wargo, P. Hwu, and G. Lizée, *Oncogenic BRAF(V600E) promotes stromal cell-mediated immunosuppression via induction of interleukin-1 in melanoma.* Clin Cancer Res, 2012. **18**(19): p. 5329-40.

55. Bradley, S.D., Z. Chen, B. Melendez, A. Talukder, J.S. Khalili, T. Rodriguez-Cruz, S. Liu, M. Whittington, W. Deng, F. Li, C. Bernatchez, L.G. Radvanyi, M.A. Davies, P. Hwu, and G. Lizée, *BRAFV600E Co-opts a Conserved MHC Class I Internalization Pathway to Diminish Antigen Presentation and CD8+ T-cell Recognition of Melanoma.* Cancer Immunol Res, 2015. **3**(6): p. 602-9.

56. Koya, R.C., S. Mok, N. Otte, K.J. Blacketor, B. Comin-Anduix, P.C. Tumeh, A. Minasyan, N.A. Graham, T.G. Graeber, T. Chodon, and A. Ribas, *BRAF inhibitor*

vemurafenib improves the antitumor activity of adoptive cell immunotherapy. Cancer Res, 2012. **72**(16): p. 3928-37.

57. Hu-Lieskovan, S., S. Mok, B. Homet Moreno, J. Tsoi, L. Robert, L. Goedert, E.M. Pinheiro, R.C. Koya, T.G. Graeber, B. Comin-Anduix, and A. Ribas, *Improved antitumor activity of immunotherapy with BRAF and MEK inhibitors in BRAF^{V600E} melanoma.* Science Translational Medicine, 2015. **7**(279): p. 279ra41.

58. Cooper, Z.A., D.T. Frederick, V.R. Juneja, R.J. Sullivan, D.P. Lawrence, A. Piris, A.H. Sharpe, D.E. Fisher, K.T. Flaherty, and J.A. Wargo, *BRAF inhibition is associated with increased clonality in tumor-infiltrating lymphocytes.* Oncoimmunology, 2013. **2**(10): p. e26615.

59. Wilmott, J.S., G.V. Long, J.R. Howle, L.E. Haydu, R.N. Sharma, J.F. Thompson, R.F. Kefford, P. Hersey, and R.A. Scolyer, *Selective BRAF inhibitors induce marked T-cell infiltration into human metastatic melanoma.* Clin Cancer Res, 2012. **18**(5): p. 1386-94.

60. Larkin, J., C.D. Lao, W.J. Urba, D.F. McDermott, C. Horak, J. Jiang, and J.D. Wolchok, *Efficacy and Safety of Nivolumab in Patients With BRAF V600 Mutant and BRAF Wild-Type Advanced Melanoma: A Pooled Analysis of 4 Clinical Trials.* JAMA Oncol, 2015. **1**(4): p. 433-40.

61. Aguissa-Touré, A.H. and G. Li, *Genetic alterations of PTEN in human melanoma.* Cell Mol Life Sci, 2012. **69**(9): p. 1475-91.

62. Dankort, D., D.P. Curley, R.A. Cartlidge, B. Nelson, A.N. Karnezis, W.E. Damsky, M.J. You, R.A. DePinho, M. McMahon, and M. Bosenberg, *Braf(V600E)*

cooperates with Pten loss to induce metastatic melanoma. Nat Genet, 2009. **41**(5): p. 544-52.

63. Dong, Y., J.A. Richards, R. Gupta, P.P. Aung, A. Emley, Y. Kluger, S.K. Dogra, M. Mahalingam, and N. Wajapeyee, *PTEN functions as a melanoma tumor suppressor by promoting host immune response.* Oncogene, 2014. **33**(38): p. 4632-42.

64. Stark, A.K., S. Sriskantharajah, E.M. Hessel, and K. Okkenhaug, *PI3K inhibitors in inflammation, autoimmunity and cancer.* Curr Opin Pharmacol, 2015. **23**: p. 82-91.

65. Hodis, E., I.R. Watson, G.V. Kryukov, S.T. Arold, M. Imielinski, J.P. Theurillat, E. Nickerson, D. Auclair, L. Li, C. Place, D. Dicara, A.H. Ramos, M.S. Lawrence, K. Cibulskis, A. Sivachenko, D. Voet, G. Saksena, N. Stransky, R.C. Onofrio, W. Winckler, K. Ardlie, N. Wagle, J. Wargo, K. Chong, D.L. Morton, K. Stemke-Hale, G. Chen, M. Noble, M. Meyerson, J.E. Ladbury, M.A. Davies, J.E. Gershenwald, S.N. Wagner, D.S. Hoon, D. Schadendorf, E.S. Lander, S.B. Gabriel, G. Getz, L.A. Garraway, and L. Chin, *A landscape of driver mutations in melanoma.* Cell, 2012. **150**(2): p. 251-63.

66. Omholt, K., S. Karsberg, A. Platz, L. Kanter, U. Ringborg, and J. Hansson, *Screening of N-ras codon 61 mutations in paired primary and metastatic cutaneous melanomas: mutations occur early and persist throughout tumor progression.* Clin Cancer Res, 2002. **8**(11): p. 3468-74.

67. Dumaz, N., R. Hayward, J. Martin, L. Ogilvie, D. Hedley, J.A. Curtin, B.C. Bastian, C. Springer, and R. Marais, *In melanoma, RAS mutations are accompanied by*

switching signaling from BRAF to CRAF and disrupted cyclic AMP signaling. Cancer Res, 2006. **66**(19): p. 9483-91.

68. Davies, M.A., K. Stemke-Hale, E. Lin, C. Tellez, W. Deng, Y.N. Gopal, S.E. Woodman, T.C. Calderone, Z. Ju, A.J. Lazar, V.G. Prieto, K. Aldape, G.B. Mills, and J.E. Gershenwald, *Integrated Molecular and Clinical Analysis of AKT Activation in Metastatic Melanoma.* Clin Cancer Res, 2009. **15**(24): p. 7538-7546.

69. Mehnert, J.M. and H.M. Kluger, *Driver mutations in melanoma: lessons learned from bench-to-bedside studies.* Curr Oncol Rep, 2012. **14**(5): p. 449-57.

70. Joseph, R.W., R.J. Sullivan, R. Harrell, K. Stemke-Hale, D. Panka, G. Manoukian, A. Percy, R.L. Bassett, C.S. Ng, L. Radvanyi, P. Hwu, M.B. Atkins, and M.A. Davies, *Correlation of NRAS mutations with clinical response to high-dose IL-2 in patients with advanced melanoma.* J Immunother, 2012. **35**(1): p. 66-72.

71. Johnson, D.B., C.M. Lovly, M. Flavin, K.S. Panageas, G.D. Ayers, Z. Zhao, W.T. Iams, M. Colgan, S. DeNoble, C.R. Terry, E.G. Berry, A.J. Iafrate, R.J. Sullivan, R.D. Carvajal, and J.A. Sosman, *Impact of NRAS mutations for patients with advanced melanoma treated with immune therapies.* Cancer Immunol Res, 2015. **3**(3): p. 288-295.

72. Fischer, G.M., F.C.L. Carapeto, A.Y. Joon, L.E. Haydu, H. Chen, F. Wang, J.S. Van Arnam, J.L. McQuade, K. Wani, J.M. Kirkwood, J.F. Thompson, M.T. Tetzlaff, A.J. Lazar, H.A. Tawbi, J.E. Gershenwald, R.A. Scolyer, G.V. Long, and M.A. Davies, *Molecular and immunological associations of elevated serum lactate dehydrogenase in metastatic melanoma patients: A fresh look at an old biomarker.* Cancer Med, 2020. **9**(22): p. 8650-8661.

73. Rimm, D.L., K. Caca, G. Hu, F.B. Harrison, and E.R. Fearon, *Frequent Nuclear/Cytoplasmic Localization of β-Catenin without Exon 3 Mutations in Malignant Melanoma.* The American Journal of Pathology, 1999. **154**(2): p. 325-329.

74. Reifenberger, J., C.B. Knobbe, M. Wolter, B. Blaschke, K.W. Schulte, T. Pietsch, T. Ruzicka, and G. Reifenberger, *Molecular genetic analysis of malignant melanomas for aberrations of the WNT signaling pathway genes CTNNB1, APC, ICAT and BTRC.* Int J Cancer, 2002. **100**(5): p. 549-56.

75. Spranger, S., R. Bao, and T.F. Gajewski, *Melanoma-intrinsic β-catenin signalling prevents anti-tumour immunity.* Nature, 2015. **523**(7559): p. 231-5.

76. Liang, X., C. Fu, W. Cui, J.L. Ober-Blöbaum, S.P. Zahner, P.A. Shrikant, B.E. Clausen, R.A. Flavell, I. Mellman, and A. Jiang, *β-catenin mediates tumor-induced immunosuppression by inhibiting cross-priming of $CD8^+$ T cells.* J Leukoc Biol, 2014. **95**(1): p. 179-90.

77. Hong, Y., I. Manoharan, A. Suryawanshi, T. Majumdar, M.L. Angus-Hill, P.A. Koni, B. Manicassamy, A.L. Mellor, D.H. Munn, and S. Manicassamy, *β-catenin promotes regulatory T-cell responses in tumors by inducing vitamin A metabolism in dendritic cells.* Cancer Res, 2015. **75**(4): p. 656-665.

78. Yaguchi, T., Y. Goto, K. Kido, H. Mochimaru, T. Sakurai, N. Tsukamoto, C. Kudo-Saito, T. Fujita, H. Sumimoto, and Y. Kawakami, *Immune suppression and resistance mediated by constitutive activation of Wnt/β-catenin signaling in human melanoma cells.* J Immunol, 2012. **189**(5): p. 2110-7.

79. Fu, C., X. Liang, W. Cui, J.L. Ober-Blöbaum, J. Vazzana, P.A. Shrikant, K.P. Lee, B.E. Clausen, I. Mellman, and A. Jiang, *β-Catenin in dendritic cells exerts opposite functions in cross-priming and maintenance of CD8+ T cells through regulation of IL-10.* Proc Natl Acad Sci U S A, 2015. **112**(9): p. 2823-8.

80. Snyder, A., V. Makarov, T. Merghoub, J. Yuan, J.M. Zaretsky, A. Desrichard, L.A. Walsh, M.A. Postow, P. Wong, T.S. Ho, T.J. Hollmann, C. Bruggeman, K. Kannan, Y. Li, C. Elipenahli, C. Liu, C.T. Harbison, L. Wang, A. Ribas, J.D. Wolchok, and T.A. Chan, *Genetic basis for clinical response to CTLA-4 blockade in melanoma.* N Engl J Med, 2014. **371**(23): p. 2189-2199.

81. Rizvi, N.A., M.D. Hellmann, A. Snyder, P. Kvistborg, V. Makarov, J.J. Havel, W. Lee, J. Yuan, P. Wong, T.S. Ho, M.L. Miller, N. Rekhtman, A.L. Moreira, F. Ibrahim, C. Bruggeman, B. Gasmi, R. Zappasodi, Y. Maeda, C. Sander, E.B. Garon, T. Merghoub, J.D. Wolchok, T.N. Schumacher, and T.A. Chan, *Cancer immunology. Mutational landscape determines sensitivity to PD-1 blockade in non-small cell lung cancer.* Science, 2015. **348**(6230): p. 124-8.

82. Hacohen, N., E.F. Fritsch, T.A. Carter, E.S. Lander, and C.J. Wu, *Getting personal with neoantigen-based therapeutic cancer vaccines.* Cancer Immunol Res, 2013. **1**(1): p. 11-5.

83. Tran, E., S. Turcotte, A. Gros, P.F. Robbins, Y.C. Lu, M.E. Dudley, J.R. Wunderlich, R.P. Somerville, K. Hogan, C.S. Hinrichs, M.R. Parkhurst, J.C. Yang, and S.A. Rosenberg, *Cancer immunotherapy based on mutation-specific CD4+ T cells in a patient with epithelial cancer.* Science, 2014. **344**(6184): p. 641-5.

84. Van Allen, E.M., D. Miao, B. Schilling, S.A. Shukla, C. Blank, L. Zimmer, A. Sucker, U. Hillen, M.H.G. Foppen, S.M. Goldinger, J. Utikal, J.C. Hassel, B. Weide, K.C. Kaehler, C. Loquai, P. Mohr, R. Gutzmer, R. Dummer, S. Gabriel, C.J. Wu, D. Schadendorf, and L.A. Garraway, *Genomic correlates of response to CTLA-4 blockade in metastatic melanoma.* Science, 2015. **350**(6257): p. 207-211.

85. Le, D.T., J.N. Uram, H. Wang, B.R. Bartlett, H. Kemberling, A.D. Eyring, A.D. Skora, B.S. Luber, N.S. Azad, D. Laheru, B. Biedrzycki, R.C. Donehower, A. Zaheer, G.A. Fisher, T.S. Crocenzi, J.J. Lee, S.M. Duffy, R.M. Goldberg, A. de la Chapelle, M. Koshiji, F. Bhaijee, T. Huebner, R.H. Hruban, L.D. Wood, N. Cuka, D.M. Pardoll, N. Papadopoulos, K.W. Kinzler, S. Zhou, T.C. Cornish, J.M. Taube, R.A. Anders, J.R. Eshleman, B. Vogelstein, and L.A. Diaz, *PD-1 Blockade in Tumors with Mismatch-Repair Deficiency.* N Engl J Med, 2015. **372**(26): p. 2509-20.

86. Roszik, J., L.E. Haydu, K.R. Hess, J. Oba, A.Y. Joon, A.E. Siroy, T.V. Karpinets, F.C. Stingo, V. Baladandayuthapani, M.T. Tetzlaff, J.A. Wargo, K. Chen, M.A. Forget, C.L. Haymaker, J.Q. Chen, F. Meric-Bernstam, A.K. Eterovic, K.R. Shaw, G.B. Mills, J.E. Gershenwald, L.G. Radvanyi, P. Hwu, P.A. Futreal, D.L. Gibbons, A.J. Lazar, C. Bernatchez, M.A. Davies, and S.E. Woodman, *Novel algorithmic approach predicts tumor mutation load and correlates with immunotherapy clinical outcomes using a defined gene mutation set.* BMC Med, 2016. **14**(1): p. 168.

87. Riaz, N., J.J. Havel, S.M. Kendall, V. Makarov, L.A. Walsh, A. Desrichard, N. Weinhold, and T.A. Chan, *Recurrent SERPINB3 and SERPINB4 mutations in*

patients who respond to anti-CTLA4 immunotherapy. Nat Genet, 2016. **48**(11): p. 1327-1329.

88. Gao, J., L.Z. Shi, H. Zhao, J. Chen, L. Xiong, Q. He, T. Chen, J. Roszik, C. Bernatchez, S.E. Woodman, P.L. Chen, P. Hwu, J.P. Allison, A. Futreal, J.A. Wargo, and P. Sharma, *Loss of IFN-γ Pathway Genes in Tumor Cells as a Mechanism of Resistance to Anti-CTLA-4 Therapy.* Cell, 2016. **167**(2): p. 397-404.e9.

89. Zaretsky, J.M., A. Garcia-Diaz, D.S. Shin, H. Escuin-Ordinas, W. Hugo, S. Hu-Lieskovan, D.Y. Torrejon, G. Abril-Rodriguez, S. Sandoval, L. Barthly, J. Saco, B. Homet Moreno, R. Mezzadra, B. Chmielowski, K. Ruchalski, I.P. Shintaku, P.J. Sanchez, C. Puig-Saus, G. Cherry, E. Seja, X. Kong, J. Pang, B. Berent-Maoz, B. Comin-Anduix, T.G. Graeber, P.C. Tumeh, T.N. Schumacher, R.S. Lo, and A. Ribas, *Mutations Associated with Acquired Resistance to PD-1 Blockade in Melanoma.* N Engl J Med, 2016. **375**(9): p. 819-29.

90. Hugo, W., J.M. Zaretsky, L. Sun, C. Song, B.H. Moreno, S. Hu-Lieskovan, B. Berent-Maoz, J. Pang, B. Chmielowski, G. Cherry, E. Seja, S. Lomeli, X. Kong, M.C. Kelley, J.A. Sosman, D.B. Johnson, A. Ribas, and R.S. Lo, *Genomic and Transcriptomic Features of Response to Anti-PD-1 Therapy in Metastatic Melanoma.* Cell, 2016. **165**(1): p. 35-44.

91. Johnson, D.B., G.M. Frampton, M.J. Rioth, E. Yusko, Y. Xu, X. Guo, R.C. Ennis, D. Fabrizio, Z.R. Chalmers, J. Greenbowe, S.M. Ali, S. Balasubramanian, J.X. Sun, Y. He, D.T. Frederick, I. Puzanov, J.M. Balko, J.M. Cates, J.S. Ross, C. Sanders, H. Robins, Y. Shyr, V.A. Miller, P.J. Stephens, R.J. Sullivan, J.A. Sosman, and

C.M. Lovly, *Targeted Next Generation Sequencing Identifies Markers of Response to PD-1 Blockade.* Cancer Immunol Res, 2016. **4**(11): p. 959-967.

92. Chen, P.L., W. Roh, A. Reuben, Z.A. Cooper, C.N. Spencer, P.A. Prieto, J.P. Miller, R.L. Bassett, V. Gopalakrishnan, K. Wani, M.P. De Macedo, J.L. Austin-Breneman, H. Jiang, Q. Chang, S.M. Reddy, W.S. Chen, M.T. Tetzlaff, R.J. Broaddus, M.A. Davies, J.E. Gershenwald, L. Haydu, A.J. Lazar, S.P. Patel, P. Hwu, W.J. Hwu, A. Diab, I.C. Glitza, S.E. Woodman, L.M. Vence, I.I. Wistuba, R.N. Amaria, L.N. Kwong, V. Prieto, R.E. Davis, W. Ma, W.W. Overwijk, A.H. Sharpe, J. Hu, P.A. Futreal, J. Blando, P. Sharma, J.P. Allison, L. Chin, and J.A. Wargo, *Analysis of Immune Signatures in Longitudinal Tumor Samples Yields Insight into Biomarkers of Response and Mechanisms of Resistance to Immune Checkpoint Blockade.* Cancer Discov, 2016. **6**(8): p. 827-37.

93. Roh, W., P.L. Chen, A. Reuben, C.N. Spencer, P.A. Prieto, J.P. Miller, V. Gopalakrishnan, F. Wang, Z.A. Cooper, S.M. Reddy, C. Gumbs, L. Little, Q. Chang, W.S. Chen, K. Wani, M.P. De Macedo, E. Chen, J.L. Austin-Breneman, H. Jiang, J. Roszik, M.T. Tetzlaff, M.A. Davies, J.E. Gershenwald, H. Tawbi, A.J. Lazar, P. Hwu, W.J. Hwu, A. Diab, I.C. Glitza, S.P. Patel, S.E. Woodman, R.N. Amaria, V.G. Prieto, J. Hu, P. Sharma, J.P. Allison, L. Chin, J. Zhang, J.A. Wargo, and P.A. Futreal, *Integrated molecular analysis of tumor biopsies on sequential CTLA-4 and PD-1 blockade reveals markers of response and resistance.* Sci Transl Med, 2017. **9**(379).

94. Ribas, A., F.S. Hodi, D.P. Lawrence, V. Atkinson, A. Starodub, M.S. Carlino, R.A. Fisher, G.V. Long, W.H. Miller, and Y. Huang, *Pembrolizumab (pembro) in*

combination with dabrafenib (D) and trametinib (T) for BRAF-mutant advanced melanoma: Phase 1 KEYNOTE-022 study. 2016, American Society of Clinical Oncology.

95. Ribas, A., F.S. Hodi, M. Callahan, C. Konto, and J. Wolchok, *Hepatotoxicity with combination of vemurafenib and ipilimumab.* N Engl J Med, 2013. **368**(14): p. 1365-6.

96. Puzanov, I., M.K. Callahan, G.P. Linette, S.P. Patel, J.J. Luke, J.A. Sosman, J.D. Wolchok, O. Hamid, D.R. Minor, and K.W. Orford, *Phase 1 study of the BRAF inhibitor dabrafenib (D) with or without the MEK inhibitor trametinib (T) in combination with ipilimumab (Ipi) for V600E/K mutation–positive unresectable or metastatic melanoma (MM)*. 2014, American Society of Clinical Oncology.

97. Amin, A., D.H. Lawson, A.K. Salama, H.B. Koon, T. Guthrie, S.S. Thomas, S.J. O'Day, M.F. Shaheen, B. Zhang, S. Francis, and F.S. Hodi, *Phase II study of vemurafenib followed by ipilimumab in patients with previously untreated BRAF-mutated metastatic melanoma.* J Immunother Cancer, 2016. **4**: p. 44.

98. Cooper, Z.A., V.R. Juneja, P.T. Sage, D.T. Frederick, A. Piris, D. Mitra, J.A. Lo, F.S. Hodi, G.J. Freeman, M.W. Bosenberg, M. McMahon, K.T. Flaherty, D.E. Fisher, A.H. Sharpe, and J.A. Wargo, *Response to BRAF inhibition in melanoma is enhanced when combined with immune checkpoint blockade.* Cancer Immunol Res, 2014. **2**(7): p. 643-54.

99. Minor, D.R., I. Puzanov, M.K. Callahan, B.A. Hug, and A. Hoos, *Severe gastrointestinal toxicity with administration of trametinib in combination with dabrafenib and ipilimumab.* Pigment Cell Melanoma Res, 2015. **28**(5): p. 611-2.

100. Ribas, A., M. Butler, J. Lutzky, D.P. Lawrence, C. Robert, W. Miller, G.P. Linette, P.A. Ascierto, T. Kuzel, and A.P. Algazi, *Phase I study combining anti-PD-L1 (MEDI4736) with BRAF (dabrafenib) and/or MEK (trametinib) inhibitors in advanced melanoma*. 2015, American Society of Clinical Oncology.

101. Gutzmer, R., D. Stroyakovskiy, H. Gogas, C. Robert, K. Lewis, S. Protsenko, R.P. Pereira, T. Eigentler, P. Rutkowski, L. Demidov, G.M. Manikhas, Y. Yan, K.C. Huang, A. Uyei, V. McNally, G.A. McArthur, and P.A. Ascierto, *Atezolizumab, vemurafenib, and cobimetinib as first-line treatment for unresectable advanced BRAF(V600) mutation-positive melanoma (IMspire150): primary analysis of the randomised, double-blind, placebo-controlled, phase 3 trial.* Lancet, 2020. **395**(10240): p. 1835-1844.

102. Chow, S.C., *Adaptive clinical trial design.* Annu Rev Med, 2014. **65**: p. 405-15.

103. Wargo, J.A., S.M. Reddy, A. Reuben, and P. Sharma, *Monitoring immune responses in the tumor microenvironment.* Curr Opin Immunol, 2016. **41**: p. 23-31.

104. Basler, L., H.S. Gabryś, S.A. Hogan, M. Pavic, M. Bogowicz, D. Vuong, S. Tanadini-Lang, R. Förster, K. Kudura, M.W. Huellner, R. Dummer, M. Guckenberger, and M.P. Levesque, *Radiomics, Tumor Volume, and Blood Biomarkers for Early Prediction of Pseudoprogression in Patients with Metastatic Melanoma Treated with Immune Checkpoint Inhibition.* Clin Cancer Res, 2020. **26**(16): p. 4414-4425.

105. Schmauch, B., A. Romagnoni, E. Pronier, C. Saillard, P. Maillé, J. Calderaro, A. Kamoun, M. Sefta, S. Toldo, M. Zaslavskiy, T. Clozel, M. Moarii, P. Courtiol, and

G. Wainrib, *A deep learning model to predict RNA-Seq expression of tumours from whole slide images.* Nat Commun, 2020. **11**(1): p. 3877.

106. Gerlinger, M., A.J. Rowan, S. Horswell, M. Math, J. Larkin, D. Endesfelder, E. Gronroos, P. Martinez, N. Matthews, A. Stewart, P. Tarpey, I. Varela, B. Phillimore, S. Begum, N.Q. McDonald, A. Butler, D. Jones, K. Raine, C. Latimer, C.R. Santos, M. Nohadani, A.C. Eklund, B. Spencer-Dene, G. Clark, L. Pickering, G. Stamp, M. Gore, Z. Szallasi, J. Downward, P.A. Futreal, and C. Swanton, *Intratumor heterogeneity and branched evolution revealed by multiregion sequencing.* N Engl J Med, 2012. **366**(10): p. 883-892.

107. Zhang, J., J. Fujimoto, D.C. Wedge, X. Song, S. Seth, C.W. Chow, Y. Cao, C. Gumbs, K.A. Gold, N. Kalhor, L. Little, H. Mahadeshwar, C. Moran, A. Protopopov, H. Sun, J. Tang, X. Wu, Y. Ye, W.N. William, J.J. Lee, J.V. Heymach, W.K. Hong, S. Swisher, I.I. Wistuba, and P.A. Futreal, *Intratumor heterogeneity in localized lung adenocarcinomas delineated by multiregion sequencing.* Science, 2014. **346**(6206): p. 256-9.

108. Lee, Y., M. Kim, J. Han, K.H. Yeom, S. Lee, S.H. Baek, and V.N. Kim, *MicroRNA genes are transcribed by RNA polymerase II.* EMBO J, 2004. **23**(20): p. 4051-60.

109. Lee, Y., K. Jeon, J.T. Lee, S. Kim, and V.N. Kim, *MicroRNA maturation: stepwise processing and subcellular localization.* EMBO J, 2002. **21**(17): p. 4663-70.

110. Zeng, Y. and B.R. Cullen, *Sequence requirements for micro RNA processing and function in human cells.* RNA, 2003. **9**(1): p. 112-23.

111. Gregory, R.I., K.P. Yan, G. Amuthan, T. Chendrimada, B. Doratotaj, N. Cooch, and R. Shiekhattar, *The Microprocessor complex mediates the genesis of microRNAs.* Nature, 2004. **432**(7014): p. 235-40.

112. Denli, A.M., B.B. Tops, R.H. Plasterk, R.F. Ketting, and G.J. Hannon, *Processing of primary microRNAs by the Microprocessor complex.* Nature, 2004. **432**(7014): p. 231-5.

113. Yi, R., Y. Qin, I.G. Macara, and B.R. Cullen, *Exportin-5 mediates the nuclear export of pre-microRNAs and short hairpin RNAs.* Genes Dev, 2003. **17**(24): p. 3011-6.

114. Grishok, A., A.E. Pasquinelli, D. Conte, N. Li, S. Parrish, I. Ha, D.L. Baillie, A. Fire, G. Ruvkun, and C.C. Mello, *Genes and mechanisms related to RNA interference regulate expression of the small temporal RNAs that control C. elegans developmental timing.* Cell, 2001. **106**(1): p. 23-34.

115. Ketting, R.F., S.E. Fischer, E. Bernstein, T. Sijen, G.J. Hannon, and R.H. Plasterk, *Dicer functions in RNA interference and in synthesis of small RNA involved in developmental timing in C. elegans.* Genes Dev, 2001. **15**(20): p. 2654-9.

116. Hu, H.Y., Z. Yan, Y. Xu, H. Hu, C. Menzel, Y.H. Zhou, W. Chen, and P. Khaitovich, *Sequence features associated with microRNA strand selection in humans and flies.* BMC Genomics, 2009. **10**: p. 413.

117. Yoda, M., T. Kawamata, Z. Paroo, X. Ye, S. Iwasaki, Q. Liu, and Y. Tomari, *ATP-dependent human RISC assembly pathways.* Nat Struct Mol Biol, 2010. **17**(1): p. 17-23.

118. Khvorova, A., A. Reynolds, and S.D. Jayasena, *Functional siRNAs and miRNAs exhibit strand bias.* Cell, 2003. **115**(2): p. 209-16.

119. Wyman, S.K., E.C. Knouf, R.K. Parkin, B.R. Fritz, D.W. Lin, L.M. Dennis, M.A. Krouse, P.J. Webster, and M. Tewari, *Post-transcriptional generation of miRNA variants by multiple nucleotidyl transferases contributes to miRNA transcriptome complexity.* Genome Res, 2011. **21**(9): p. 1450-61.

120. Barman, B. and S.N. Bhattacharyya, *mRNA Targeting to Endoplasmic Reticulum Precedes Ago Protein Interaction and MicroRNA (miRNA)-mediated Translation Repression in Mammalian Cells.* J Biol Chem, 2015. **290**(41): p. 24650-6.

121. Gebert, L.F.R. and I.J. MacRae, *Regulation of microRNA function in animals.* Nat Rev Mol Cell Biol, 2019. **20**(1): p. 21-37.

122. Bartel, D.P., *MicroRNAs: target recognition and regulatory functions.* Cell, 2009. **136**(2): p. 215-33.

123. Agarwal, V., G.W. Bell, J.W. Nam, and D.P. Bartel, *Predicting effective microRNA target sites in mammalian mRNAs.* Elife, 2015. **4**.

124. McCall, M.N., M.S. Kim, M. Adil, A.H. Patil, Y. Lu, C.J. Mitchell, P. Leal-Rojas, J. Xu, M. Kumar, V.L. Dawson, T.M. Dawson, A.S. Baras, A.Z. Rosenberg, D.E. Arking, K.H. Burns, A. Pandey, and M.K. Halushka, *Toward the human cellular microRNAome.* Genome Res, 2017. **27**(10): p. 1769-1781.

125. Peng, Y. and C.M. Croce, *The role of MicroRNAs in human cancer.* Signal Transduct Target Ther, 2016. **1**: p. 15004.

126. Network, C.G.A., *Genomic Classification of Cutaneous Melanoma.* Cell, 2015. **161**(7): p. 1681-96.

127. Stark, M.S., S. Tyagi, D.J. Nancarrow, G.M. Boyle, A.L. Cook, D.C. Whiteman, P.G. Parsons, C. Schmidt, R.A. Sturm, and N.K. Hayward, *Characterization of the Melanoma miRNAome by Deep Sequencing.* PLoS One, 2010. **5**(3): p. e9685.

128. Thyagarajan, A., A. Shaban, and R.P. Sahu, *MicroRNA-Directed Cancer Therapies: Implications in Melanoma Intervention.* J Pharmacol Exp Ther, 2018. **364**(1): p. 1-12.

129. Chen, S., L. Wang, J. Fan, C. Ye, D. Dominguez, Y. Zhang, T.J. Curiel, D. Fang, T.M. Kuzel, and B. Zhang, *Host miR155 promotes tumor growth through a myeloid-derived suppressor cell-dependent mechanism.* Cancer Res, 2015. **75**(3): p. 519-31.

130. Ji, Y., C. Wrzesinski, Z. Yu, J. Hu, S. Gautam, N.V. Hawk, W.G. Telford, D.C. Palmer, Z. Franco, M. Sukumar, R. Roychoudhuri, D. Clever, C.A. Klebanoff, C.D. Surh, T.A. Waldmann, N.P. Restifo, and L. Gattinoni, *miR-155 augments CD8+ T-cell antitumor activity in lymphoreplete hosts by enhancing responsiveness to homeostatic γc cytokines.* Proc Natl Acad Sci U S A, 2015. **112**(2): p. 476-81.

131. Dudda, J.C., B. Salaun, Y. Ji, D.C. Palmer, G.C. Monnot, E. Merck, C. Boudousquie, D.T. Utzschneider, T.M. Escobar, R. Perret, S.A. Muljo, M. Hebeisen, N. Rufer, D. Zehn, A. Donda, N.P. Restifo, W. Held, L. Gattinoni, and P. Romero, *MicroRNA-155 is required for effector CD8+ T cell responses to virus infection and cancer.* Immunity, 2013. **38**(4): p. 742-53.

132. Achberger, S., W. Aldrich, R. Tubbs, J.W. Crabb, A.D. Singh, and P.L. Triozzi, *Circulating immune cell and microRNA in patients with uveal melanoma developing metastatic disease.* Mol Immunol, 2014. **58**(2): p. 182-6.

133. Venza, I., M. Visalli, C. Beninati, S. Benfatto, D. Teti, and M. Venza, *IL-10Rα expression is post-transcriptionally regulated by miR-15a, miR-185, and miR-211 in melanoma.* BMC Med Genomics, 2015. **8**: p. 81.

134. Chen, L., D.L. Gibbons, S. Goswami, M.A. Cortez, Y.H. Ahn, L.A. Byers, X. Zhang, X. Yi, D. Dwyer, W. Lin, L. Diao, J. Wang, J. Roybal, M. Patel, C. Ungewiss, D. Peng, S. Antonia, M. Mediavilla-Varela, G. Robertson, M. Suraokar, J.W. Welsh, B. Erez, I.I. Wistuba, S. Wang, S.E. Ullrich, J.V. Heymach, J.M. Kurie, and F.X. Qin, *Metastasis is regulated via microRNA-200/ZEB1 axis control of tumour cell PD-L1 expression and intratumoral immunosuppression.* Nat Commun, 2014. **5**: p. 5241.

135. Wei, J., F. Wang, L.Y. Kong, S. Xu, T. Doucette, S.D. Ferguson, Y. Yang, K. McEnery, K. Jethwa, O. Gjyshi, W. Qiao, N.B. Levine, F.F. Lang, G. Rao, G.N. Fuller, G.A. Calin, and A.B. Heimberger, *miR-124 inhibits STAT3 signaling to enhance T cell-mediated immune clearance of glioma.* Cancer Res, 2013. **73**(13): p. 3913-26.

136. Wei, J., E.K. Nduom, L.Y. Kong, Y. Hashimoto, S. Xu, K. Gabrusiewicz, X. Ling, N. Huang, W. Qiao, S. Zhou, C. Ivan, G.N. Fuller, M.R. Gilbert, W. Overwijk, G.A. Calin, and A.B. Heimberger, *MiR-138 exerts anti-glioma efficacy by targeting immune checkpoints.* Neuro Oncol, 2016. **18**(5): p. 639-48.

137. Mastroianni, J., N. Stickel, H. Andrlova, K. Hanke, W. Melchinger, S. Duquesne, D. Schmidt, M. Falk, G. Andrieux, D. Pfeifer, H. Dierbach, A. Schmitt-Graeff, F. Meiss, M. Boerries, and R. Zeiser, *miR-146a Controls Immune Response in the Melanoma Microenvironment.* Cancer Res, 2019. **79**(1): p. 183-195.

138. Siegel, R.L., K.D. Miller, and A. Jemal, *Cancer statistics, 2018.* CA Cancer J Clin, 2018. **68**(1): p. 7-30.

139. Iwai, Y., M. Ishida, Y. Tanaka, T. Okazaki, T. Honjo, and N. Minato, *Involvement of PD-L1 on tumor cells in the escape from host immune system and tumor immunotherapy by PD-L1 blockade.* Proc Natl Acad Sci U S A, 2002. **99**(19): p. 12293-7.

140. Wolchok, J.D., V. Chiarion-Sileni, R. Gonzalez, P. Rutkowski, J.J. Grob, C.L. Cowey, C.D. Lao, J. Wagstaff, D. Schadendorf, P.F. Ferrucci, M. Smylie, R. Dummer, A. Hill, D. Hogg, J. Haanen, M.S. Carlino, O. Bechter, M. Maio, I. Marquez-Rodas, M. Guidoboni, G. McArthur, C. Lebbé, P.A. Ascierto, G.V. Long, J. Cebon, J. Sosman, M.A. Postow, M.K. Callahan, D. Walker, L. Rollin, R. Bhore, F.S. Hodi, and J. Larkin, *Overall Survival with Combined Nivolumab and Ipilimumab in Advanced Melanoma.* N Engl J Med, 2017. **377**(14): p. 1345-1356.

141. Sade-Feldman, M., Y.J. Jiao, J.H. Chen, M.S. Rooney, M. Barzily-Rokni, J.P. Eliane, S.L. Bjorgaard, M.R. Hammond, H. Vitzthum, S.M. Blackmon, D.T. Frederick, M. Hazar-Rethinam, B.A. Nadres, E.E. Van Seventer, S.A. Shukla, K. Yizhak, J.P. Ray, D. Rosebrock, D. Livitz, V. Adalsteinsson, G. Getz, L.M. Duncan, B. Li, R.B. Corcoran, D.P. Lawrence, A. Stemmer-Rachamimov, G.M. Boland, D.A. Landau, K.T. Flaherty, R.J. Sullivan, and N. Hacohen, *Resistance to checkpoint blockade therapy through inactivation of antigen presentation.* Nat Commun, 2017. **8**(1): p. 1136.

142. Friedman, R.C., K.K. Farh, C.B. Burge, and D.P. Bartel, *Most mammalian mRNAs are conserved targets of microRNAs.* Genome Res, 2009. **19**(1): p. 92-105.

143. Calin, G.A., C.G. Liu, C. Sevignani, M. Ferracin, N. Felli, C.D. Dumitru, M. Shimizu, A. Cimmino, S. Zupo, M. Dono, M.L. Dell'Aquila, H. Alder, L. Rassenti, T.J. Kipps, F. Bullrich, M. Negrini, and C.M. Croce, *MicroRNA profiling reveals distinct signatures in B cell chronic lymphocytic leukemias.* Proc Natl Acad Sci U S A, 2004. **101**(32): p. 11755-60.

144. Olive, V., I. Jiang, and L. He, *mir-17-92, a cluster of miRNAs in the midst of the cancer network.* Int J Biochem Cell Biol, 2010. **42**(8): p. 1348-54.

145. Kundu, S.T., L.A. Byers, D.H. Peng, J.D. Roybal, L. Diao, J. Wang, P. Tong, C.J. Creighton, and D.L. Gibbons, *The miR-200 family and the miR-183~96~182 cluster target Foxf2 to inhibit invasion and metastasis in lung cancers.* Oncogene, 2016. **35**(2): p. 173-86.

146. Zehavi, L., R. Avraham, A. Barzilai, D. Bar-Ilan, R. Navon, Y. Sidi, D. Avni, and R. Leibowitz-Amit, *Silencing of a large microRNA cluster on human chromosome 14q32 in melanoma: biological effects of mir-376a and mir-376c on insulin growth factor 1 receptor.* Mol Cancer, 2012. **11**: p. 44.

147. Galore-Haskel, G., Y. Nemlich, E. Greenberg, S. Ashkenazi, M. Hakim, O. Itzhaki, N. Shoshani, R. Shapira-Fromer, E. Ben-Ami, E. Ofek, L. Anafi, M.J. Besser, J. Schachter, and G. Markel, *A novel immune resistance mechanism of melanoma cells controlled by the ADAR1 enzyme.* Oncotarget, 2015. **6**(30): p. 28999-9015.

148. Bonazzi, V.F., M.S. Stark, and N.K. Hayward, *MicroRNA regulation of melanoma progression.* Melanoma Res, 2012. **22**(2): p. 101-13.

149. Fattore, L., A. Sacconi, R. Mancini, and G. Ciliberto, *MicroRNA-driven deregulation of cytokine expression helps development of drug resistance in metastatic melanoma.* Cytokine Growth Factor Rev, 2017. **36**: p. 39-48.

150. Luo, C., C.E. Weber, W. Osen, A.K. Bosserhoff, and S.B. Eichmüller, *The role of microRNAs in melanoma.* Eur J Cell Biol, 2014. **93**(1-2): p. 11-22.

151. Fattore, L., S. Costantini, D. Malpicci, C.F. Ruggiero, P.A. Ascierto, C.M. Croce, R. Mancini, and G. Ciliberto, *MicroRNAs in melanoma development and resistance to target therapy.* Oncotarget, 2017. **8**(13): p. 22262-22278.

152. Xu, S., J. Wei, F. Wang, L.Y. Kong, X.Y. Ling, E. Nduom, K. Gabrusiewicz, T. Doucette, Y. Yang, N.K. Yaghi, V. Fajt, J.M. Levine, W. Qiao, X.G. Li, F.F. Lang, G. Rao, G.N. Fuller, G.A. Calin, and A.B. Heimberger, *Effect of miR-142-3p on the M2 macrophage and therapeutic efficacy against murine glioblastoma.* J Natl Cancer Inst, 2014. **106**(8).

153. Rooney, M.S., S.A. Shukla, C.J. Wu, G. Getz, and N. Hacohen, *Molecular and genetic properties of tumors associated with local immune cytolytic activity.* Cell, 2015. **160**(1-2): p. 48-61.

154. Newman, A.M., C.L. Liu, M.R. Green, A.J. Gentles, W. Feng, Y. Xu, C.D. Hoang, M. Diehn, and A.A. Alizadeh, *Robust enumeration of cell subsets from tissue expression profiles.* Nat Methods, 2015. **12**(5): p. 453-7.

155. Huang, T., W. Kang, B. Zhang, F. Wu, Y. Dong, J.H. Tong, W. Yang, Y. Zhou, L. Zhang, A.S. Cheng, J. Yu, and K.F. To, *miR-508-3p concordantly silences NFKB1 and RELA to inactivate canonical NF-κB signaling in gastric carcinogenesis.* Mol Cancer, 2016. **15**: p. 9.

156. Ayers, M., J. Lunceford, M. Nebozhyn, E. Murphy, A. Loboda, D.R. Kaufman, A. Albright, J.D. Cheng, S.P. Kang, V. Shankaran, S.A. Piha-Paul, J. Yearley, T.Y. Seiwert, A. Ribas, and T.K. McClanahan, *IFN-γ-related mRNA profile predicts clinical response to PD-1 blockade.* J Clin Invest, 2017. **127**(8): p. 2930-2940.

157. Riaz, N., J.J. Havel, V. Makarov, A. Desrichard, W.J. Urba, J.S. Sims, F.S. Hodi, S. Martín-Algarra, R. Mandal, W.H. Sharfman, S. Bhatia, W.J. Hwu, T.F. Gajewski, C.L. Slingluff, D. Chowell, S.M. Kendall, H. Chang, R. Shah, F. Kuo, L.G.T. Morris, J.W. Sidhom, J.P. Schneck, C.E. Horak, N. Weinhold, and T.A. Chan, *Tumor and Microenvironment Evolution during Immunotherapy with Nivolumab.* Cell, 2017. **171**(4): p. 934-949.e16.

158. Grasso, C.S., J. Tsoi, M. Onyshchenko, G. Abril-Rodriguez, P. Ross-Macdonald, M. Wind-Rotolo, A. Champhekar, E. Medina, D.Y. Torrejon, D.S. Shin, P. Tran, Y.J. Kim, C. Puig-Saus, K. Campbell, A. Vega-Crespo, M. Quist, C. Martignier, J.J. Luke, J.D. Wolchok, D.B. Johnson, B. Chmielowski, F.S. Hodi, S. Bhatia, W. Sharfman, W.J. Urba, C.L. Slingluff, A. Diab, J.B.A.G. Haanen, S.M. Algarra, D.M. Pardoll, V. Anagnostou, S.L. Topalian, V.E. Velculescu, D.E. Speiser, A. Kalbasi, and A. Ribas, *Conserved Interferon-γ Signaling Drives Clinical Response to Immune Checkpoint Blockade Therapy in Melanoma.* Cancer Cell, 2020. **38**(4): p. 500-515.e3.

159. Taube, J.M., G.D. Young, T.L. McMiller, S. Chen, J.T. Salas, T.S. Pritchard, H. Xu, A.K. Meeker, J. Fan, C. Cheadle, A.E. Berger, D.M. Pardoll, and S.L. Topalian, *Differential Expression of Immune-Regulatory Genes Associated with PD-L1*

Display in Melanoma: Implications for PD-1 Pathway Blockade. Clin Cancer Res, 2015. **21**(17): p. 3969-76.

160. Auslander, N., G. Zhang, J.S. Lee, D.T. Frederick, B. Miao, T. Moll, T. Tian, Z. Wei, S. Madan, R.J. Sullivan, G. Boland, K. Flaherty, M. Herlyn, and E. Ruppin, *Robust prediction of response to immune checkpoint blockade therapy in metastatic melanoma.* Nat Med, 2018. **24**(10): p. 1545-1549.

161. Becht, E., N.A. Giraldo, L. Lacroix, B. Buttard, N. Elarouci, F. Petitprez, J. Selves, P. Laurent-Puig, C. Sautès-Fridman, W.H. Fridman, and A. de Reyniès, *Estimating the population abundance of tissue-infiltrating immune and stromal cell populations using gene expression.* Genome Biol, 2016. **17**(1): p. 218.

162. Hodi, F.S., V. Chiarion-Sileni, R. Gonzalez, J.J. Grob, P. Rutkowski, C.L. Cowey, C.D. Lao, D. Schadendorf, J. Wagstaff, R. Dummer, P.F. Ferrucci, M. Smylie, A. Hill, D. Hogg, I. Marquez-Rodas, J. Jiang, J. Rizzo, J. Larkin, and J.D. Wolchok, *Nivolumab plus ipilimumab or nivolumab alone versus ipilimumab alone in advanced melanoma (CheckMate 067): 4-year outcomes of a multicentre, randomised, phase 3 trial.* Lancet Oncol, 2018. **19**(11): p. 1480-1492.

163. Hamid, O., C. Robert, A. Daud, F.S. Hodi, W.J. Hwu, R. Kefford, J.D. Wolchok, P. Hersey, R. Joseph, J.S. Weber, R. Dronca, T.C. Mitchell, A. Patnaik, H.M. Zarour, A.M. Joshua, Q. Zhao, E. Jensen, S. Ahsan, N. Ibrahim, and A. Ribas, *Five-year survival outcomes for patients with advanced melanoma treated with pembrolizumab in KEYNOTE-001.* Ann Oncol, 2019. **30**(4): p. 582-588.

164. Serrone, L., M. Zeuli, F.M. Sega, and F. Cognetti, *Dacarbazine-based chemotherapy for metastatic melanoma: thirty-year experience overview.* J Exp Clin Cancer Res, 2000. **19**(1): p. 21-34.

165. Tumeh, P.C., C.L. Harview, J.H. Yearley, I.P. Shintaku, E.J. Taylor, L. Robert, B. Chmielowski, M. Spasic, G. Henry, V. Ciobanu, A.N. West, M. Carmona, C. Kivork, E. Seja, G. Cherry, A.J. Gutierrez, T.R. Grogan, C. Mateus, G. Tomasic, J.A. Glaspy, R.O. Emerson, H. Robins, R.H. Pierce, D.A. Elashoff, C. Robert, and A. Ribas, *PD-1 blockade induces responses by inhibiting adaptive immune resistance.* Nature, 2014. **515**(7528): p. 568-71.

166. Taube, J.M., A. Klein, J.R. Brahmer, H. Xu, X. Pan, J.H. Kim, L. Chen, D.M. Pardoll, S.L. Topalian, and R.A. Anders, *Association of PD-1, PD-1 ligands, and other features of the tumor immune microenvironment with response to anti-PD-1 therapy.* Clin Cancer Res, 2014. **20**(19): p. 5064-74.

167. Vilain, R.E., A.M. Menzies, J.S. Wilmott, H. Kakavand, J. Madore, A. Guminski, E. Liniker, B.Y. Kong, A.J. Cooper, J.R. Howle, R.P.M. Saw, V. Jakrot, S. Lo, J.F. Thompson, M.S. Carlino, R.F. Kefford, G.V. Long, and R.A. Scolyer, *Dynamic Changes in PD-L1 Expression and Immune Infiltrates Early During Treatment Predict Response to PD-1 Blockade in Melanoma.* Clin Cancer Res, 2017. **23**(17): p. 5024-5033.

168. Prat, A., A. Navarro, L. Paré, N. Reguart, P. Galván, T. Pascual, A. Martínez, P. Nuciforo, L. Comerma, L. Alos, N. Pardo, S. Cedrés, C. Fan, J.S. Parker, L. Gaba, I. Victoria, N. Viñolas, A. Vivancos, A. Arance, and E. Felip, *Immune-Related Gene Expression Profiling After PD-1 Blockade in Non-Small Cell Lung*

Carcinoma, Head and Neck Squamous Cell Carcinoma, and Melanoma. Cancer Res, 2017. **77**(13): p. 3540-3550.

169. Gopalakrishnan, V., C.N. Spencer, L. Nezi, A. Reuben, M.C. Andrews, T.V. Karpinets, P.A. Prieto, D. Vicente, K. Hoffman, S.C. Wei, A.P. Cogdill, L. Zhao, C.W. Hudgens, D.S. Hutchinson, T. Manzo, M. Petaccia de Macedo, T. Cotechini, T. Kumar, W.S. Chen, S.M. Reddy, R. Szczepaniak Sloane, J. Galloway-Pena, H. Jiang, P.L. Chen, E.J. Shpall, K. Rezvani, A.M. Alousi, R.F. Chemaly, S. Shelburne, L.M. Vence, P.C. Okhuysen, V.B. Jensen, A.G. Swennes, F. McAllister, E. Marcelo Riquelme Sanchez, Y. Zhang, E. Le Chatelier, L. Zitvogel, N. Pons, J.L. Austin-Breneman, L.E. Haydu, E.M. Burton, J.M. Gardner, E. Sirmans, J. Hu, A.J. Lazar, T. Tsujikawa, A. Diab, H. Tawbi, I.C. Glitza, W.J. Hwu, S.P. Patel, S.E. Woodman, R.N. Amaria, M.A. Davies, J.E. Gershenwald, P. Hwu, J.E. Lee, J. Zhang, L.M. Coussens, Z.A. Cooper, P.A. Futreal, C.R. Daniel, N.J. Ajami, J.F. Petrosino, M.T. Tetzlaff, P. Sharma, J.P. Allison, R.R. Jenq, and J.A. Wargo, *Gut microbiome modulates response to anti-PD-1 immunotherapy in melanoma patients.* Science, 2018. **359**(6371): p. 97-103.

170. Wong, P.F., W. Wei, S. Gupta, J.W. Smithy, D. Zelterman, H.M. Kluger, and D.L. Rimm, *Multiplex quantitative analysis of cancer-associated fibroblasts and immunotherapy outcome in metastatic melanoma.* J Immunother Cancer, 2019. **7**(1): p. 194.

171. Helmink, B.A., S.M. Reddy, J. Gao, S. Zhang, R. Basar, R. Thakur, K. Yizhak, M. Sade-Feldman, J. Blando, G. Han, V. Gopalakrishnan, Y. Xi, H. Zhao, R.N. Amaria, H.A. Tawbi, A.P. Cogdill, W. Liu, V.S. LeBleu, F.G. Kugeratski, S. Patel,

M.A. Davies, P. Hwu, J.E. Lee, J.E. Gershenwald, A. Lucci, R. Arora, S. Woodman, E.Z. Keung, P.O. Gaudreau, A. Reuben, C.N. Spencer, E.M. Burton, L.E. Haydu, A.J. Lazar, R. Zapassodi, C.W. Hudgens, D.A. Ledesma, S. Ong, M. Bailey, S. Warren, D. Rao, O. Krijgsman, E.A. Rozeman, D. Peeper, C.U. Blank, T.N. Schumacher, L.H. Butterfield, M.A. Zelazowska, K.M. McBride, R. Kalluri, J. Allison, F. Petitprez, W.H. Fridman, C. Sautès-Fridman, N. Hacohen, K. Rezvani, P. Sharma, M.T. Tetzlaff, L. Wang, and J.A. Wargo, *B cells and tertiary lymphoid structures promote immunotherapy response.* Nature, 2020. **577**(7791): p. 549-555.

172. Si, W., J. Shen, H. Zheng, and W. Fan, *The role and mechanisms of action of microRNAs in cancer drug resistance.* Clin Epigenetics, 2019. **11**(1): p. 25.

173. Pencheva, N., H. Tran, C. Buss, D. Huh, M. Drobnjak, K. Busam, and S.F. Tavazoie, *Convergent multi-miRNA targeting of ApoE drives LRP1/LRP8-dependent melanoma metastasis and angiogenesis.* Cell, 2012. **151**(5): p. 1068-82.

174. Yu, H. and W. Yang, *MiR-211 is epigenetically regulated by DNMT1 mediated methylation and inhibits EMT of melanoma cells by targeting RAB22A.* Biochem Biophys Res Commun, 2016. **476**(4): p. 400-405.

175. Golan, T., A.R. Messer, A. Amitai-Lange, Z. Melamed, R. Ohana, R.E. Bell, O. Kapitansky, G. Lerman, S. Greenberger, M. Khaled, N. Amar, J. Albrengues, C. Gaggioli, P. Gonen, Y. Tabach, D. Sprinzak, R. Shalom-Feuerstein, and C. Levy, *Interactions of Melanoma Cells with Distal Keratinocytes Trigger Metastasis via Notch Signaling Inhibition of MITF.* Mol Cell, 2015. **59**(4): p. 664-76.

176. Vergani, E., L. Di Guardo, M. Dugo, S. Rigoletto, G. Tragni, R. Ruggeri, F. Perrone, E. Tamborini, A. Gloghini, F. Arienti, B. Vergani, P. Deho, L. De Cecco, V. Vallacchi, P. Frati, E. Shahaj, A. Villa, M. Santinami, F. De Braud, L. Rivoltini, and M. Rodolfo, *Overcoming melanoma resistance to vemurafenib by targeting CCL2-induced miR-34a, miR-100 and miR-125b.* Oncotarget, 2016. **7**(4): p. 4428-41.

177. Dragomir, M., A.C.P. Mafra, S.M.G. Dias, C. Vasilescu, and G.A. Calin, *Using microRNA Networks to Understand Cancer.* Int J Mol Sci, 2018. **19**(7).

178. Duroux-Richard, I., C. Roubert, M. Ammari, J. Présumey, J.R. Grün, T. Häupl, A. Grützkau, C.H. Lecellier, V. Boitez, P. Codogno, J. Escoubet, Y.M. Pers, C. Jorgensen, and F. Apparailly, *miR-125b controls monocyte adaptation to inflammation through mitochondrial metabolism and dynamics.* Blood, 2016. **128**(26): p. 3125-3136.

179. Haq, R., J. Shoag, P. Andreu-Perez, S. Yokoyama, H. Edelman, G.C. Rowe, D.T. Frederick, A.D. Hurley, A. Nellore, A.L. Kung, J.A. Wargo, J.S. Song, D.E. Fisher, Z. Arany, and H.R. Widlund, *Oncogenic BRAF regulates oxidative metabolism via PGC1α and MITF.* Cancer Cell, 2013. **23**(3): p. 302-15.

180. Fischer, G.M., Y.N. Vashisht Gopal, J.L. McQuade, W. Peng, R.J. DeBerardinis, and M.A. Davies, *Metabolic strategies of melanoma cells: Mechanisms, interactions with the tumor microenvironment, and therapeutic implications.* Pigment Cell Melanoma Res, 2018. **31**(1): p. 11-30.

181. Hwang, H.W., E.A. Wentzel, and J.T. Mendell, *Cell-cell contact globally activates microRNA biogenesis.* Proc Natl Acad Sci U S A, 2009. **106**(17): p. 7016-21.

182. Huber, V., V. Vallacchi, V. Fleming, X. Hu, A. Cova, M. Dugo, E. Shahaj, R. Sulsenti, E. Vergani, P. Filipazzi, A. De Laurentiis, L. Lalli, L. Di Guardo, R. Patuzzo, B. Vergani, E. Casiraghi, M. Cossa, A. Gualeni, V. Bollati, F. Arienti, F. De Braud, L. Mariani, A. Villa, P. Altevogt, V. Umansky, M. Rodolfo, and L. Rivoltini, *Tumor-derived microRNAs induce myeloid suppressor cells and predict immunotherapy resistance in melanoma.* J Clin Invest, 2018. **128**(12): p. 5505-5516.

183. Fischer, G.M., A. Jalali, D.A. Kircher, W.C. Lee, J.L. McQuade, L.E. Haydu, A.Y. Joon, A. Reuben, M.P. de Macedo, F.C.L. Carapeto, C. Yang, A. Srivastava, C.R. Ambati, A. Sreekumar, C.W. Hudgens, B. Knighton, W. Deng, S.D. Ferguson, H.A. Tawbi, I.C. Glitza, J.E. Gershenwald, Y.N. Vashisht Gopal, P. Hwu, J.T. Huse, J.A. Wargo, P.A. Futreal, N. Putluri, A.J. Lazar, R.J. DeBerardinis, J.R. Marszalek, J. Zhang, S.L. Holmen, M.T. Tetzlaff, and M.A. Davies, *Molecular Profiling Reveals Unique Immune and Metabolic Features of Melanoma Brain Metastases.* Cancer Discov, 2019. **9**(5): p. 628-645.

184. Jaiswal, A.R., A.J. Liu, S. Pudakalakatti, P. Dutta, P. Jayaprakash, T. Bartkowiak, C.R. Ager, Z.Q. Wang, A. Reuben, Z.A. Cooper, C. Ivan, Z. Ju, F. Nwajei, J. Wang, M.A. Davies, R.E. Davis, J.A. Wargo, P.K. Bhattacharya, D.S. Hong, and M.A. Curran, *Melanoma Evolves Complete Immunotherapy Resistance through the Acquisition of a Hypermetabolic Phenotype.* Cancer Immunol Res, 2020. **8**(11): p. 1365-1380.

185. Najjar, Y.G., A.V. Menk, C. Sander, U. Rao, A. Karunamurthy, R. Bhatia, S. Zhai, J.M. Kirkwood, and G.M. Delgoffe, *Tumor cell oxidative metabolism as a barrier to PD-1 blockade immunotherapy in melanoma.* JCI Insight, 2019. **4**(5).

186. González-Silva, L., L. Quevedo, and I. Varela, *Tumor Functional Heterogeneity Unraveled by scRNA-seq Technologies.* Trends Cancer, 2020. **6**(1): p. 13-19.

187. Fattore, L., C.F. Ruggiero, D. Liguoro, R. Mancini, and G. Ciliberto, *Single cell analysis to dissect molecular heterogeneity and disease evolution in metastatic melanoma.* Cell Death Dis, 2019. **10**(11): p. 827.

188. McCart Reed, A.E., J. Bennett, J.R. Kutasovic, E. Kalaw, K. Ferguson, J. Yeong, P.T. Simpson, and S.R. Lakhani, *Digital spatial profiling application in breast cancer: a user's perspective.* Virchows Arch, 2020. **477**(6): p. 885-890.

189. Oba, J., S.H. Kim, W.L. Wang, M.P. Macedo, F. Carapeto, M.A. McKean, J. Van Arnam, A.K. Eterovic, S. Sen, C.R. Kale, X. Yu, C.L. Haymaker, M. Routbort, L.E. Haydu, C. Bernatchez, A.J. Lazar, E.A. Grimm, D.S. Hong, and S.E. Woodman, *Targeting the HGF/MET Axis Counters Primary Resistance to KIT Inhibition in.* JCO Precis Oncol, 2018. **2018**.

190. Park, J., A.H. Talukder, S.A. Lim, K. Kim, K. Pan, B. Melendez, S.D. Bradley, K.R. Jackson, J.S. Khalili, J. Wang, C. Creasy, B.F. Pan, S.E. Woodman, C. Bernatchez, D. Hawke, P. Hwu, K.M. Lee, J. Roszik, G. Lizée, and C. Yee, *SLC45A2: A Melanoma Antigen with High Tumor Selectivity and Reduced Potential for Autoimmune Toxicity.* Cancer Immunol Res, 2017. **5**(8): p. 618-629.

191. Li, Y., M. Bleakley, and C. Yee, *IL-21 influences the frequency, phenotype, and affinity of the antigen-specific CD8 T cell response.* J Immunol, 2005. **175**(4): p. 2261-9.

192. Li, Y. and C. Yee, *IL-21 mediated Foxp3 suppression leads to enhanced generation of antigen-specific CD8+ cytotoxic T lymphocytes.* Blood, 2008. **111**(1): p. 229-35.

VITA

Robert Andrew Szczepaniak Sloane was born in Canterbury, Kent, England in July 1987. After completing his work at Barton Court Grammar School, Canterbury, Kent in 2005, he entered The University of Manchester in Manchester, England. He received the degree Bachelor of Science with honours in June 2008. For the next seven years, he worked as a scientific officer in the laboratory of Caroline Dive, CBE, PhD, FBPhS, FMedSci, at the Cancer Research UK Manchester Institute. In August 2015 he entered the PhD program at The University of Texas MD Anderson Cancer Center UTHealth Graduate School of Biomedical Sciences.